



January 2012

Assessing The Biophysical Naturalness Of Grassland In Eastern North Dakota With Hyperspectral Imagery

Qiang Zhou

[How does access to this work benefit you? Let us know!](#)

Follow this and additional works at: <https://commons.und.edu/theses>

Recommended Citation

Zhou, Qiang, "Assessing The Biophysical Naturalness Of Grassland In Eastern North Dakota With Hyperspectral Imagery" (2012). *Theses and Dissertations*. 1218.
<https://commons.und.edu/theses/1218>

This Thesis is brought to you for free and open access by the Theses, Dissertations, and Senior Projects at UND Scholarly Commons. It has been accepted for inclusion in Theses and Dissertations by an authorized administrator of UND Scholarly Commons. For more information, please contact und.common@library.und.edu.

ASSESSING THE BIOPHYSICAL NATURALNESS OF GRASSLAND IN EASTERN
NORTH DAKOTA WITH HYPERSPECTRAL IMAGERY

by

Qiang Zhou

Bachelor of Science, HeFei University of Technology, 2006

Master of Science, Institute of Remote Sensing Applications Chinese Academy of
Sciences, 2009

A Thesis

Submitted to the Graduate Faculty

of the

University of North Dakota

In partial fulfillment of the requirements

for the degree of

Master of Science

Grand Forks, North Dakota

December

2011

This thesis, submitted by Qiang Zhou in partial fulfillment of the requirements for the Degree of Master of Science from the University of North Dakota, has been read by the Faculty Advisory Committee under whom the work has been done and is hereby approved.

Michael J. Hill

Chairperson

Soizik Laguette

Bradley Rundquist

This thesis meets the standards for appearance, conforms to the style and format requirements of the Graduate School of the University of North Dakota, and is hereby approved.

Wayne Swisher

Dean of the Graduate School

April 3, 2012

Date

TABLE OF CONTENTS

LIST OF FIGURES	vii
LIST OF TABLES	xiv
ACKNOWLEDGEMENTS	xv
ABSTRACT	xvi
CHAPTER	
I. INTRODUCTION	1
Thesis Overview: Outline of Thesis Structure and Chapters	4
II. LITERATURE REVIEW	6
Prairie Grassland Characteristics	6
Key Features of Grasslands That Could Be Spectrally Discriminatory	8
Multispectral Remote Sensing of Grassland and Spectral indices...	9
Hyperspectral Remote Sensing of Grassland	12
Ecosystem Parameters	12
Biophysical Grassland Parameters	14
Species Discrimination - Case Studies	16
Spectral Identification Techniques	19
Other Potentially Important Grassland Properties	21
Summary	21
III. IMAGE PROCESSING	25
Introduction	25
Sites	25

	Hyperion Sensor.....	31
	Data Processing.....	31
	Grassland Classification and Mask.....	34
	Image Analysis: Fractional Cover.....	38
	Linear Unmixing under NDVI and CAI space	38
	Fractional Cover.....	40
IV.	FIELD SPECTRA.....	44
	The Spectroradiometer.....	44
	Data Processing.....	45
	Field Measurements Result.....	50
	Discussion.....	60
V.	SPECTRUM MATCHING.....	63
	Introduction.....	63
	Spectral Library	63
	Methods.....	71
	Matching Methods.....	71
	Adaptive Coherence Estimator (ACE).....	72
	Dominance Analysis.....	73
	Texture Co-occurrence Measurements: Spatial Grain	74
	Results.....	77
	Matching.....	77
	Dominance	89
	Discussion.....	93
VI.	NATURALNESS MODELING	95
	MCAS-S - Multi-Criteria Analysis Shell for Spatial Decision Support.....	96

	Summary of Potential Input Data Layers for Modeling	96
	Model 1: Introduced Grass Model	104
	Introduced Grass Model applied to Oakville Prairie	104
	Introduced Grass Model applied to Woodworth	108
	Model 2: Native Grass Model.....	110
	Native Grass Model Applied To Oakville Prairie	111
	Native Grass Model Applied on Woodworth	114
	Model 3: Decision Tree (Based on later growing Season)	118
	Final Model Assessment at an Independent Field Site	123
	Discussion and Conclusion	129
VII.	CONCLUSION, LIMITATION AND FUTURE WORK FOR THE STUDY	132
	Conclusion and Discussion	132
	Limitations of the Study and Future Work.....	139
	REFERENCES	142

LIST OF FIGURES

Figure	Page
1. Flow Diagram Of Thesis Chapters And Relationship To Main Contents.....	4
2. General Spectrum Of Vegetation. The Reflectance Is Calculated As Average Of Various Species Field Measurements In Oakville Area.	9
3. Flow Diagram Of The Analytical Process	24
4. Locations Of Three Sites In North Dakota. The Background Is North Dakota GAP Analysis Map (Strong Et Al., 2005).....	27
5. Oakville Site. Background Is NAIP Map; The Red Box Shows The Boundary Of Oakville Prairie And The Blue Box Is School Trust Land	28
6. Mekinock Site Within The Red Boundary	28
7. Woodworth Site In The Red Boundary. The Yellow Boundary Suggests The Restored Area.....	29
8. Process Step For Hyperion Data.....	33
9. Results For Hyperion Data.....	36
10. Hyperion Image Classification Map And Mask Result (The Black Means Remove And The White Part Means Grassland And Will Be Maintained)	37
11. An Example Of The Scatter Plot Of CAI And NDVI Showing The Location Of The Three Endmembers.	40
12. Result Of The Green Vegetation, Dry And Soil Factional Cover Unmixing Based On The NDVI And CAI For The Oakville Prairie	42
13. Result Of The Green Vegetation, Dry And Soil Factional Cover Unmixing Based On The NDVI And CAI For The Woodworth And Masked To Grassland Areas Only.....	43
14. Overview Of The Field Spectra Processing And Transformation Steps.....	46
15. Average Of 10 Raw Measurements In Order To Reduce Noise	47

16. Reflectance Calculated As Ratio Between Measurements From Certain Species And White Reference.....	47
17. The First Detector Is Corrected And Adjusted To The Second Detector	49
18. Water Vapour Bands Are Removed And Replaced With Linear Interpolations....	49
19. Field Measurements Locations At Oakville Site. The Overview Image Shows Oakville North Section Region.	51
20. The Overall Variation In Vegetation Spectra At Oakville (Aug 06 2009; May 16 2011; Jun 28 2011; Jul 07 2011; Aug 25 2011)	52
21. The Overall Variation In Spectra At Woodworth (Aug 09 2011)	52
22. Photos Of Golden Rod; Wheat Grass Patch At Three Dates A-C); And D) Patch Spectra Collected At Four Times In 2001; And E) Fractional Cover Of Green, Dry And Bare Soil For The Image Pixel Corresponding To This Location.	53
23. Photo Of Triglochin Patch At Three Dates A-C); And D) Patch Spectra Collected At Four Times In 2001; And E) Fractional Cover Of Green, Dry And Bare Soil For The Image Pixel Corresponding To This Location.....	53
24. Photo Of Wheat Grass Patch Spectra Of Wheat Grass Patch At Three Dates A-C); And D) Patch Spectra Collected At Four Times In 2001; And E) Fractional Cover Of Green, Dry And Bare Soil For The Image Pixel Corresponding To This Location.	54
25. Photo Of Cord Grass; Hairy Aster Patch At Three Dates A-C); And D) Patch Spectra Collected At Four Times In 2001; And E) Fractional Cover Of Green, Dry And Bare Soil For The Image Pixel Corresponding To This Location.	54
26. Photo Of An Area Dominated By Wild Rye (Elymus Spp) At Three Dates A-C); And D) Patch Spectra Collected At Four Times In 2001; And E) Fractional Cover Of Green, Dry And Bare Soil For The Image Pixel Corresponding To This Location.	55
27. Photo Of Wheat Grass Patch At Three Dates A-C); And D) Patch Spectra Collected At Four Times In 2001; And E) Fractional Cover Of Green, Dry And Bare Soil For The Image Pixel Corresponding To This Location.....	55
28. Photo Of Golden Rod; Poaceae Patch At Three Dates A-C); And D) Patch Spectra Collected At Four Times In 2001; And E) Fractional Cover Of Green, Dry And Bare Soil For The Image Pixel Corresponding To This Location.....	56

29. Photo Of Cord Grass Patch At Three Dates A-C); And D) Patch Spectra Collected At Four Times In 2001; And E) Fractional Cover Of Green, Dry And Bare Soil For The Image Pixel Corresponding To This Location.....	56
30. Photo Of Wheat Grass Patch At Three Dates A-C); And D) Patch Spectra Collected At Four Times In 2001; And E) Fractional Cover Of Green, Dry And Bare Soil For The Image Pixel Corresponding To This Location.....	57
31. Photo Of Patch At Three Dates A-C); And D) Patch Spectra Collected At Four Times In 2001; And E) Fractional Cover Of Green, Dry And Bare Soil For The Image Pixel Corresponding To This Location.	57
32. Photo Of Patch At Three Dates A-B); And C) Patch Spectra Collected At Four Times In 2001; And D) Fractional Cover Of Green, Dry And Bare Soil For The Image Pixel Corresponding To This Location.	58
33. Photo Of Snow Berrypatch At Three Dates A-C); And D) Patch Spectra Collected At Four Times In 2001; And E) Fractional Cover Of Green, Dry And Bare Soil For The Image Pixel Corresponding To This Location.....	58
34. Photo Of Brome Grass Patch At Three Dates A-B); And C) Patch Spectra Collected At Four Times In 2001; And D) Fractional Cover Of Green, Dry And Bare Soil For The Image Pixel Corresponding To This Location.....	59
35. Field Condition Of Spectral Library	66
36. Early Growing Season Spectral Library	67
37. Late Growing Season Spectra Library	67
38. Early Growing Season Spectral Library Continuum Removal.....	69
39. Late Growing Season Spectra Library Continuum Removal	69
40. Early Growing Season Spectral Library Area Of Absorption Features	70
41. Later Growing Season Spectral Library Area Of Absorption Features	70
42. Illustration Of ACE Detector (Manolakis, 2002).....	73
43. Example Of Image Texture	75
44. Illustration Of Four Nearest-Neighbor (Distance Is 1 Pixel) Directions	75
45. (A)4 By 4 Image With Four Gray-Tone Values 0-3; (B) General Form Of Any Gray-Tone Spatial-Dependence Matrix For Image With Gray-Tone Values 0-3; (C)-(F) Calculation Of All Four Distance 1 Gray-Tone Spatial-Dependence Matrices.....	76

46. A) Methods Test Of Oakville May 20 2010. For Each Method, 11 Endmembers Are Included. B) Legend For Data Layers.....	79
47. A) Methods Test Of Oakville May 24 2009. For Each Method, 11 Endmembers Are Included. B) Legend For Data Layers.....	80
48. A) Methods Test Of Oakville August 08 2010. For Each Method, 11 Endmembers Are Included. B) Legend For Data Layers.....	81
49. A) Methods Test Of Woodworth June 04 2010. For Each Method, 11 Endmembers Are Included. B) Legend For Data Layers.....	82
50. A) Methods Test Of Woodworth June 29 2009. For Each Method, 11 Endmembers Are Included. B) Legend For Data Layers.....	83
51. A) Methods Test Of Oakville September 01 2009. For Each Method, 12 Endmembers Are Included. B) Legend For Data Layers.....	84
52. A) Methods Test Of Woodworth September 18 2009. For Each Method, 12 Endmembers Are Included. B) Legend For Data Layers.....	85
53. Mean Possibility Of Species In Oakville September 01 2009. (X Axis From 1 To 11 Are June Grass; Maximilian Sunflower; Cord Grass; Wheat Grass; Wild Rye; Brome Grass Green; Brome Grass Flowering; Sage; Sage Willow; Thistle Green; Thistle Flowering).....	87
54. Mean Possibility Of Species In Woodworth September 18 2009. (X Axis From 1 To 11 Are June Grass; Maximilian Sunflower; Cord Grass; Wheat Grass; Wild Rye; Brome Grass Green; Brome Grass)	87
55. Possibility Standard Deviation Of Species In Oakville September 01 2009. (X Axis From 1 To 11 Are June Grass; Maximilian Sunflower; Cord Grass; Wheat Grass; Wild Rye; Brome Grass Green; Brome Grass Flowering; Sage; Sage Willow; Thistle Green; Thistle Flowering).....	88
56. Possibility Standard Deviation Of Species In Woodworth September 18 2009. (X Axis From 1 To 11 Are June Grass; Maximilian Sunflower; Cord Grass; Wheat Grass; Wild Rye; Brome Grass Green; Brome Grass Flowering; Sage; Sage Willow; Thistle Green; Thistle Flowering).....	88
57. Level Of Dominance.....	89
58. Band Variance.....	89
59. Scatter Plot Of Band Variance And Level Of Dominance In Oakville And Woodworth.....	89

60. Texture Co-Occurrence Measurements Of Level Dominance In Oakville September 01 2009 (Upper From Left To Right: Mean, Variance, Homogeneity, Contrast; Bottom From Left To Right: Dissimilarity, Entropy, Second Moment).....	90
61. Scatter Plot Of Texture Co-Occurrence Measurements In Multi Directions For Level Dominance In Oakville For September 1, 2009.	91
62. Scatter Plot Of Texture Co-Occurrence Measurements In Multi Directions For Level Dominance In Woodworth September 18 2009. The Cyan Area Suggests Disagreements Between 45 Degree And 135 Degree Measurements.....	92
63. A) Legend For Data Layers B) Data Layers Derived For Oakville Site May 20 2010 (Early Growing Season).....	99
64. A) Legend For Data Layers; B) Data Layers Derived For Oakville Site September 01 2009 (Later Growing Season).....	100
65. A) Legend For Data Layers. B) Data Layers Derived For Woodworth Site June 04 2010(Early Growing Season).	101
66. A) Legend For Data Layers; B) Data Layers Derived For Woodworth Site September 18 2009 (Later Growing Season).....	102
67. Introduced Grass Detection Model. The Character “I” Before Parameters Means Inverse, Which Inverted Maximum Value To 0 And Minimum To 1.....	105
68. Oakville Early Growing Season Model. Color From Blue To Red Indicates Value Or Model Score From Low To High.....	106
69. Oakville Later Growing Season Model. Color From Blue To Red Indicates Value Or Model Score From Low To High.....	106
70. Combined Time Series Model Of Oakville Prairie Grass. Color From Blue To Red Indicates Value Or Model Score From Low To High.....	107
71. Histogram Of Oakville Prairie. Color From Blue To Red Indicates Value Or Model Score From Low To High.....	107
72. Woodworth Early Growing Season Model. Color From Blue To Red Indicates Value Or Model Score From Low To High.....	108
73. Woodworth Later Growing Season Model. Color From Blue To Red Indicate Value Or Model Score From Low To High.....	109
74. Combined Time Series Model Of Woodworth Grass. Color From Blue To Red Indicate Value Or Model Score From Low To High.....	109

75. Histogram Of Disturbed Area At Woodworth. Color From Blue To Red Indicate Value Or Model Score From Low To High.....	110
76. Native Grass Detection Model. The Character “I” Before Parameters Means Inverse, Which Inverted Maximum Value To 0 And Minimum To 1.	111
77. Oakville Early Growing Season Model. Color From Blue To Red Indicates Value Or Model Score From Low To High.....	112
78. Oakville Later Growing Season Model. Color From Blue To Red Indicates Value Or Model Score From Low To High.....	113
79. Combined Time Series Model Of Oakville Prairie Grass. Color From Blue To Red Indicates Value Or Model Score From Low To High.....	113
80. Histogram Of Left Half Section Above School Trust Land Including Oakville Prairie And Part Of Forb Area. Color From Blue To Red Indicates Value Or Model Score From Low To High.....	114
81. Woodworth Early Growing Season Model. Color From Blue To Red Indicates Value Or Model Score From Low To High.....	116
82. Woodworth Later Growing Season Model. Color From Blue To Red Indicates Value Or Model Score From Low To High.....	116
83. Combined Time Series Model Of Woodworth Grass. Color From Blue To Red Indicates Value Or Model Score From Low To High	117
84. Histogram Of Woodworth Disturbed Area. The Replanted Area Has Been Removed From Statistic. Color From Blue To Red Indicates Value Or Model Score From Low To High	117
85. Decision Tree To Identify Brome Grass Patches From Native Grassland.	119
86. Decision Tree Applied On Oakville Site. Color From Blue To Red Indicate Value Or Model Score From Low To High.....	121
87. Decision Tree Applied On Woodworth Site. Color From Blue To Red Indicate Value Or Model Score From Low To High.....	122
88. Mekinock Survey At August 26 2010.....	124
89. Grassland Combinations Of 27 Sample Points. All Points Are Classified Into Three Groups: Mixed Native Grassland, Pure Native Or Forb And Pure Brome Grass Patch.....	125
90. Decision Tree Applied On Mekinock Site. Color From Blue To Red Indicate Value Or Model Score From Low To High.....	128

91. Decision Tree Model Results Distribution Based On Field Survey Points	129
92. Land Cover Proportion Of Three Sites: Oakville Prairie In A Half Section; Woodworth Without The Replanted Area And Mekinock	129

LIST OF TABLES

Table	Page
1. Main Species Appear In Oakville Prairie.....	30
2. Wavelength Ranges Used In This Study.....	39
3. Texture Statistics defined i, j are row and column.....	77
4. Factors Response At Early Growing Season And Later Growing Season.....	103
5. Confusion Matrix of Decision Tree Model.....	127
6. Grassland Condition Distribution of Three Sites: Oakville Prairie in a Half Section; Woodworth Without The Replanted Area And Mekinock.....	127

ACKNOWLEDGEMENTS

I would like to thank Dr. Michael J. Hill for his continuous guidance and encouragement and support. I wish to express my honest appreciation to Dr. Soizik Laguette and Dr. Bradley Rundquist for review and guidance for this work. I would also like to thank Dr. Hojin Kim for assistance on my field measurements. Deepest thankfulness is also due to Earth System Science and Policy (ESSP) for providing me this opportunity. At last, but not the least, I wish to express my love and gratitude to my family and my friends who supported me through the duration of my study.

ABSTRACT

Over the past two decades, non-native species within grassland communities have quickly developed due to human migration and commerce. Invasive species like Smooth Brome grass (*Bromus inermis*) and Kentucky Blue Grass (*Poa pratensis*), seriously threaten conservation of native grasslands. This study aims to discriminate between native grasslands and planted hayfields and conservation areas dominated by introduced grasses using hyperspectral imagery.

Hyperspectral imageries from the Hyperion sensor on EO-1 were acquired in late spring and late summer on 2009 and 2010. Field spectra for widely distributed species as well as smooth brome grass and Kentucky blue grass were collected from the study sites throughout the growing season. Imagery was processed with an unmixing algorithm to estimate fractional cover of green and dry vegetation and bare soil. As the spectrum is significantly different through growing season, spectral libraries for the most common species are then built for both the early growing season and late growing season. After testing multiple methods, the Adaptive Coherence Estimator (ACE) was used for spectral matching analysis between the imagery and spectral libraries. Due in part to spectral similarity among key species, the results of spectral matching analysis were not definitive. Additional indexes, “Level of Dominance” and “Band variance”, were calculated to measure the predominance of spectral signatures in any area. A Texture co-occurrence analysis was also performed on both “Level of Dominance” and “Band variance” indexes

to extract spatial characteristics. The results suggest that compared with disturbed area, native prairie tend to have generally lower “Level of Dominance” and “Band variance” as well as lower spatial dissimilarity.

A final decision tree model was created to predict presence of native or introduced grassland. The model was more effective for identification of Mixed Native Grassland than for grassland dominated by a single species. The discrimination of native and introduced grassland was limited by the similarity of spectral signatures between forb-dominated native grasslands and brome-grass stands. However, saline native grasslands were distinguishable from brome grass.

CHAPTER I

INTRODUCTION

The Central Plains of North America is a large area that was once covered by grassland and savanna. The Great Plains stretches from Alberta south through southern Texas and Mexico, and approximately 1,000 miles from western Indiana westward to the Rocky Mountains (Conner et al., 2002). Eighteen U.S. states have land management responsibilities within the Great Plains, and the Great Plains accounts for approximately 29% of that land area of the U.S. Mexico contains the least amount (4%) of the Great Plains, restricted to 5% of the country's land area. About 16% of the area of the Great Plains lies in Canada and this represents about 5% of the landmass of Canada (Gauthier et al. 1998). Four major grassland regions are generally identified with the Physical Provinces of the Central Plains (Conner et al., 2002):

- 1) short-grass prairies of the Great Plains;
- 2) mixed-grass prairies of the Great Plains;
- 3) tall-grass prairies of the Central Lowlands and Coastal Plains;
- 4) the savannas of the Central Lowlands and Coastal Plains.

North Dakota (ND), at the center of the North America, approximately covers the whole Great Plains physiographic provinces (Fenneman 1931). From west to east in ND, annual precipitation gradually increases, and grassland ecosystems correspondingly shift from Wheatgrass-Needle grass, to Wheatgrass-Bluestem-Needle grass, and, finally,

Bluestem Prairie (Kuchler, 1964).

Native grasslands directly support the livestock industry. Take school trust land as example, there are about 288,945.548 ha in North Dakota and managed by ND State Land Department. Most of that grassland is semi-natural and leased for grazing (Brand et al. 1988). Over 86% of the breeding sheep in the U.S. are located west of the Mississippi River along with numerous domestic goats and horses whose main feed source is derived from grasslands. In South Dakota, as of 1997, approximately 9.7 million ha of non-federal lands were in native rangeland or introduced pasture grasses (grazing lands). But, in the 15 years prior to 1997, South Dakota lost about 0.5 million ha of its non-federal native rangeland (~5.3%), only about 3% of which was transferred to federal ownership. Of that native rangeland loss, about 68% was a conversion to cropland, 46% (255.842 ha) being under cultivation by 1997.

In North Dakota, grassland habitat loss is extensive. The remaining blocks of habitat are highly fragmented by agricultural lands and a relatively dense network of roads. Only a little intact habitat remains in the Northern Tall Grasslands (Ricketts et al. 1999). For example, the Sheyenne Delta Grasslands Reserve, in southeastern North Dakota, stabilized in an area of sand dunes of about 465 km². The Sheyenne Delta has been protected (about 70 percent public owned) but heavily grazed. Agricultural conversion continues to threaten habitats, which include: potato farming in the Sheyenne Delta, mining in the Lake Agassiz beach ridges and dunes, and drainage of moist prairie wetlands throughout (Ricketts et al. 1999).

However, over the past two decades, the number of non-native species within grassland communities increased rapidly due to human migration and commerce

(Hodkinson et al. 1997; Kowarik 2003; Mack et al. 2000; Mooney et al. 1986; Vitousek 1997). Some introduced species, like Smooth Brome grass (*Bromus inermis*) and Kentucky Blue Grass (*Poa pratensis*), seriously threaten native grass and forbs (Whitman & Barker 1994). Relatively undisturbed and pure stands of native grasses are rare now, but it is still important for biodiversity. Invasive species, on the other hand, threaten native species restoration in many ways. For example, due to aggressive rhizome of smooth brome grass, other species are depressed (Sedivec et al. 2011). Besides, invasive plants, like *Bromus* spp, can also modify attributes of soil. For example, invasive modification of soil micro biota can facilitate plant invasive species, and moreover has potential to impede restoration of native communities after removal of an invasive species (Jordan et al. 2008).

There is a need to document the presence of native grasses and the extent to which they are invaded by or replaced by exotic introduced grasses. This is particularly important for the areas that originally supported tall grass prairie, as this is the most converted and threatened of the major prairie grassland associations. In addition, there is a need to know the relative composition of grasslands on a continuum from pristine native stands to completely exotic hayfields and volunteer stands. This is important since insect and bird biodiversity may depend upon the extent to which native prairie species important for pollination and nectar are excluded (Isaacs et al., 2008). Remote sensing may provide a means to develop indicators of relative naturalness using the full spectral coverage available from hyperspectral sensors (He et al. 2011). Hyperspectral imagery further provides a wealth of spectral information which is related biophysical information of plants (Mutanga & Skidmore, 2004; Darvishzadeh & Skidmore, 2008). Based on the

assumption that various biophysical structures of species represent different spectrum characteristics, there is a possibility that the hyperspectral imagery is capable to identify certain species or species combination. This study will focus on discriminating between pure native grasslands and planted hayfields and conservation areas dominated by introduced grasses using hyperspectral imagery acquired at two times during the growing season, and calibrated with spectral libraries acquired in the field.

Thesis Overview: Outline of Thesis Structure and Chapters

The general flow of the research undertaken is demonstrated at Figure 1 as well as the relationship between chapters.

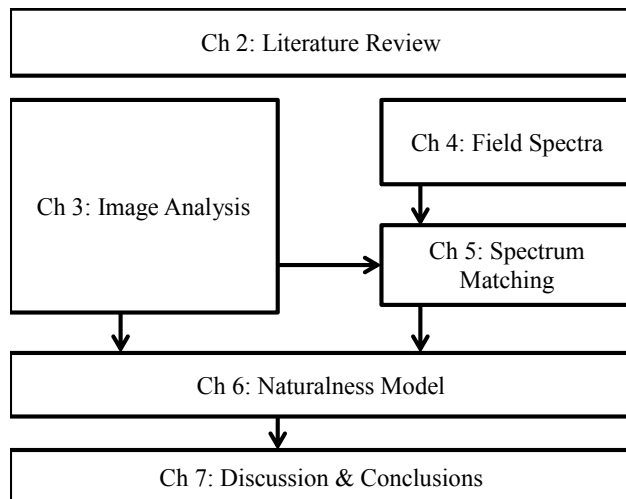


Figure 1 Flow diagram of thesis chapters and relationship to main contents

Chapter 2 provides a review of current remote sensing applications in grasslands with particular focus on the use of hyperspectral imagery. It outlines the ability of hyperspectral imagery for estimation of vegetation properties, explores the current methodology and provides some examples of recent case studies.

Chapter 3 describes the processing of images from the Hyperion hyperspectral sensor on the EO-1 satellite. A detailed process flow is provided to explain how radiance

data are converted to land surface reflectance. It also describes the linear unmixing procedure used to assess proportion of green vegetation, dry litter and bare soil within each pixel which aims to explore different proportion change patterns from native and disturbed area.

Chapter 4 describes the characteristics of the field spectroradiometer and the collection of field measurements for further application. In addition, observations of changes in grassland, spectral signature and fractional cover are presented for a range of grassland patches and types.

Chapter 5 explores the relationship between field measured spectra and remote sensing reflectance extracted from Chapter 3. Due to the change in spectral signatures of species as the growing season progressed, two spectral libraries were built: one for early in the season and one for late in the season. In addition, eight methods of spectral matching are compared and discussed, and the best method is selected. The development of additional measures of spectral variance and dominance and spatial hetero- and homogeneity are also described.

Chapter 6 explores different models for discrimination of native and introduced grasslands at the two study sites, and for early and late growing season. The models from the early and late growing periods are then combined. A final model is tested at an independent conservation area in the Township of Mekeonock where a naturalness assessment of the grassland (including photography) had been carried out.

Finally, in Chapter 7, the overall results are discussed and some conclusions are presented.

CHAPTER II

LITERATURE REVIEW

Prairie Grassland Characteristics

Grassland not only contributes to agricultural production, but also significantly impacts on environmental and societal functions. Increasingly, scientific evidence supports important functions of grassland, especially native grasses, such as conservation of biodiversity, in the regulation of physical and chemical fluxes in ecosystems, and the mitigation of pollution (Gibon, 2005).

Grassland structure also affects biodiversity. Rahmig (2008) examined bird diversity in the Flint Hills of Kansas, and found that bird diversity was higher in native prairie, hayfields and grazed pastures than in CRP fields that were dominated by *Spiza americana*. The U.S. grasslands probably have the most altered biodiversity from human impacts compared to the other terrestrial ecosystems. The ecological status of many existing grassland systems are heavily influenced at the local level by combinations of habitat fragmentation, undesirable habitat changes due to fire exclusion, declining range conditions due to improper grazing management, and loss of habitat values due to the spread of invasive and non-native plants. Further complications come from demographic trends related to changes in land ownership. As a result, many species that live in grassland habitats have declined substantially in the recent past (Conner et al. 2002). The

grasslands of North Dakota are important areas for breeding populations of several endemic grassland birds, like *Ammodramus bairdii* (Conner et al. 2002). This species seems to depend upon large expanses of native prairie with minimal shrub cover (Dechant et al. 2001). During the period from 1966 to 1999, Breeding Bird Survey records indicate that Baird's sparrow experienced one of the most drastic declines of any endemic grassland bird in the U.S.; decreasing at an average rate of 3.4% per year (Conner et al. 2002).

Grasslands provide valuable ecological services such as carbon sequestration from the atmosphere as well as nutrient cycling. For example, Biondini (1998) found that heavy grazing leads to declines in standing dead biomass and biomass nitrogen content. However, he concluded that ecological function can be better sustained under moderate to light grazing. Grassland soils probably lost up to 50% of their original carbon within the first half of the 20th Century as a result of cultivation (Conner et al. 2002). Grasslands are also key components in an efficient hydrologic cycle. The quality and quantity of water runoff and infiltration is dependent upon the quality of ground cover. Converting grasslands to other uses, like cropping, will lead to more serious soil erosion and decreased water quality (Conner et al. 2002).

Biological diversity is an important indicator of the effectiveness of ecosystem in rural areas (Schwab, 2002). However, most grassland has been converted because of human activities, especially in the early 20th Century. The remaining habitat is also highly fragmented. During recent decades, semi-natural grasslands have been more and more protected, and the loss of biodiversity on agricultural land has been an increasing concern (Franzén, 2008). Agricultural intensification, encouraged by market and policy

incentives may lead to biodiversity decline (Questad, 2011). For example market or policy incentives for bioenergy may cause significant conversion from native and semi-natural ecosystems to production fields (Questad, 2011). Soil quality and plant diversity have already been steadily decreasing along with loss of scale-dependent community patch structure due to historical cultivation (Questad, 2011).

Key Features of Grasslands That Could Be Spectrally Discriminatory

Remote sensing provides the capability to rapidly and synoptically monitor large areas. Previous studies have successfully used spectro-radiometer and remotely sensed data to estimate and assess heterogeneous grasslands (e.g., Price et al. 2002, Zhang et al. 2007, Guo et al. 2003, Foster et al. 2009, Guo et al. 2004, Hurst 2006, Chen et al. 2010, Peterson et al. 2002, Zhang et al. 2006, Douglas et al. 2004).

The reflectance spectrum (Figure 2) of vegetation is well-known. Key features in the visible spectrum are the green (550nm) peak and strong chlorophyll absorption at about 700 nm (Figure 3). The sharp rise in reflectance between red and near infrared (NIR) wavelengths is commonly known as the "red edge". Leaf water absorption features occur on the NIR plateau at about 1000 nm and 1200 nm. Then two valleys appear at short-wave infrared (SWIR) because of water absorption. The two peaks in SWIR decrease with wavelength. Based on these reflectance features, numerous indexes have been developed such as the Photochemical Reflectance Index (PRI; Gamon, et al. 1992) and Cellulose Absorption Index (CAI; Daughtry, et al. 1996) to infer physiological conditions of leaves and canopies.

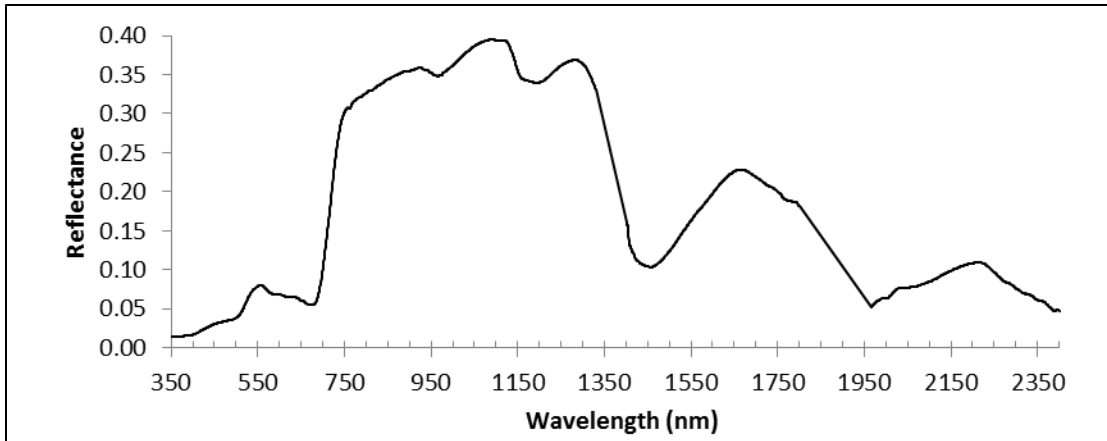


Figure 2 General Spectrum of Vegetation. The reflectance is calculated as average of various species field measurements in Oakville area.

Multispectral Remote Sensing of Grassland and Spectral indices

Normalized Difference Vegetation Index (NDVI) (Deering 1978) is defined as $(NIR - RED) / (NIR + RED)$. It is widely used in vegetation remote sensing, because it amplifies differences between red and NIR channels, which appears as the “red edge” in vegetation spectrum (Figure 3). Besides, NDVI is also correlated with leaf area index (LAI), biomass and other parameters. In addition, due to the normalization of the ratio between red and NIR, NDVI can reduce part of the influence from cloud, shadow, and sun elevation. However, because NDVI represents a non-linear data transform, it is relatively insensitive to low and high vegetation coverage.

The PRI (Gamon, et al. 1992) is defined as normalization between reflectance at 531 nanometer and 570 nanometers. $((R_{531} - R_{570}) / (R_{531} + R_{570}))$, which is sensitive to change in xanthophyll pigments. The xanthophyll, on the other hand, is important in the process of photosynthesis. Hence, it can be used to indicate vegetation health and light-use efficiency (Sabrina et al., 2005).

The Normalized Difference Water Index (NDWI) (Gao, 1996) is defined as $(NIR -$

SWIR)/(NIR+SWIR). SWIR reflectance is sensitive to changes in vegetation water content, while the NIR reflectance is affected by leaf internal structure. The combination of the NIR with the SWIR removes variations induced by leaf internal structure, improving the accuracy in retrieving the vegetation water content (Ceccato et al. 2001).

The CAI, describes the depth of the lignocellulose absorption feature in the shortwave infrared region: $0.5*(R_{2000}+R_{2200})-R_{2100}$, where R_{2000} , R_{2100} , and R_{2200} are reflectance 2000–2050, 2080–2130, and 2190–2240 nm, respectively (Pamela, et al. 2003). This index is helpful in discriminating plant litter from soil (Daughtry, et al. 1996). Pamela (2003) suggests that the CAI of litter was significantly greater than the CAI of soils. Besides, the decay of plant litter over time has a significant effect on reflectance (Pamela, et al. 2003). This index has been used in combination with the NDVI to unmix fractional cover of photosynthetic (PV) and non-photosynthetic vegetation (NPV) and bare soil (BS) in Australian savannas (Guerschmann et al., 2008). Differences in proportion of photosynthetic, non-photosynthetic vegetation and bare soil could be indicators or differences between native and disturbed grasslands in North Dakota, particularly if introduced species had different green-up and senescence characteristics with native species.

Since the vegetation spectral response changes with the seasons, including the effect of soil background, there may be temporal variation in discrimination. For example, Price (2002) compared Landsat Thematic Mapper (TM) bands as well as vegetation indices for discrimination of six grassland types in eastern Kansas between May and September. The research area included both C4 grasses (Big Bluestem – *Andropogon gerardii*; Little Bluestem – *Schizachyrium scoparium*; Indian grass – *Sorghastrum nutans*; and Switch

grass – *Panicum virgatum*) and C3 grasses (Smooth Bromegrass ; Tall Fescue – *Festuca arundinacea*; Kentucky Bluegrass; and Orchard Grass- *Dactylis glomerata*). All grasses were then combined into six types:

- 1) cool season grasslands being managed under the USDA Conservation Reserve Program (CRP)
- 2) cool season grazed
- 3) cool season hayed
- 4) warm season CRP
- 5) warm season grazed
- 6) Warm season hayed.

Price (2002) concluded that in May, reflectance at TM4, 5, 7 (NIR and two SWIR bands) are most distinct among grassland types, while the near infrared band (TM4) is more distinctive in July and September. The author also concluded that compared with raw TM bands, vegetation indices were more helpful during the growing season (May and especially July), but little advantage in time series model. The Green Vegetation Index (GVI) was the most effective index over all seasons (Price 2002).

A large number of studies have been done on the application of broad bands imagery to retrieval of vegetation properties. Various vegetation indexes, that retrieve different properties of plant, have been developed. Some of these indexes provide a guide for potential application of hyperspectral imagery. This study will also test some indexes in order to extract differences between smooth brome grass and various native grasses.

Hyperspectral Remote Sensing of Grassland

Multispectral sensors such as Landsat TM have only 7 bands and provide limited discrimination between grassland types. Hyperspectral imagery, on the other hand, provides a wealth of spectral information which is related biophysical information of plants. There have been numerous studies on the utility of hyperspectral imagery for discrimination of vegetation types and characteristics (e.g. Schaepman et al., 2009). However, less attention has been paid to grasslands than forested systems. Nonetheless, there are many examples of grassland applications, for example, Asner (2002) compared the ability of unmixing vegetation, soil and dry carbon cover in arid regions by using hyperspectral observations and multispectral observations. The wavelength peaks of different grass species was also extracted from derivative spectroscopy of hyperspectral reflectance of grassland vegetation (Yamano, 2003).

Ecosystem Parameters

Since smooth brome grass dominated area is usually lack of biodiversity such as richness and heterogeneity, an estimation of those ecosystem factors would be also helpful. Some studies have explored the potential capability of hyperspectral imagery for estimating the status of ecosystems using metrics that relate to biodiversity. For instance, spectral radiance, reflectance and band ratios from hyperspectral imagery were evaluated as potential indicators of vascular plant species richness in a mesic grassland in Konza Prairie Biological Station in northeastern Kansas (Carter, 2005). The results suggested that the 856 nm and 780 nm reflectance ratio produced highest adjusted coefficients (R^2 approximately equal to 0.4) with richness when both bison-grazed and ungrazed areas were included (Carter, 2005). The author also suggested that the relationship between

species richness and species spectral features is affected by soil exposure (Carter, 2005).

In 2007, Zhang investigated the northern Mixed Native Grassland biological heterogeneity at Grasslands National Park (GNP), Canada, using ground level hyperspectral imagery, biological data like leaf area index, biomass, and vegetation cover) and environmental data including soil moisture, organic content, and bulk density(Zhang, C. 2007). The result showed that indices extracted from ground level remote sensing data is capable to explain about 40% to 60% of biological variation (Zhang, C. 2007).

Lucas (2008) used the HyMap airborne imaging spectrometer to examine plant species richness for several habitat-types on Horn Island, Mississippi, northern Gulf of Mexico. The HyMap image system contains 126 bands, which cover the 450-2500nm spectrum (Lucas, 2008). The author suggested that no index extracted from HyMap imagery could be related to species richness when all habitat-types were considered, however a number of indices showed significant relationships and reflectance for individual habitat types (Lucas, 2008). For example, the result showed that the reflectance ratio between 1056 nm and 966 nm and the ratio between 920 nm and 834nm were negatively related with species richness in meadows and transition zones. This indicated that richness of habitat declined when soil exposure increased. In marsh habitat, species richness was positive related with reflectance ratio between 618 nm and 2475 nm and the ratio between 514 nm and 2459 nm, mainly due to increasing broadleaved vegetation patches (Lucas, 2008).

Biophysical Grassland Parameters

In this section, a hyperspectral remote sensing application on biophysical grassland parameters like nitrogen content, leaf area index (LAI) is reviewed. Since brome grass grows early than most of native species, brome grass dominated area may show different biophysical properties from native grassland in the early of growing season. Since the shape of a plant spectrum contains information on the biophysical properties of plants, a growing number of studies focus on spectral inversion. Mutanga and Skidmore (2004) used high spectral resolution reflectance to discriminate differences in nitrogen concentration in an African savanna rangeland. The continuum removal was first used to extract absorption features and reduce dimensionality in the data (Mutanga & Skidmore, 2004). Then a neural network algorithm was used for nitrogen concentration mapping (Mutanga & Skidmore, 2004). This approach explained 60% of the nitrogen concentration variation in savanna grassland, which was better than standard multiple linear regression techniques (Mutanga & Skidmore, 2004).

Rahman and Gamon (2004) examined the utility of hyperspectral remote sensing to map vegetation types, including identifying riparian forests, burnt grasslands and resurgence zones, crops and several types of savannah and pastures in southern California. They found that, compared with the previously commonly used NDVI, the water band index (WBI), was a better indicator of important biophysical properties, like fresh and dry biomass and water content, in semi-arid ecosystem, especially after regeneration (Rahman & Gamon, 2004).

Gianelle and Guastella (2007) applied hyperspectral, multi-angular approaches as well as broad bands (Landsat bands) in order to estimate biophysical grassland

parameters such as biomass, total and percent nitrogen content, phytomass (leaf) and its total and percent nitrogen content. Although they found no significant difference between off-nadir and nadir data in predicting biophysical variables, but both measurements were better than broad bands indices (Gianelle&Guastella2007).

Darvishzadeh and Skidmore (2008) successfully mapped to LAI, leaf chlorophyll content (LCC) and canopy chlorophyll content (CCC) in a heterogeneous Mediterranean grassland based on radioactive transfer model of canopy spectral reflectance measurements (Darvishzadeh & Skidmore, 2008). Darvishzadeh and Skidmore (2008) concluded that, compared with univariate methods such as vegetation indices, multivariate techniques such as partial least squares regression is more helpful in the process of mapping.

Cho and Skidmore (2009) simulated commonly used vegetation indexes such as NDVI, the modified soil adjusted vegetation index (MSAVI), the soil adjusted and atmospherically resistant vegetation index (SARVI) and the NDWI from HyMap imagery. The simulated results were then used to retrieve grass/herb biomass production on a yearly basis in the Majella National Park, Italy (Cho& Skidmore, 2009). Based on the linear regression analysis, authors found that indexes like MSAVI, SARVI and NDWI are more stable along year's prediction compared with NDVI.

Chen and Gu (2009) examined the utility of the spectral features on estimating aboveground green biomass by using partial least squares (PLS) regression between above ground green biomass and original reflectance, first-order derivative reflectance (FDR), as well as band-depth indices. The NIR region bands and red-edge bands were

effective in estimating high-cover meadow biomass and the band-depth indices improved the estimation accuracy (RMSE = 40.2 g m⁻²) (Chen & Gu, 2009).

A variety of vegetation indexes had been successfully migrated from broad band remote sensing and diversified for hyperspectral imagery. A number of techniques have been developed, like first-order derivative reflectance and band-depth measurements from continuum removal in order to utilize spectral absorption features in image spectra. These techniques have enabled retrieval of different biophysical information from grassland. These approaches may help to indicate differences between introduced and native grassland. Thus a range of these vegetation indexes and a range of techniques will be applied in this study.

Species Discrimination - Case Studies

Since there are distinct biophysical differences among species, hyperspectral imagery also has the potential to discriminate between individual species. For example, Underwood et al. (2003) were able to discriminate between ice plant (*Carpobrotus edulis*) and jubata grass (*Cortaderia jubata*) in California's coastal habitat. Three methods, including minimum noise fraction (MNF), continuum removal, and band ratio indices, were used in order to reduce data dimension and then a maximum likelihood supervised classification was performed (Underwood et al., 2003). Based on field validation, author found that all methods showed high accuracy (about 97%) for determine presence or absence of iceplant (Underwood et al., 2003). However, when classes were divided into pristine area, and areas with iceplant coverage between 51%-75%, 76%-90% and 91%-100%, only the MNF showed relatively high estimating accuracy (55%) (Underwood et al., 2003). In later work (Underwood et al., 2007); the

author detected three invasive species: iceplant, jubata grass, and blue gum (*Eucalyptus globulus*) at Vandenberg Air Force Base, California, using AVIRIS imagery (174 wavebands, 4m spatial resolution). The authors first divided the research area into six vegetation classes: intact coastal scrub, iceplant invaded coastal scrub, iceplant invaded chaparral, jubata grass invaded chaparral, blue gum invaded chaparral, and intact chaparral. A maximum likelihood supervised classification was performed based on field survey and the result showed a 75% overall accuracy across all classes. Imagery spatially degraded to Hyperion resolution (174 bands, 30m) was also subjected to the same classification procedure. In this case accuracy was reduced to 58%. The limitation of the two projects, as authors suggested, mainly came from a mismatch between field-measured training data and image registration (Underwood et al., 2007). On the other hand, this research also suggested that a spatially degraded image has lower capability to detect invasive species as more species variation may be contained in one pixel in the lower spatial resolution image (Underwood et al., 2007).

Andrew and Ustin (2008) applied a series of approaches including: aggregated classification, spectral physiological indexes, regression tree models and mixture tuned matched filtering (MTMF) to detect invasive *Lepidium latifolium* (perennial pepperweed) at California's San Francisco Bay. Three sites were tested in the research: least diverse site, several co-occurring species with enough spectral variability; least spectral variability site (Andrew & Ustin, 2008). The authors found that the identification accuracy was significantly affected by site complexity (Andrew & Ustin, 2008). For example the detecting accuracy is about 90% at first two sites, but failed at the last one (Andrew & Ustin, 2008). As the author suggested, the identification accuracy is limited

by site complexity represented by species, structural, and landscape diversity, and the consequent spectral variability (Andrew & Ustin, 2008). This is because with the increasing to site complexity, the certain invasive species is more and more spectrally distinctive from others and others' combination (Andrew & Ustin, 2008).

The invasive weed yellow star thistle (*Centaurea solstitialis*) at the western edge of California's Central Valley grassland was detected from Compact Airborne Spectrographic Imager 2 (CASI - 2) hyperspectral imagery by using linear spectral mixture models (LSMM)(Miao et al., 2006). The research area was first divided into six endmembers: live yellow star thistle; dead star thistle; riparian vegetation; Oak; burn scar and background (Miao et al., 2006). Four LSMMs, from unconstrained to fully constrained, were then performed. The author concluded that all models, except unconstrained LSMMs, showed consistent results (Miao et al., 2006).

Yang et al. (2009) mapped Ashe juniper distribution from mixed woody, herbaceous species and other land cover types like bare soil and water in airborne hyperspectral imagery. Four supervised classification methods: minimum distance, Mahalanobis distance, maximum likelihood and spectral angle mapper (SAM) was applied on the first 10 and 20 MNF bands (Yang et al. 2009). Based on the authors' analysis, classification accuracy varied around 90% and the first 10 MNF bands were sufficient of discrimination.

This section reviews previous studies of using hyperspectral imagery to identify invasive species. Plenty of approaches had been developed, such as SAM and LSMM, and those approaches will also be test in this study. However, previous work suggest that the spatial resolution and low SNR of Hyperion imagery may have reduced identification

accuracy for grassland types compared with analysis undertaken with airborne hyperspectral data. Therefore, it may be important to develop additional measures of spectral variability and spatial variability to assist direct spectral matching techniques.

Spectral Identification Techniques

Over many years of research with airborne and space borne hyperspectral sensors, a wide range of techniques have been developed for processing hyperspectral data to distinguish between species, including linear regression, MNF and various supervised classification methods.

The MNF transformation is a commonly used method for reducing the dimensionality of hyperspectral data, especially in species discrimination. The MNF transformation is essentially a two phase principal components analysis that rescales noise and reduces data dimensionality for subsequent analyses. Rotated or transformed data, such as MNF or PCA, is characterized by high data variance in the first few bands then decrease in later bands, and the last bands are usually dominated by noise (Mundt et al., 2005). So it is also commonly used to smooth spectrum by removing the last of the noise-dominated bands and re-process MNF inversion to create a clean data stack with reduced dimensions. For example, Mundt (2005) used MNF to smooth hyperspectral data first, and then the SAM (Spectral Angle Mapper) algorithm was used to discriminate hoary cress. Addinck et al. (2007) also used a MNF product as input to estimate biomass and leaf area index (LAI).

Linear Spectral Unmixing, such as Singular Value Decomposition (SVD), is a group of classical techniques, which assumes that the reflectance spectrum of pixel is a linear

combination of the spectra of all objects inside the pixel where the coefficients are the area proportion of objects. In order to solve the linear equations for the unknown pixel fractions, objects must be less than the number of spectral bands.

Various supervised classification methods have been used in species detection. For example the SAM (Yuhas et al., 1992) computes a spectral angle between each pixel spectrum and each target spectrum. The spectral angle shows similarity between pixel and targets, the smaller the angle, the greater the similarity. This spectral angle can ignore influence of pixel illumination caused by system error, because increasing or decreasing illumination only affects its magnitude instead of its direction. Supervised classification is limited by its efficiency (Underwood et al., 2007), but classification algorithms may be helpful in this study and will be tested in the process of spectrum discrimination.

On the basis of the case studies examined above, the accuracy of species discrimination largely depends upon the spectral complexity of the research area (Andrew & Ustin, 2008) as well as spectral and spatial resolution of the sensor (Underwood et al., 2007). Based on the Hyperion spatial resolution of 30 m, and the variety of species combinations occurring especially on the native grassland, it is likely that additional surface characteristics will be needed in order to assess the naturalness of these grasslands. Thus, it will be necessary to utilize spectral processing methods to identify spectral features that are sensitive to biophysical properties. Techniques like continuum removal may be used to estimate biophysical properties of grassland, and various narrow band vegetation indexes may also be used to capture spectral features. Continuum removal standardizes reflectance spectra to allow for comparison of absorption features (Underwood et al., 2003). Continuum removal of the water absorption bands is assumed

to be particularly sensitive to the fleshy succulent leaves (Underwood et al., 2003). The process involves spectrally subsetting images to known spectral regions with key absorption bands. In this research, the absorption bands defined by Thulin (2009) were used: 408-518nm, 588-750nm, 1116-1284nm, 1652-1770nm, 2006-2196nm and 2222-2378nm. Water absorption can be estimated using area or depth of absorption regions.

Other Potentially Important Grassland Properties

Beside techniques for species discrimination, other factors like patch structure, soil effects on species composition, and the spatial structure of the landscape may also be helpful in characterizing the grassland. For example, smooth brome grass is less compatible with other species because of its rhizomatous crown structure and aggressive spread and (Sedivec et al. 2009). Therefore, it might be expected that a disturbed area dominated by smooth brome grass, would exhibit less spectral variance and more spatial homogeneity than more diverse natural areas. Another potential discriminatory characteristic of smooth brome grass as a cool season grass is the tendency to initiate growth earlier than most of native grasses. However, later in the growing season, most smooth brome grass may have a mixture of seed heads and green leaves, while many cool season native grasses are predominantly covered in seed heads. These phenological differences in growth and flowering behavior between native grasses and smooth brome grass may be very critical for discrimination between grassland types both early and late in the growing season.

Summary

The review of research methods shows that there are a number of approaches that may be used ranging from empirical to analytical. However, the likelihood of there being

one single method that is better performing in all circumstances is low, which provides a solid and positive platform to combine different methods for research into using hyperspectral data to estimate naturalness of grassland. Therefore, the following analytical process was adopted (Figure 3).

First **Hyperion images were acquired from 2009 to 2010**. As mentioned above, sampling in both early and later growing season periods was considered to be very important. Field spectra for relatively abundant grasses and forbs as well as smooth brome grass and Kentucky blue grass at were then collected throughout the growing seasons in in 2010 and 2011. Field measurements were collected each month from early May to late August in order to capture spectrum changes of species in the whole growing season.

Level 1R Hyperion images were processed and corrected. Field spectra were also corrected and imported into spectral libraries. Independent spectral libraries were created for early and late growing season data.

In order to capture any differences in the overall proportions of photosynthetic and non-photosynthetic surfaces between native and introduced grasslands, **fractional cover of non-photosynthetic vegetation (NPV; litter), photosynthetic vegetation (PV) and bare soil (BS)** was estimated using published methods. Differences in fractional cover may also indicate disturbance. The fractional cover is estimated by using NDVI and CAI (Guerschman et al., 2009).

In order to detect individual species, and mixtures of species at sub pixel level, **spectral matching** techniques were examined, and a total of eight target detecting

algorithms were tested. Based on assessment of matching results in relation to the field survey of patch distribution and their structure, the **Adaptive Coherence Estimator (ACE)** was finally selected.

In order to capture any spatial characteristics that could help in grassland discrimination, **Texture co-occurrence analysis** was applied to the match images from the ACE analysis. Textural differences were hypothesized to be potential source of discrimination between native grassland, with various species and patches, and areas dominated by smooth brome grasses.

Finally, **a number of multi-criteria naturalness models were developed in the Multi-Criteria Analysis Shell for Spatial decision support (MCAS-S)**. These were assessed for effectiveness and then combined to form a final model. This model was tested at an independent location. Three types of data were used in the final modeling: fractional cover maps; spectral matching results and measures of variance and dominance of spectral match; and textural measures of spatial patterns. Since texture analysis was applied to the spectral matching maps, the final result of the modeling was still highly dependent on the quality of the spectral match.

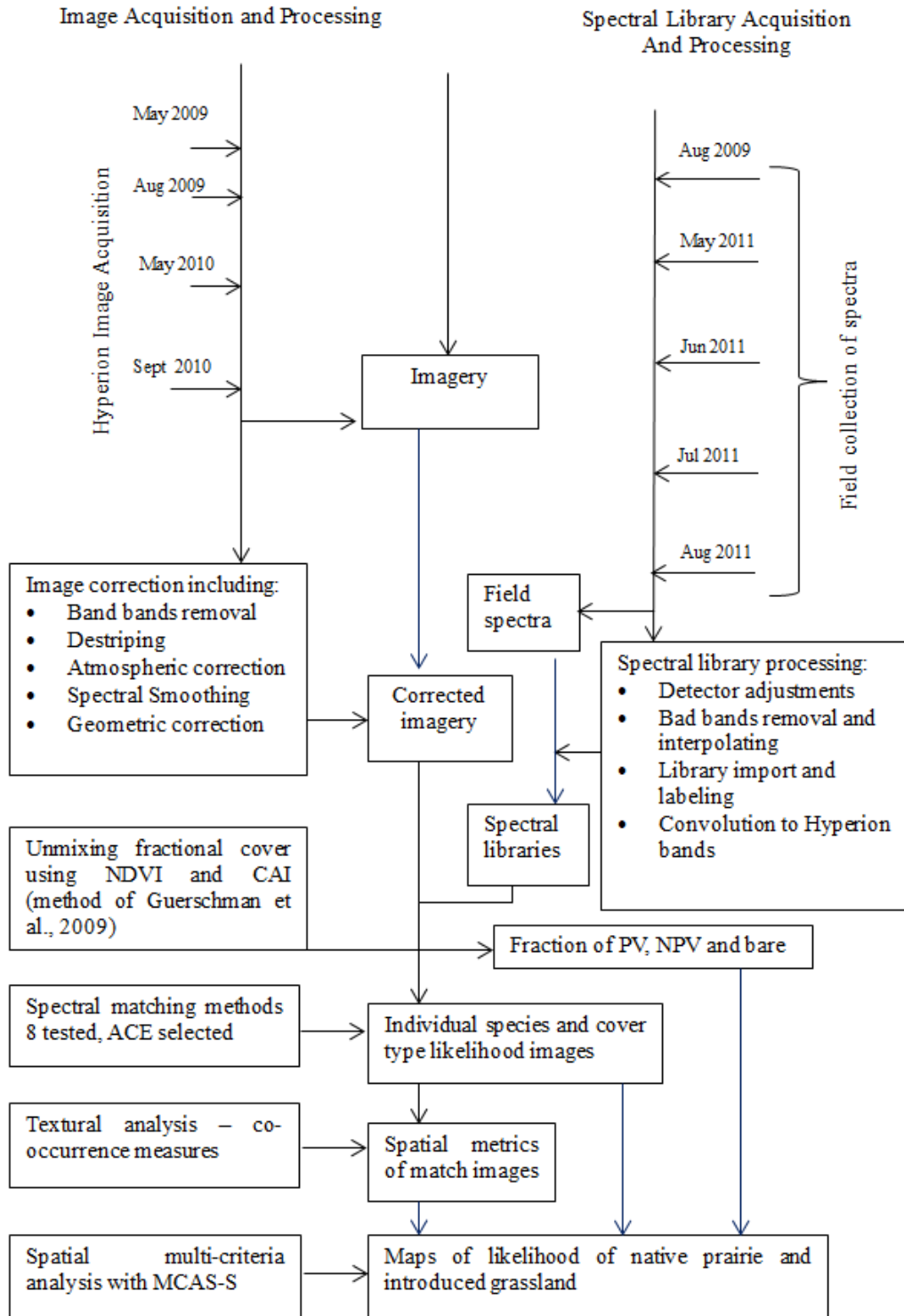


Figure 3 Flow diagram of the analytical process

CHAPTER III

IMAGE PROCESSING

Introduction

In this chapter, firstly, the study areas including Oakville, Woodworth and Mekinock are described. Secondly, the characteristics of the Hyperion Sensor and the companion ALI imager are described. Thirdly, the steps involved in processing the Hyperion images are documented. As this research focuses only on the grassland, other land cover types are then identified, classified and masked from subsequent image analysis. Finally, this chapter also describes the calculation of fractional cover of PV, NPV and BS (Guerschman et al., 2009).

Sites

This research was concentrated on three sites: Oakville Prairie near Emerado and, Mekinock Water Fowl Production Area near Grand Forks Airbase (both in Grand Forks County), and Woodworth Waterfowl Production Area near Carrington in Stutsman County (Figure4).

Oakville Prairie is located 19km west of Grand Forks, North Dakota ($97^{\circ} 19'W$, $47^{\circ} 55'N$) in Oakville township (Redmann, 1972). Mekinock is ($97.363W$, $48.013N$) close to Oakville Prairie, and they both are located in the Red River Valley. The Red River Valley in North Dakota is a broad plain which slopes gradually to the northeast (Redmann,

1972). The beach ridges which were formed on the western shore of Glacial Lake Agassiz are the most prominent topographic features in the Oakville Prairie area (Redmann,1972). The flat topography with poor surface and internal drainage results in a high water table (Redmann, 1972). At Oakville Prairie (Figure 5) the most saline areas are the "alkali- or salt-flats" which have a high and fluctuating water table (Redmann,1972). A wide variety of prairie grasses and forbs (Table 1) are supported by the soil complex in Oakville Prairie and about 236 species have been recorded from the site (Kannowski, 1988). Thus, Oakville is a site that represents undisturbed native prairie on saline and wet land; aside from *Spartinia pectinata*, the site is too wet to support the other major tall grasses. Mekinock (Figure 6), on the other hand, has some introduced species and many areas are dominated by *Typha* spp. As such it provides a good test of any naturalness model since it should indicate both native and introduced components.

Woodworth (Figure 7) is located in the Missouri Coteau Physiographic region, which is a large stagnation moraine, formed of low-permeability glacial till (Mushet, 2004). The topography is very hummocky with most of the depressions containing wetlands (Mushet, 2004). The Woodworth Chase Lake Wildlife Refuge (http://www.fws.gov/arrowwood/chaselake_nwr/) established in 1908, is significantly more disturbed (non-natural) than the recently restored prairie grassland (National Ecological Observatory Network site). Thus Woodworth is used to represent stands of well-established smooth brome grass in this research.

Woodworth contains one of the core sites for the National Ecological Observatory Network (NEON). In early June 2009 this site was planted with a 22 species mix. Seven native mixed grass prairie species as follows: Western Wheat grass *Agropyron smithii*,

Green Needle *Stipa viridula*, Little Bluestem *Schizachyrium scoparium*, Blue Grama *Bouteloua gracilis*, Big Bluestem *Andropogon gerardii*, Sideoats grama *Bouteloua curtipendula*, and Prairie June grass *Koeleria macrantha*. Fifteen native forbs: *Achillea millefolium* (White Yarrow), *Astragalus crassicaarpus* (Ground Plum milkvetch), *Coreopsis tinctoria* (Plains coreopsis), *Echinaca epurpurea* (Purple Coneflower), *Gaillardia aristata* (Blanket flower), *Helianthus maximiliani* (Maximillian Sunflower), *Liatris pycnostachya* (Prairie Blazing Star), *Linum lewisii* (Blue flax), *Oerotherabiennis* (Evening Primrose), *Petalostemum candidum* (White Prairie Clover), *Petalostemum purpureum* (Purple Prairie Clover), *Ratibida pinnata* (Yellow Coneflower), *Rudbeckia hirta* (Black-eyed Susan), *Verbena stricta* (Hoary Vervain) and *Amorpha canescens* (Leadplant).

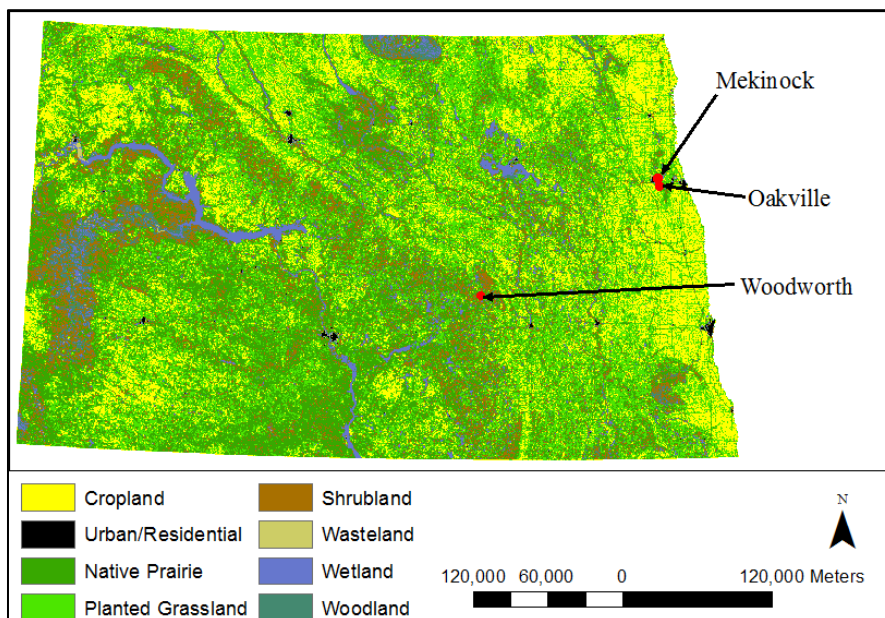


Figure 4. Locations of three sites in North Dakota. The background is North Dakota GAP analysis map (Strong et al., 2005)

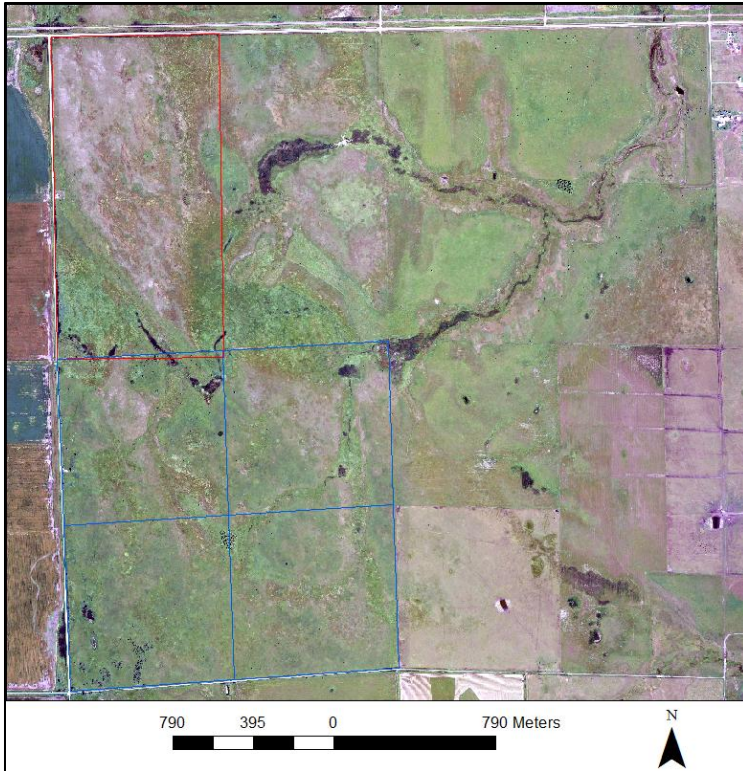


Figure 5 Oakville Site. Background is NAIP map; the red box shows the boundary of Oakville Prairie and the blue box is School Trust land

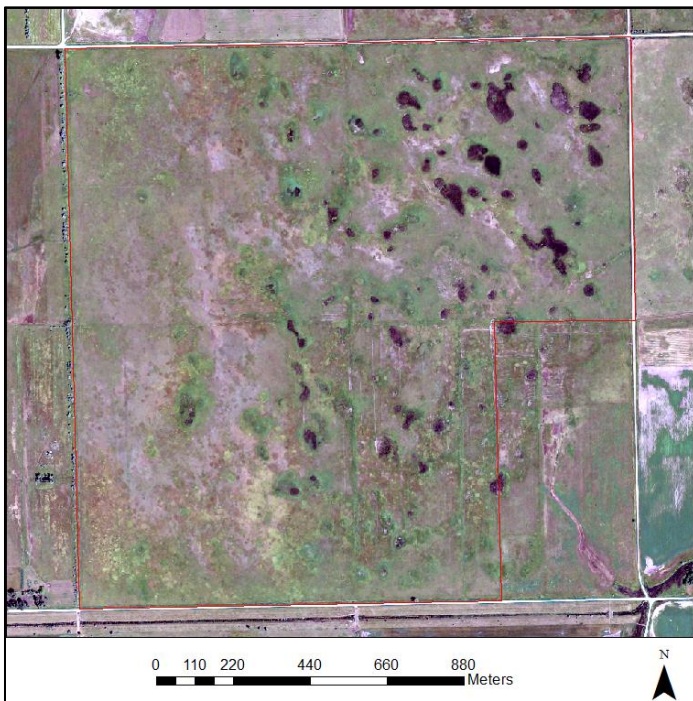


Figure 6 Mekinock Site within the red boundary

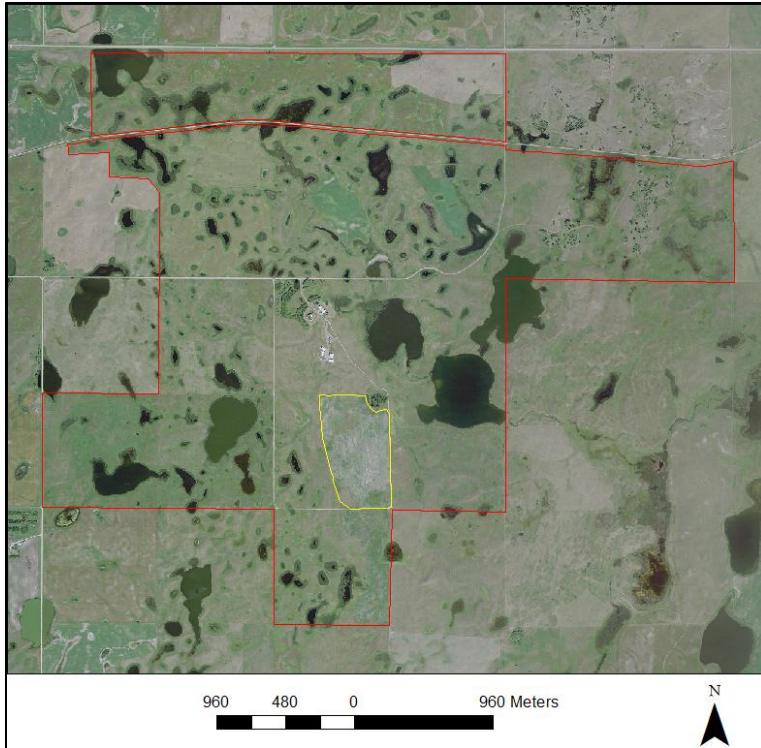


Figure 7 Woodworth Site in the red boundary. The yellow boundary suggests the restored area.

Table 1. Main Species Found At Oakville Prairie

Name	Scientific Name
June grass	Koeleria macrantha
Maximilian sunflower	Helianthus maximilianii
Goldenrod	Solidago virgaurea
Prairie cord grass	Spartinia pectinata
Wheat grass	Agropyron specie
Canada wildrye	Elymus canadiensis
Hairy aster	Aster pilosis
Prairie dandelion	Agoseriscuspidata
Hairy aster	Aster pilosis
Prairie brome	Bromus calmanii
Bluegrass	Poa pratensis L.
Indiangrass	Sorghastrum nutans
Smooth Brome	Bromus inermis Leyss
Little blue stem	Schizachyrium scoparium
Big blue stem	Andropogon gerardii
Switchgrass	Panicum virgatum
Sweet Clover	Melilotus
SlimstemReedgrass	Calamagrostis stricta

Hyperion Sensor

The Hyperion sensor provides hyperspectral imagery with a 30 meter spatial resolution in 220 spectral bands (10nm spectral resolution from 0.4 to 2.5 μm). The images cover 7.5 km swath width and either full (225 km) or quarter (~ 60 km) swath lengths at nadir or near nadir look angles within a Landsat path and row framework. The data provide detailed spectral mapping across from 400 to 2500nm with high radiometric accuracy. Because of the recent development in image spectroscopy, hyperion has been widely used to extract various terrestrial features (Mutanga et al. 2009). For example, Dadon et al. (2011) used hyperion imageries to map stratigraphic and lithologic in the Dana Geology National Park, Jordan. A supervised classification was used in the research and the overall accuracy was 57% for stratigraphic and 79% for lithologic (Dadon et al. 2011). Petropoulos et al. (2011) produced land use/cover map by using hyperion image. He et al. (2011) compared utility of various hyperspectral data for tracking invasive species and concluded that the hyperspectral remote sensing had great potential for invasion research.

Another sensor carried on the same satellite is multispectral Advanced Land Imager (ALI). The ALI supports a continuous $15^\circ \times 1.625^\circ$ field of view with 10 bands (Bicknell et al., 1999). It provides 7 visible and near infrared (VNIR) band and 3 short wave infrared (SWIR) bands (Lencioni et al., 1999). The panchromatic within sensor support 10 meter resolution and multispectral detector support 30 meters resolution (Bicknell et al., 1999). The ALI data is used in this research as geo-registration base map.

Data Processing

Hyperion data processing workshop is provided by CSIRO Earth Observation

Center (Datt&Jupp, 2004; Datt et al. 2003; Jupp et al. 2002; Apan& Held, 2002). Processing steps and their descriptions are listed as follows (Figure 8):

Bad Pixel Fix: In push-broom sensors such as Hyperion, detectors that failed to response signals will leave vertical stripes or ‘streaks’ in an image band. The aim of this process is detecting and replacing those vertical stripes or ‘streaks’ with averages of data from adjacent pixels. This procedure is provided by ENVI-CSIRO workshop.

Re-calibration of Hyperion Data: Re-calibration of the Level 1B1 data convert each band into a uniform calibration gain for later processing, and also provides better interpretation of radiance spectra. Bad bands including 1-7, 58-76, and 225-242 were set to zero. This procedure is provided by ENVI-CSIRO workshop.

De_Smile: The processing aims to correct distortion in the spectral dimension so that DN value across the spatial dimension is comparable within each band. This procedure is provided by ENVI-CSIRO workshop.

Column Stats De-streak: The process aims to remove pixel streaks or vertical stripes from images. This research only uses Global de-streaking method, which uses the whole image mean and standard deviation for each band as the reference values to correct columns within the band. This procedure is provided by ENVI-CSIRO workshop.

Atmosphere Correction: Atmosphere correction aims to convert the DN value of remotely sensed imagery into surface reflectance. ACRON MODE 1.5 is used in this process.

Smooth: The MNF transformation is first used to smooth both visible-NIR and short

wave infrared (SWIR) data separately. The MNF transformation first rotated and decorrelated data. The transformed data associated with eigenvalues which indicated amount of information within each layer. Then only first few images with large eigenvalues are converted back. The two sets of smoothed data are then combined. At last the data set is smoothed again in the workshop, which calculates run

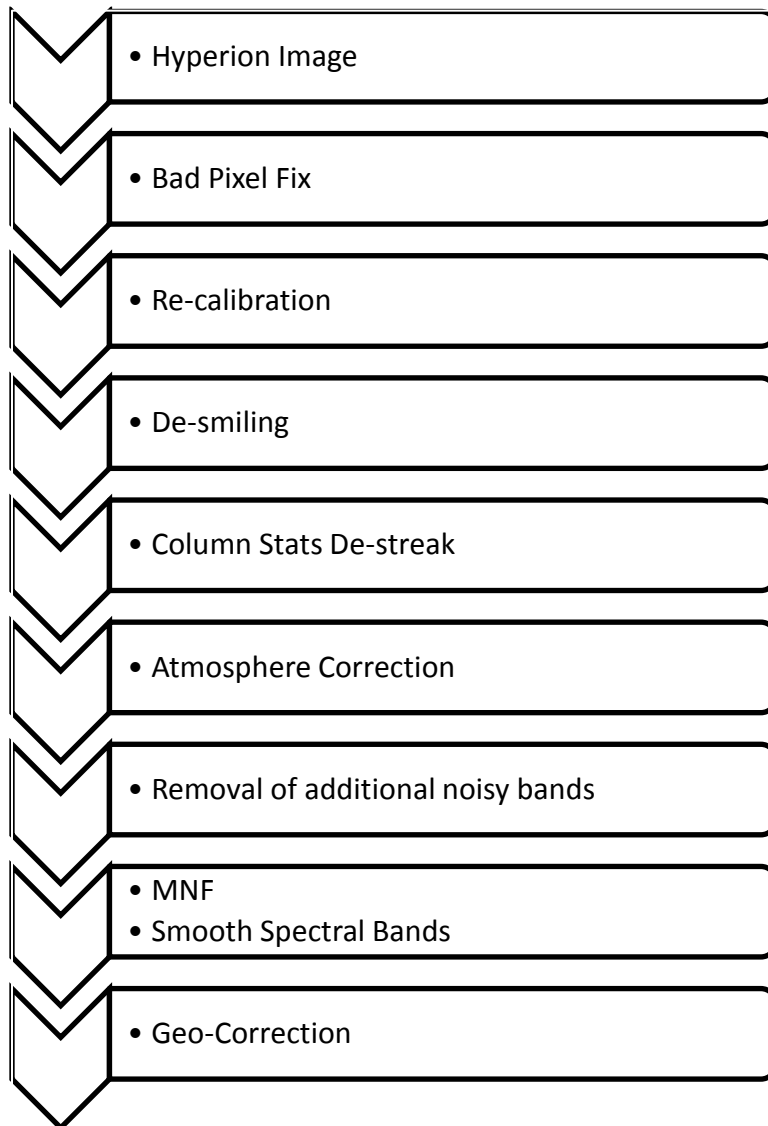


Figure 8 Process Step for Hyperion Data

mean for each pixel in spectral dimension. The last smooth step is performed in

ENVI-CSIRO workshop.

Geo-correction: Finally, Hyperion data is geo-corrected based on ALI geo-corrected data, which is radiometrically corrected and resampled for geometric correction and registered to a geographic map projection. This procedure is provided by ENVI Registration module.

Figure 9 suggests the processing results on Oakville and Woodworth sites. The imagery covers research area from early growing season (May) to later growing season (September). Typical vegetation spectrum within each image is also showed. Spectrum characteristics are well conserved within visible wavelength, while many SWIR bands are removed because of water absorption effects.

Grassland Classification and Mask

To focus on grassland, hyperion imageries are further classified based on National Land Cover Data (2009) and all other land cover type are masked.

National Land Cover Data is provided by The U.S. Department of Agriculture, Service Center Agencies in terms of 30m resolution and UTM NAD83 projection (Homer et al. 2007). The land cover map is generated from multi-season Landsat5 and Landsat 7 imagery as well as DEM and other ancillary data (Homer et al. 2007).

Each Hyperion image is classified separately by using support vector machine (SVM) method. Most common land cover types (water body, grassland, soybeans, corn, spring wheat, etc) within each image were included. Then mask files were created to extract grassland. As results show (Figure 10), most of grasslands were well extracted. But some roads were also included in the mask file, especially in early growing season,

which is because the road's spectrum is close to bare soil. On the other hand, masks for the same region vary in different of time. Part of the reason is that land cover types change along growing season. For example, some area might be covered by water at early growing season, and then dried out and covered by grasses later. Another reason is that grassland spectrum varies a lot and some pixels might be misclassified into bare soil or crop land.

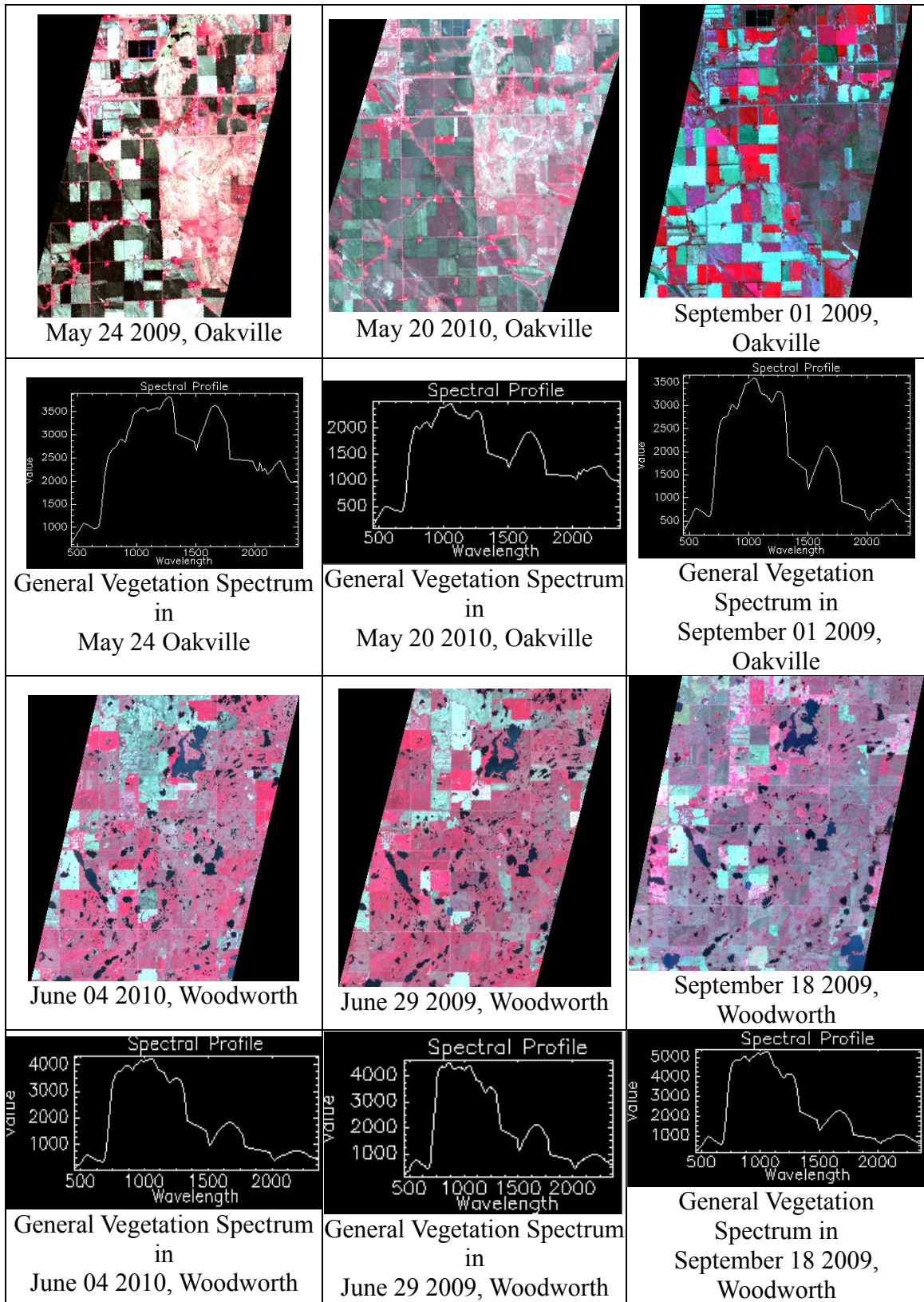


Figure 9. Results for Hyperion data

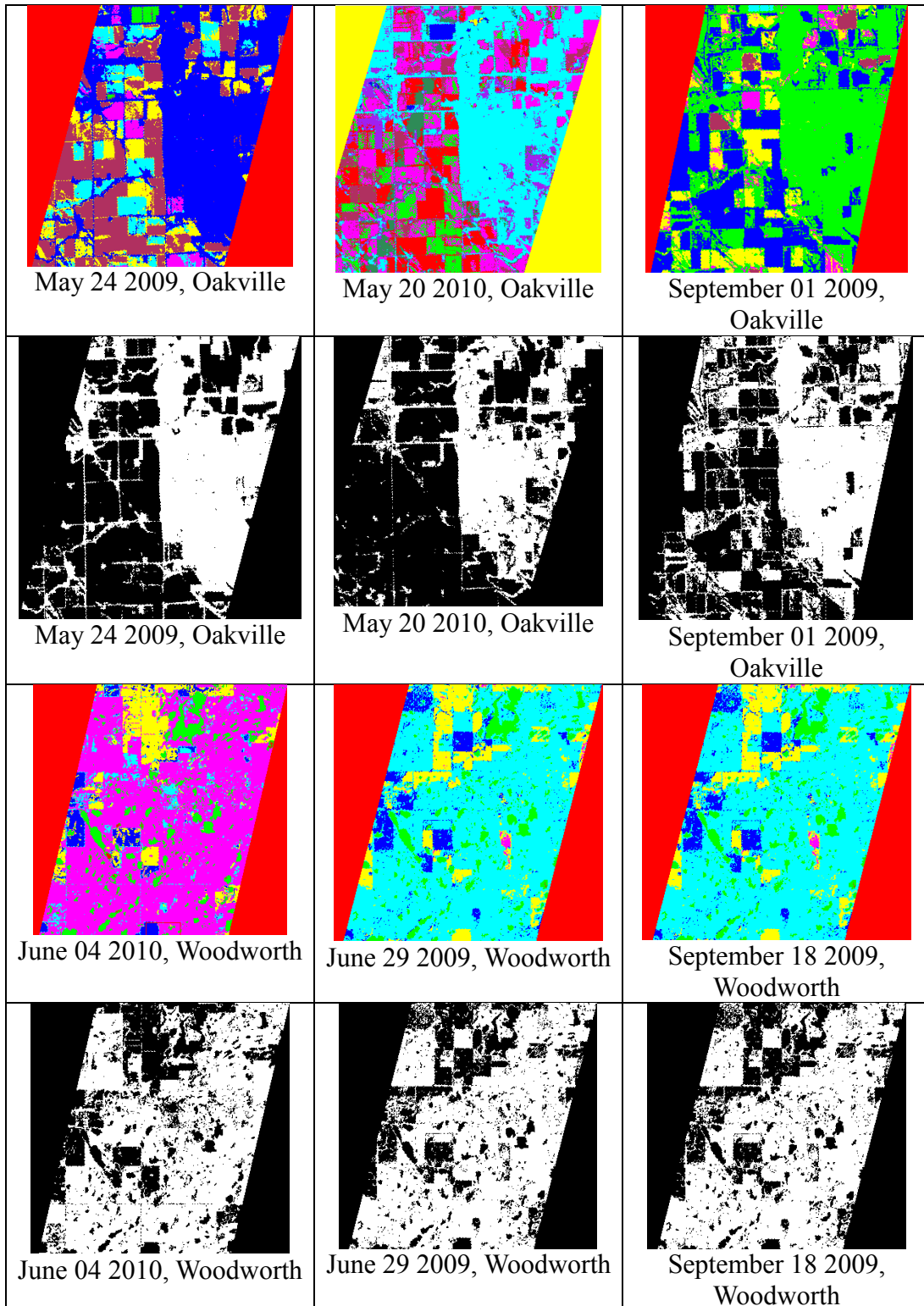


Figure 10 Hyperion image classification map and mask result (the black means remove and the white part means grassland and will be maintained)

Image Analysis: Fractional Cover

Linear Unmixing under NDVI and CAI space

This section will use NDVI and CAI to estimate fractional cover of green (photosynthetic vegetation – PV), dry (Non-photosynthetic vegetation – NPV) and bare soil (BS) using linear unmixing (Guerschman et al., 2009).

NDVI is defined as $(\text{NIR}-\text{RED}) / (\text{NIR}+\text{RED})$. It is widely used in vegetation remote sensing, because it amplifies differences between red and NIR channels, which appears as the “red edge” in vegetation spectrum (Deering 1978).

The CAI describes the depth of the lignocellulose absorption feature in the shortwave infrared region about 2000 nm. The index is calculated by:

$$\text{CAI} = 0.5 * (\text{R}2000 + \text{R}2200) - \text{R}2100 \quad (1)$$

Where R2000, R2100, and R2200 are reflectance 2000–2050, 2080–2130, and 2190–2240 nm, respectively (Pamela, et al. 2003). This index could be used to discriminate plant litter from bare soil (Daughtry, et al. 1996).

The method has been used by Daughtry in 2004 and 2006 to assess crop residue cover and soil tillage intensity. Guerschman (2009) also uses NDVI and CAI, derived from Hyperion and MODIS sensors, to estimating fractional cover of dry grass, green grass and bare soil in the Australian tropical savanna region.

This method will be used in this research to estimate fractional cover in these grasslands. As indicated at the end of Chapter 2, it is hypothesized that differences in fractional cover of PV and NPV at different times during the growing season could help

discriminate between native and introduced grasslands.

Wavelength ranges of NIR, RED, R2000, R2100 and R2200 are given in the following table (Table 2):

Table 2. Wavelength ranges used in this study

	Hyperion Wavelength (nm)	Bands Number
RED	681.198	24
NIR	803.302	36
R2000	1991.958	117
R2100	2102.9419	126
R2200	2203.8279	136

There are several assumptions are made in this research:

- a) In any canopy, fractions of green vegetation, dry vegetation and bare soil can be solved by using the complementary indices NDVI and CAI (Daughtry, et al. 2006).
- b) Pure green vegetation, dry vegetation and bare soil pixels can be found in imagery.

Then the proportions of each land cover for single pixel were found by solving equations 2:

$$\begin{cases} V_H = \sum [f_i V_i] = [f_G V_G + f_D V_D + f_S V_S] \\ C_H = \sum [f_i C_i] = [f_G C_G + f_D C_D + f_S C_S] \\ \sum f_i = [f_G + f_D + f_S] = 1 \end{cases} \quad (2)$$

Where V_H and C_H are NDVI and CAI value of single pixel and $C_G/V_G, C_D/V_D, C_S/V_S$ are NDVI/CAI values of green grass, dry grass and soil, respectively. f_G, f_D, f_S are proportions of each land covers.

The NDVI/CAI values of green grass, dry grass and soil are extracted from imagery. Based on (Guerschman et al. 2009) the three endmembers forms a triangle in a CAI

versus NDVI scatter plot (Figure 11), because green grass has a high NDVI and moderate CAI; dry grass have a high CAI but low NDVI; soil has low values for both indexes. Thus scatter plot is first made for wide agriculture and grass land area, and then three corners are extracted and assigned into three endmembers. Finally, proportion of three land cover types is calculated using “linear spectral unmixing” function in ENVI.

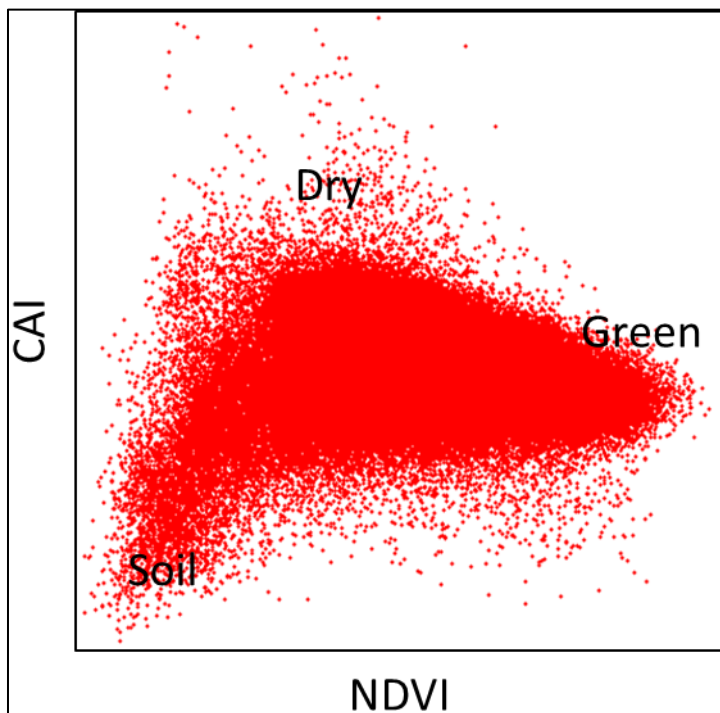


Figure 11 An example of the scatter plot of CAI and NDVI showing the location of the three endmembers.

Fractional Cover

The results (Figure 12) show that Oakville Prairie is mainly covered by dry grass or litter at the end of May. The observation is consistent in both 2009 (Figure 12a) and 2010 (Figure 12b). At early September (Figure 12c), the Oakville Prairie is mostly green grass and mixed with some dry grass or litter.

At Woodworth (Figure 13), much of the land cover is dominated by the PV by early June (Figure 13a), although there are some patches with significant fractions of NPV. At

mid-September (Figure 13c), the former green grass area is mixed with dry, while the former mixed patch turn to mostly green. This change pattern may distinguish between different grassland types at Woodworth, and illustrates the importance of fractional cover and a discriminatory property of grassland.

The two sites show distinct patterns within sub-sections. The value ranges for fractional cover of some parts of Oakville Prairie and on the replanted area at Woodworth are significantly different to the surrounding areas at Woodworth and to other parts of Oakville Prairie. This partial distinction and partial similarity indicates that fractional cover difference can only provide partial discrimination of elements of grassland naturalness. In the next chapter, field spectral libraries of common species, collected throughout the growing season are described and the libraries are formulated to support spectral image matching later in the thesis..

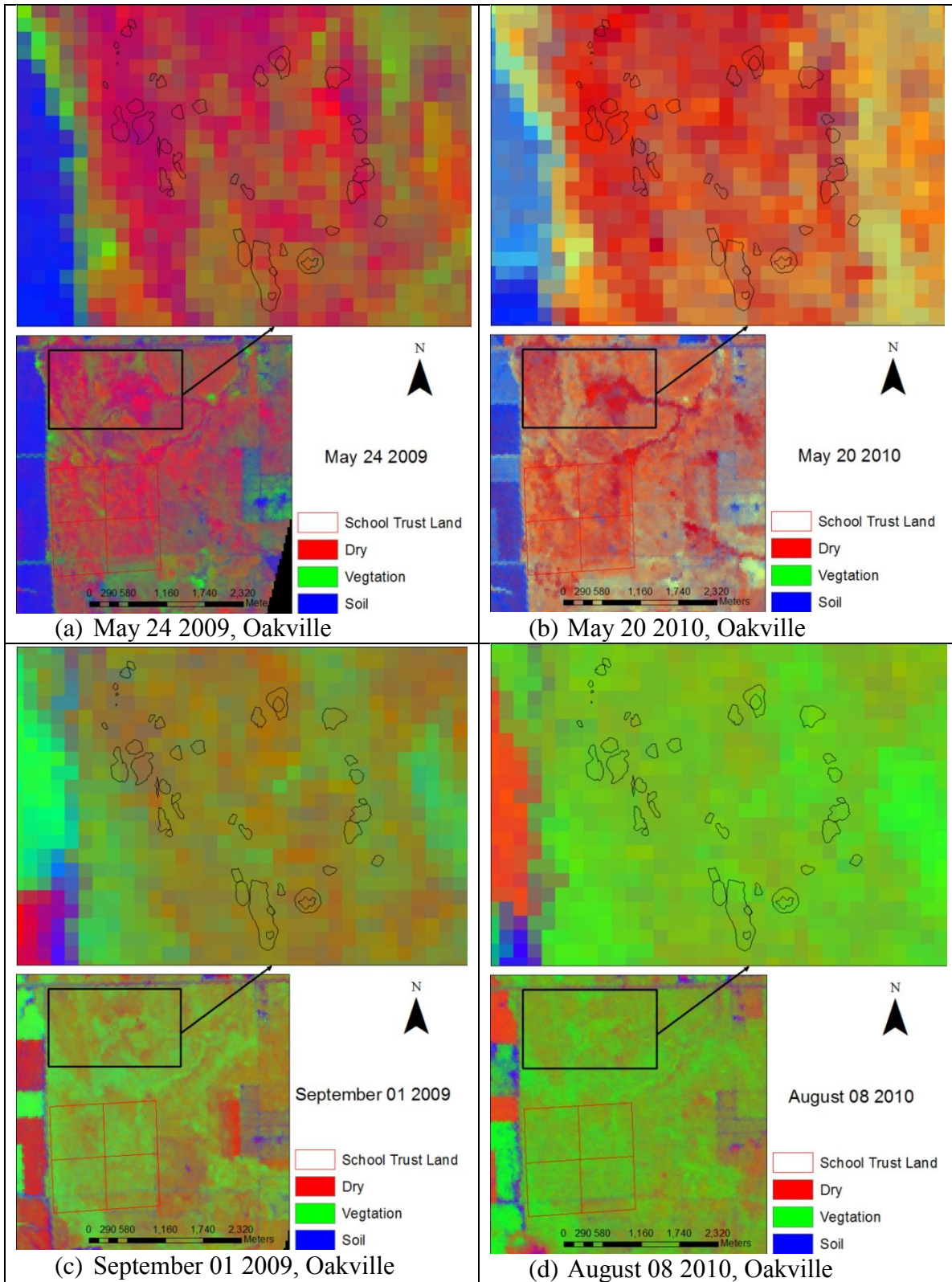


Figure 12. Result of the green vegetation, dry and soil fractional cover unmixing based on the NDVI and CAI for the Oakville Prairie

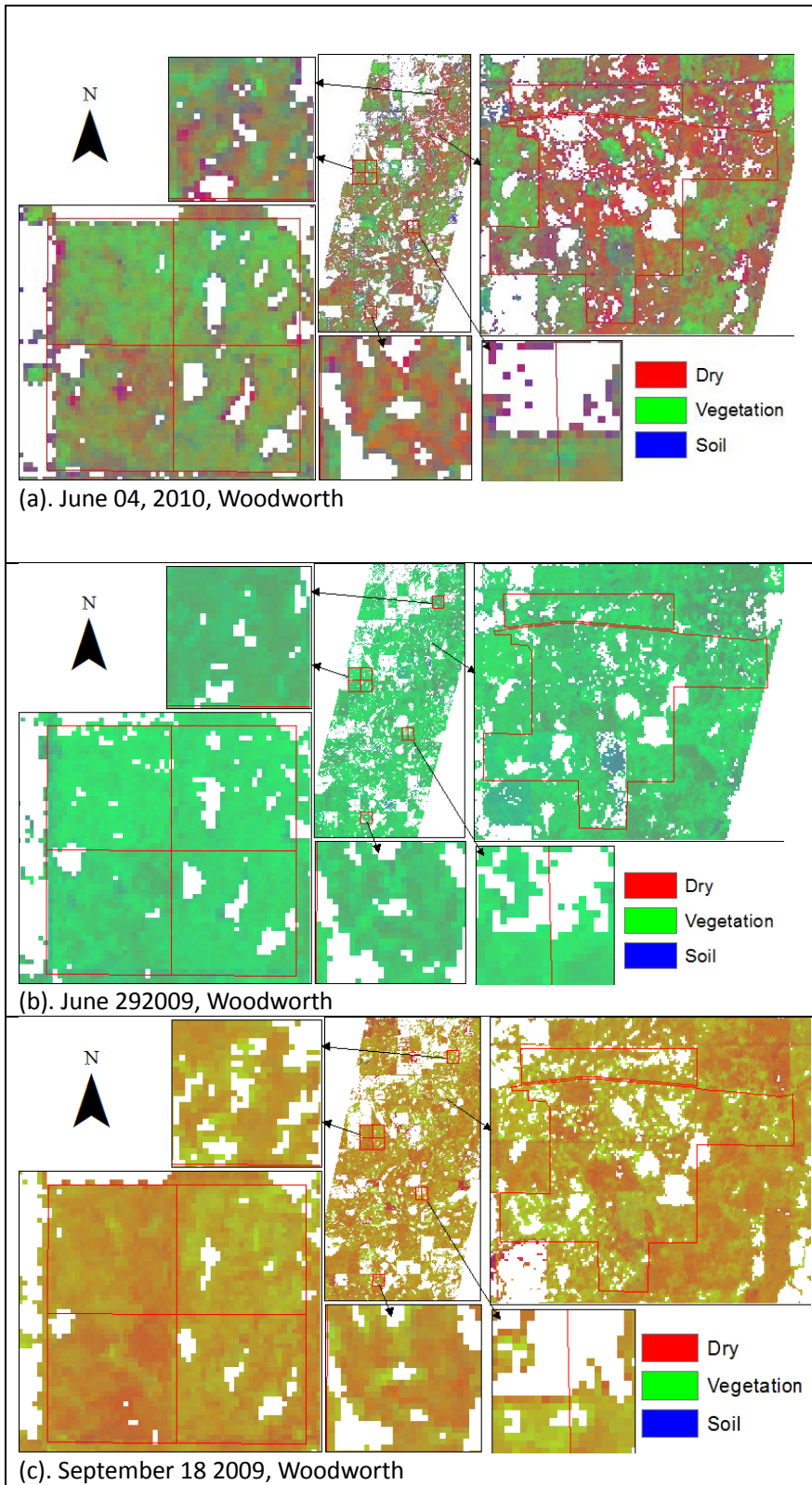


Figure 13. Result of the green vegetation, dry and soil fractional cover unmixing based on the NDVI and CAI for the Woodworth and masked to grassland areas only.

CHAPTER IV

FIELD SPECTRA

In this section the collection of spectral libraries with the Analytical Spectral Devices (ASD) spectroradiometer is described. As discussed in the previous chapter, grassland may exhibit great spatial variation at the same point in time (Thulin, 2009), and these spatial patterns may then vary with time during the growing season due to differences in phenology. Variation may also occur from year to year due to changes in dominance resulting from different spring moisture and temperature conditions. As a result, spectral signatures were collected in the field over a wide range of times. Two separate spectral libraries were constructed to represent early and late season grassland characteristics.

The Spectroradiometer

The ASD measures radiance in a continuous spectrum between 350 and 2500 nanometers. There are three separate detectors covering different spectral ranges. The Visible/Near Infrared (VNIR) portion of the spectrum, the 350 - 1050 nanometer wavelength domain, is most commonly measured by a 512-channel silicon photodiode array overlaid with an order separation filter. Each channel measures wavelength within a narrow (1.4 nm) bandwidth. The full width half maximum (FWHM) of VNIR spectrometer, known as spectral resolution, is approximately 3 nm measured at around

700 nm (FieldSpec Pro 2002).

The Short-Wave Infrared (SWIR), also called the Near Infrared (NIR), portion of the spectrum is acquired with two scanning spectrometers. Different with the array used in the VNIR, which measures wavelengths sequentially, The SWIR measures light simultaneously. The first spectrometer (SWIR1) covers the region from about 900 to 1850 nm; the second (SWIR2) measures light from about 1700 to 2500 nm. The controlling software automatically accounts for the overlap in wavelength intervals by using a preset wavelength within the common subset at which to place a “splice”. The sampling interval for each SWIR region is about 2 nm, and the spectral resolution varies between 10 nm and 12 nm, depending on the scan angle at that wavelength. (FieldSpec Pro 2002)

Data Processing

Figure 14 illustrates overall the field spectra processing and transformation steps. The ASD Raw DN mode is used in field measurement. The raw data (raw DN, for “digital numbers”) usually contains 16-bit integer numbers corresponding to the intensity of light field through a given point in space measured by VNIR and SWIR detectors, and it is a function both of the characteristics of the light field being measured and of the instrument itself (FieldSpec Pro 2002). Reflectance is calculated from these raw digital numbers (FieldSpec Pro 2002). Due to water absorption in atmosphere and electronic noise in the instrumentation, ASD suggest that an averaging method is needed to reduce noise in the desired spectrum. In field measurements, 10 spectra are collected each time. Then, if there is no significant difference between 10 spectra, average will be calculated (Figure 15).

Reflectance is the fraction of incident light that is reflected from a surface, which can be represented as a ratio between measurements from both the unknown material and a white reference (Equation 3). The white reference has approximately 100% reflectance through the entire spectrum. Thus reflectance is calibrated by using the ratio between measurements of species and white reference (Equation 4, Figure 16).

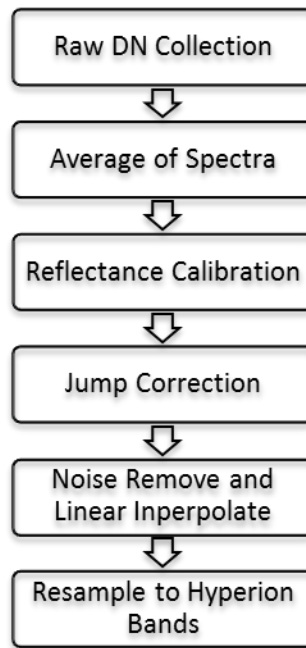


Figure 14. Overview of the field spectra processing and transformation steps

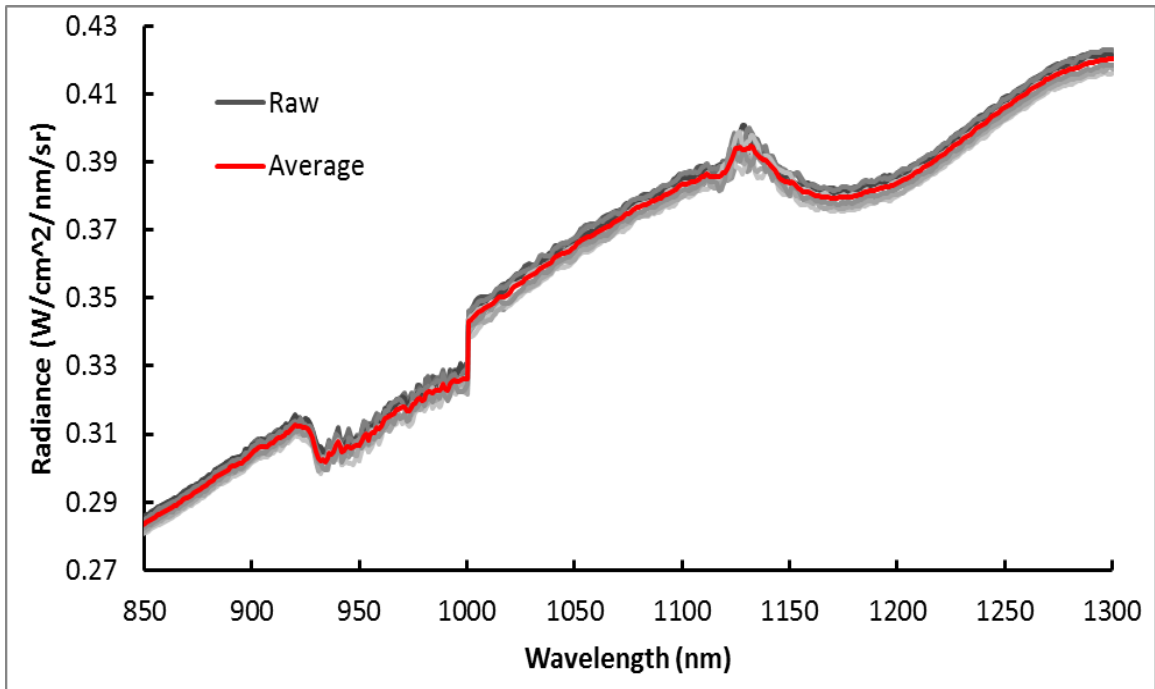


Figure 15. Average of 10 raw measurements in order to reduce noise

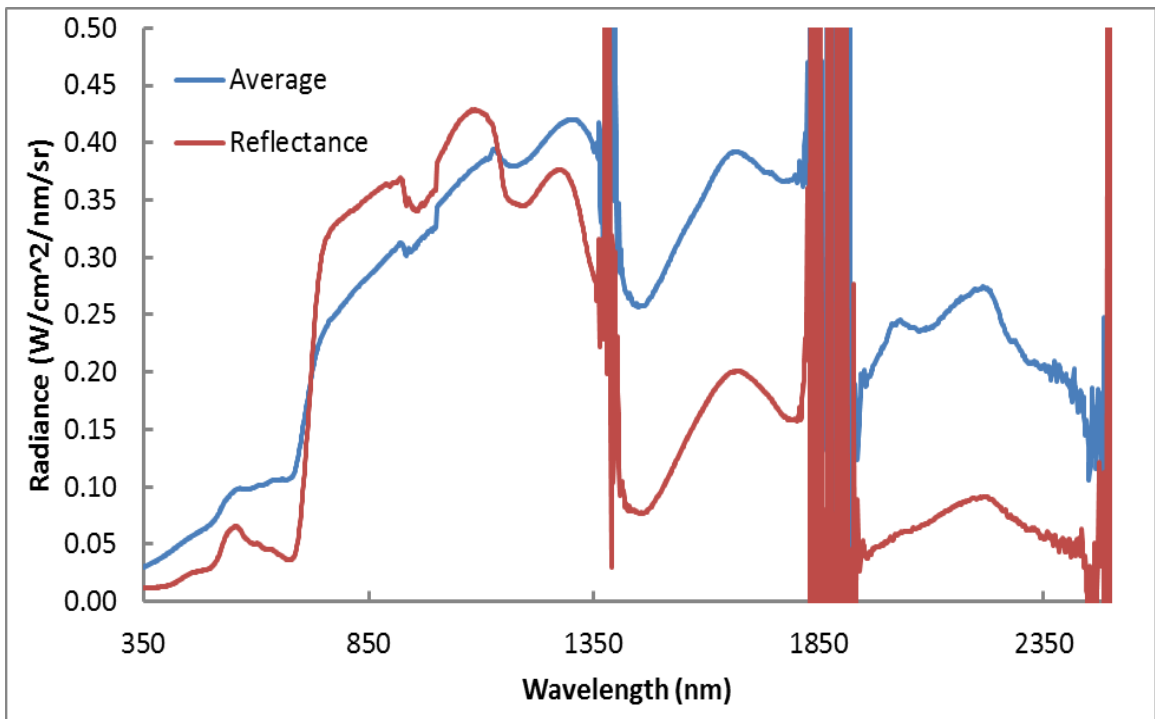


Figure 16. Reflectance calculated as ratio between measurements from certain species and white reference

$$\mathbf{R \text{ (Reflectance)}} = \frac{\mathbf{Light \text{ emitted from sample}}}{\mathbf{light \text{ emitted from white reference (WR)}}} \quad (3)$$

$$\mathbf{R} = \frac{\mathbf{Raw \text{ DN spectrum of sample}}}{\mathbf{Raw \text{ DN spectrum of WR}}} \quad (4)$$

There are three detectors in the ASD instrument measuring light continuously. One covers the VNIR, the two others the Short-Wave Infrared. However, jumps can often be observed between two detectors in the measured spectrum. This can be attributed to inadequate optimization/calibration of the detectors or to target homogeneity (Dorigo 2006). For spectra measured in the field, only the jump between the first two detectors can be observed, since the shift between the SWIR1 and SWIR2 is within a wavelength range which is governed by water vapor, and thus the jump is overshadowed by noise (Dorigo 2006). For the jump correction, one of the three detectors will be considered as a reference, and the data from the other detectors is adjusted to that reference (Figure 17). Here the second detector is assumed to be the “correct one”.

The field spectra is greatly perturbed due to the presence of water vapor absorbing light in the regions around 1400nm and 1800nm as it passes through the atmosphere. These wavelengths are usually considered to have low signal to noise ratio (SNR) and therefore were removed during analysis. The removed regions include 1336-1420nm, 1737-1952nm and region beyond 2333nm. The water vapor bands were then replaced by linear interpolation (Figure 18).

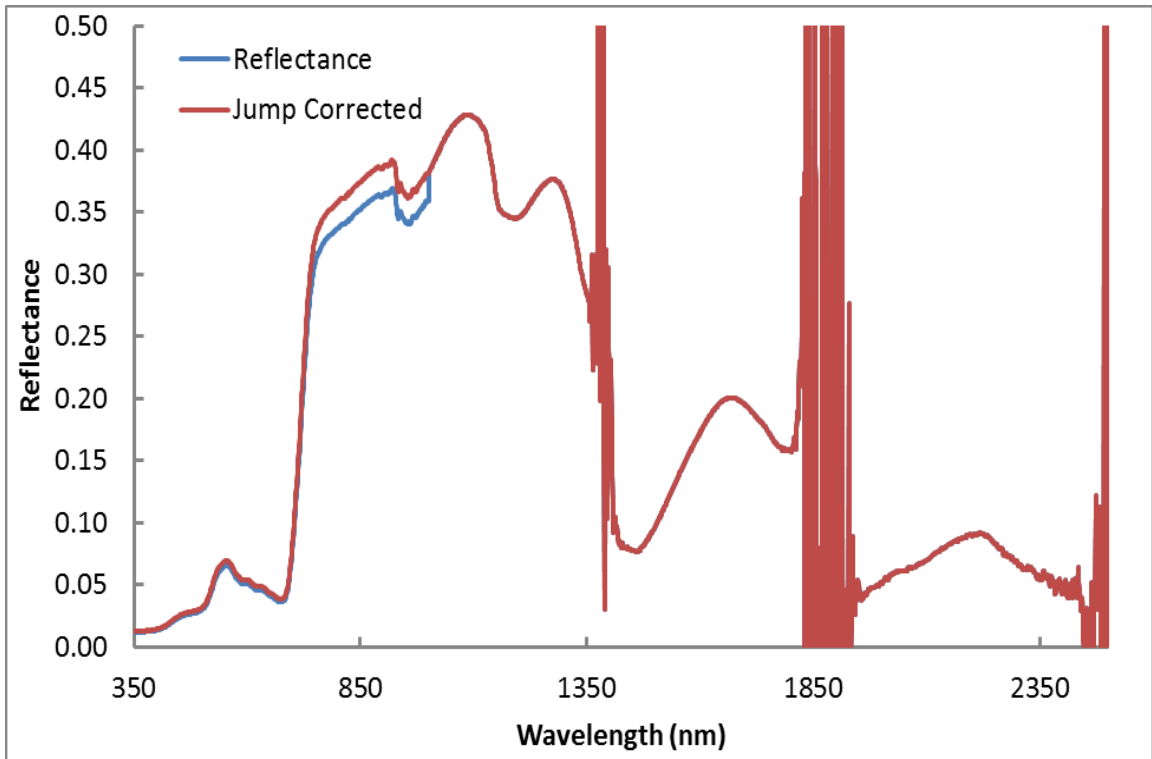


Figure 17. The First Detector Is Corrected And Adjusted To The Second Detector

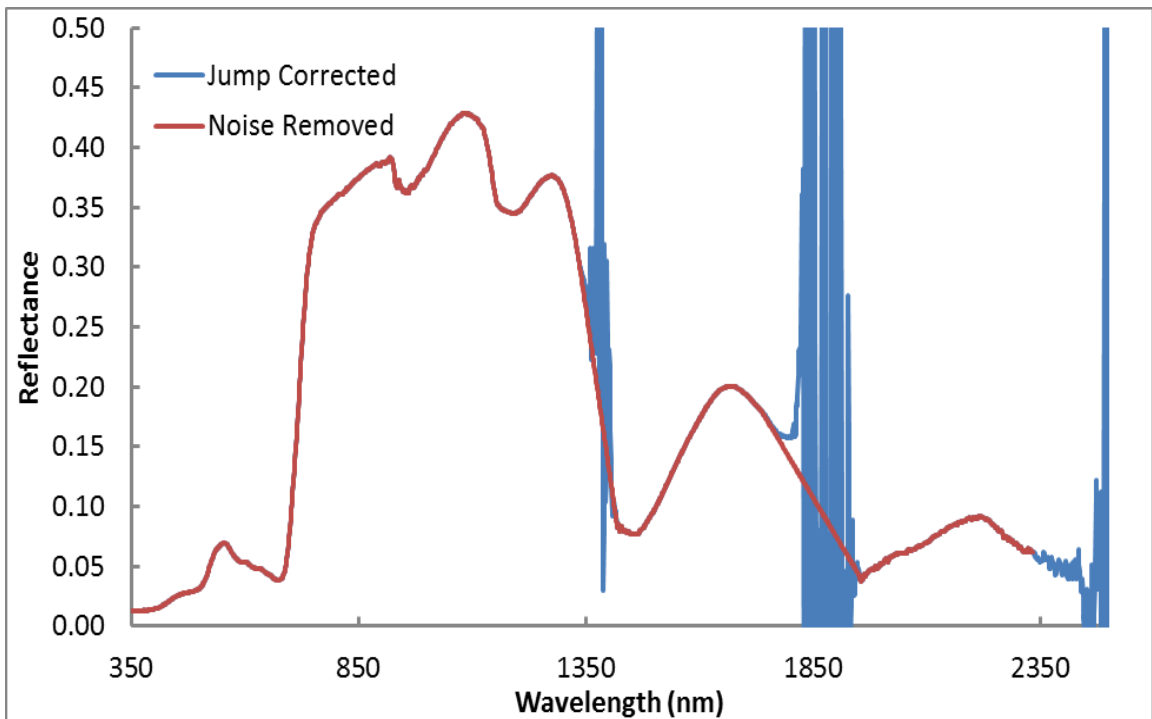


Figure 18. Water vapour bands are removed and replaced with linear interpolations

Field Measurements Result

Several locations of patches are continuously sampled (Figure 19) since May 2011 to compare spectral changes (Figure 20; Figure 21) of different species through growing season and proportion of land cover is also extracted based on their locations (Figure 22 to Figure 34).

All native spectra and land cover proportions from Figure 22 to Figure 33 are collected from Oakville Prairie. The brome grass spectra (Figure 34) are collected from both Oakville and Woodworth. The land cover proportion of brome grass (Figure 34c), however, is extracted from Woodworth, due to the lack of big patch at Oakville Prairie.

In some cases, temporal changes in the magnitude and shape of the spectra do not exhibit consistent patterns. For example, the red edge effect might usually be expected to increase from early in the growing season to later in the growing season as in Figure 29, where the green cover clearly increases (Figure 29 a-c). The disagreements may come from many factors, for example, atmosphere condition, wind, health of plants. However, temporal variability in strength and shape of spectral signatures may introduce unwanted variation and spectral confusion into the spectral analysis at the next chapter.

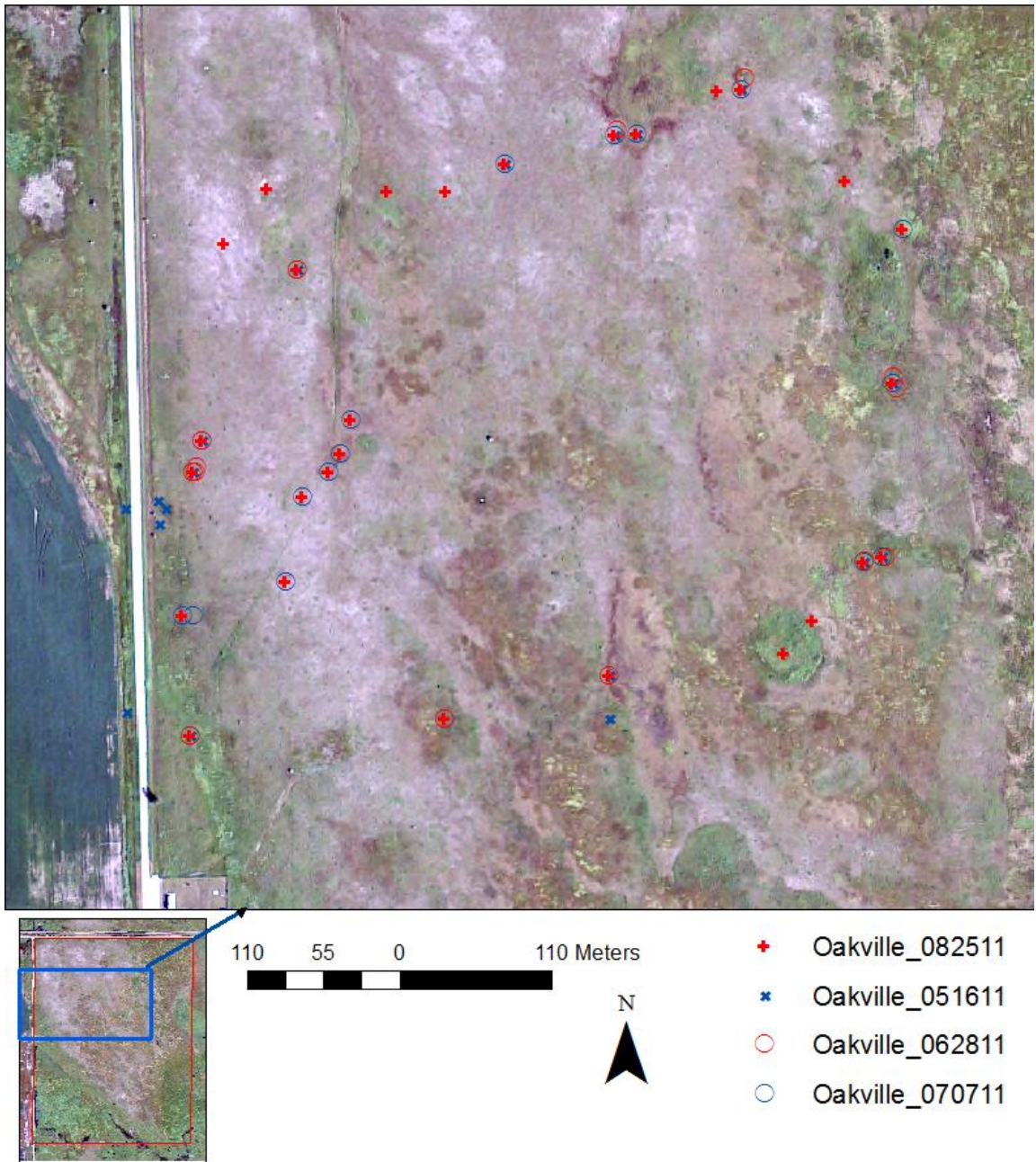


Figure 19. Field Measurements Locations At Oakville Site. The Overview Image Shows Oakville North Section Region.

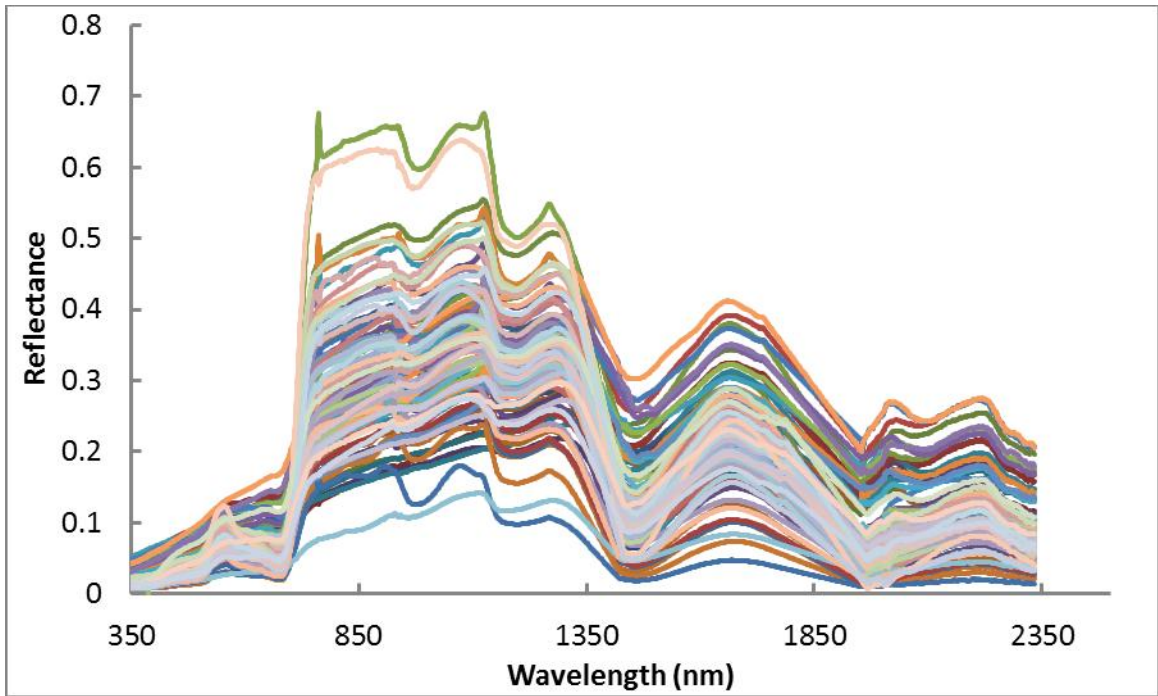


Figure 20. The Overall Variation In Vegetation Spectra at Oakville (Aug 06 2009; May 16 2011; Jun 28 2011; Jul 07 2011; Aug 25 2011)

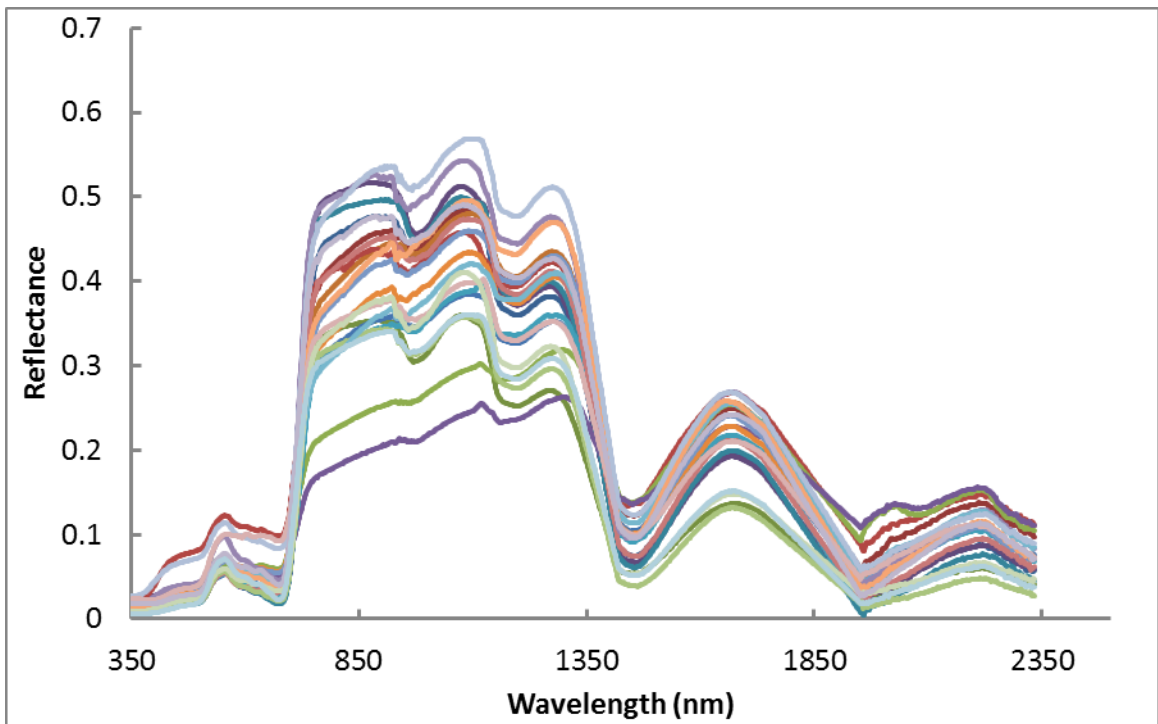
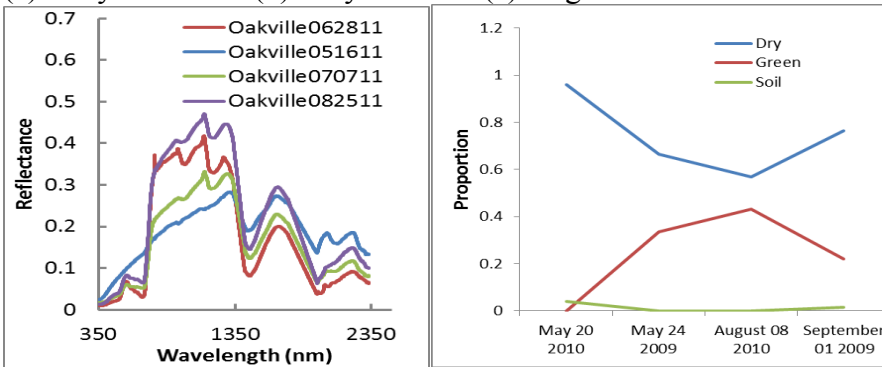


Figure 21. The Overall Variation In Spectra at Woodworth (Aug 09 2011)



(a). May-16-2011 (b). July-07-2011 (c). August-25-2011

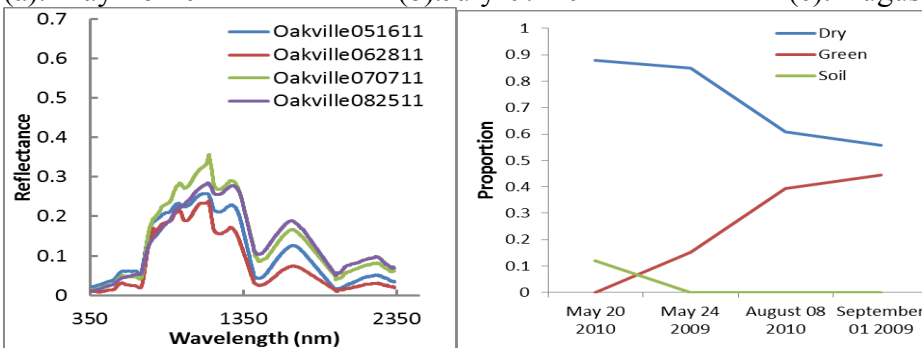


(d). Time series Spectrum (e). Fraction Cover

Figure 22. Photos of Golden Rod; Wheat Grass Patch at three dates a-c); and d) patch spectra collected at four times in 2001; and e) fractional cover of green, dry and bare soil for the image pixel corresponding to this location.



(a). May-16-2011 (b). July-07-2011 (c). August-25-2011



(d). Time series Spectrum (e). Fraction Cover

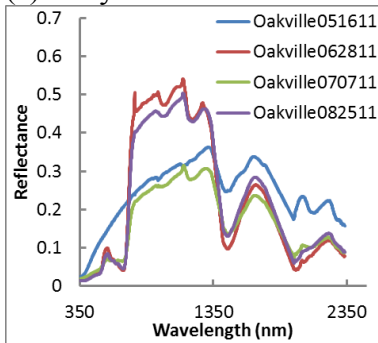
Figure 23. Photo of Triglochin Patch at three dates a-c); and d) patch spectra collected at four times in 2001; and e) fractional cover of green, dry and bare soil for the image pixel corresponding to this location.



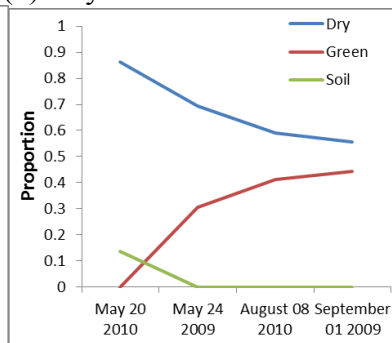
(a). May-16-2011

(b). July-07-2011

(c). August-25-2011



(d). Time series Spectrum



(e). Fraction Cover

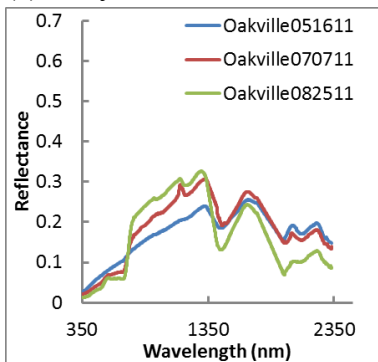
Figure 24. Photo of Wheat Grass Patch Spectra of Wheat Grass Patch at three dates a-c); and d) patch spectra collected at four times in 2001; and e) fractional cover of green, dry and bare soil for the image pixel corresponding to this location.



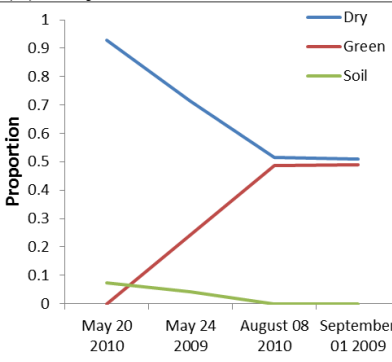
(a). May-16-2011

(b). July-07-2011

(c). August-25-2011



(d). Time series Spectrum



(e). Fraction Cover

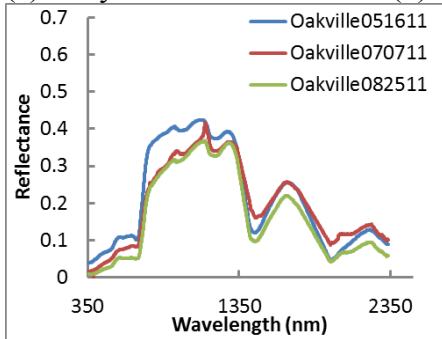
Figure 25. Photo of Cord Grass; Hairy Aster Patch at three dates a-c); and d) patch spectra collected at four times in 2001; and e) fractional cover of green, dry and bare soil for the image pixel corresponding to this location.



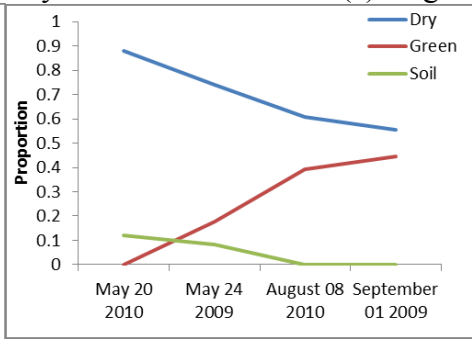
(a). May-16-2011

(b). July-07-2011

(c). August-25-2011



(d). Time series Spectrum



(e). Fraction Cover

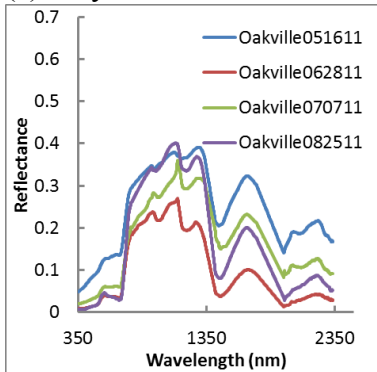
Figure 26. Photo of an area dominated by wild rye (*Elymus* spp) at three dates a-c); and d) patch spectra collected at four times in 2001; and e) fractional cover of green, dry and bare soil for the image pixel corresponding to this location.



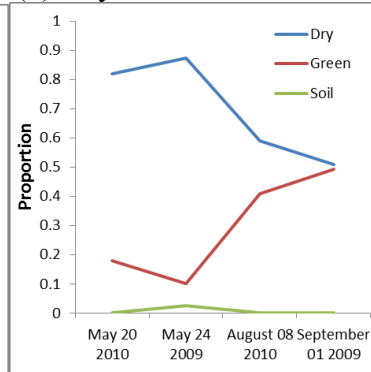
(a). May-16-2011

(b). July-07-2011

(c). August-25-2011



(d). Time series Spectrum



(e). Fraction Cover

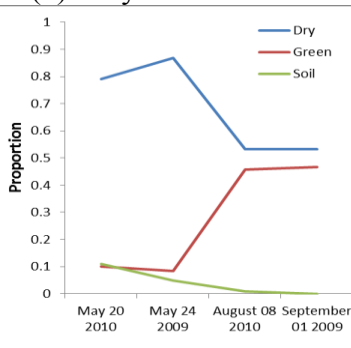
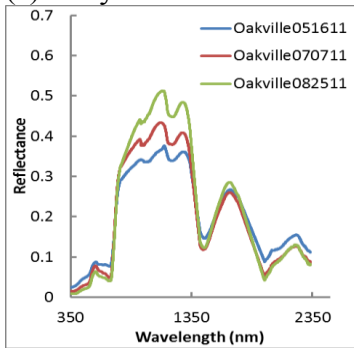
Figure 27. Photo of Wheat Grass Patch at three dates a-c); and d) patch spectra collected at four times in 2001; and e) fractional cover of green, dry and bare soil for the image pixel corresponding to this location.



(a). May-16-2011

(b). July-07-2011

(c). August-25-2011



(d). Time series Spectrum

(e). Fraction Cover

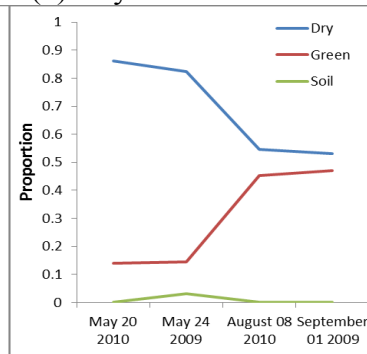
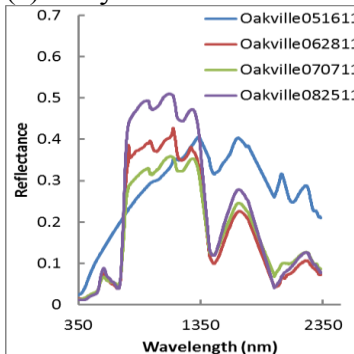
Figure 28. Photo of Golden Rod; Poaceae Patch at three dates a-c); and d) patch spectra collected at four times in 2001; and e) fractional cover of green, dry and bare soil for the image pixel corresponding to this location.



(a). May-16-2011

(b). July-07-2011

(c). August-25-2011



(d). Time series Spectrum

(e). Fraction Cover

Figure 29. Photo of Cord Grass Patch at three dates a-c); and d) patch spectra collected at four times in 2001; and e) fractional cover of green, dry and bare soil for the image pixel corresponding to this location.

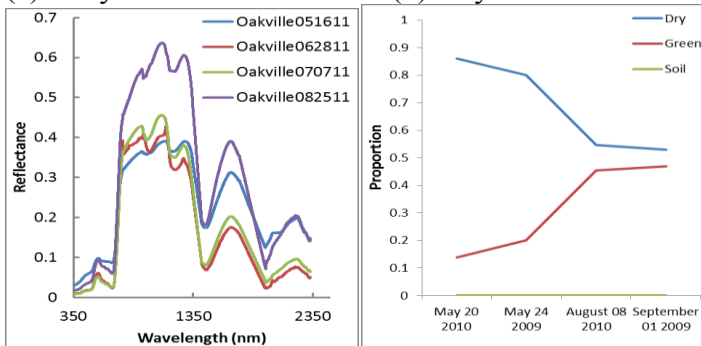


Figure 30. Photo of Wheat Grass Patch at three dates a-c); and d) patch spectra collected at four times in 2001; and e) fractional cover of green, dry and bare soil for the image pixel corresponding to this location.

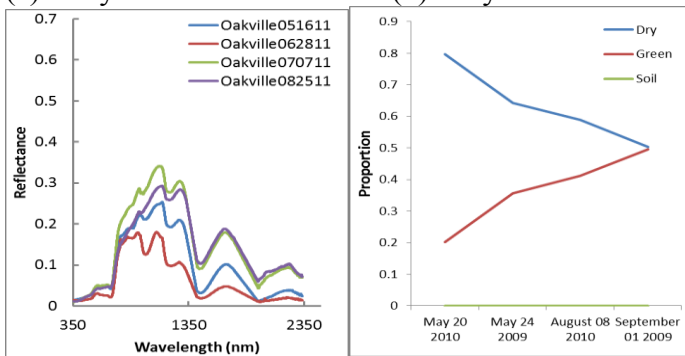
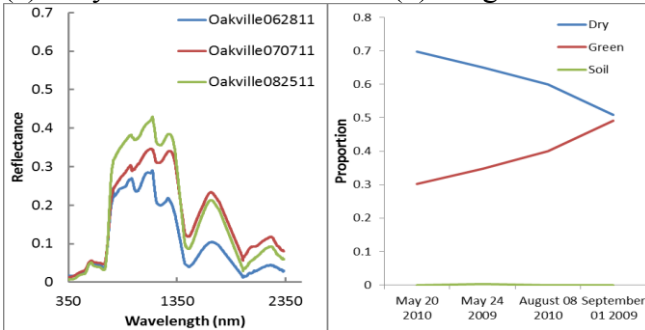


Figure 31. Photo of Patch at three dates a-c); and d) patch spectra collected at four times in 2001; and e) fractional cover of green, dry and bare soil for the image pixel corresponding to this location.



(a). July-07-2011

(b). August-25-2011



(c). Time series Spectrum (d). Fraction Cover

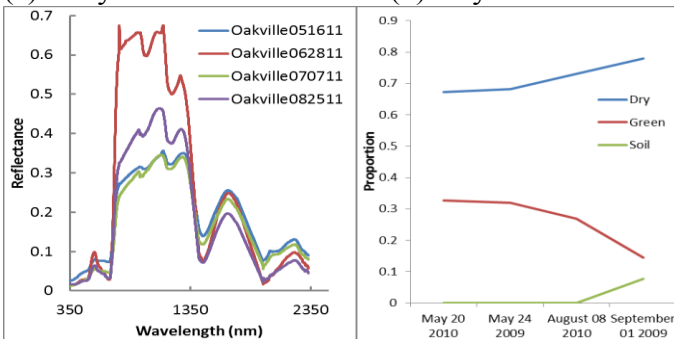
Figure 32. Photo of Patch at three dates a-b); and c) patch spectra collected at four times in 2001; and d) fractional cover of green, dry and bare soil for the image pixel corresponding to this location.



(a). May-16-2011

(b). July-07-2011

(c). August-25-2011



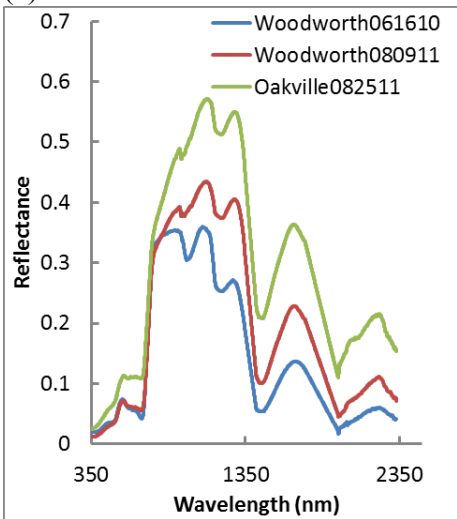
(d). Time series Spectrum (e). Fraction Cover

Figure 33. Photo of Snow Berry Patch at three dates a-c); and d) patch spectra collected at four times in 2001; and e) fractional cover of green, dry and bare soil for the image pixel corresponding to this location.

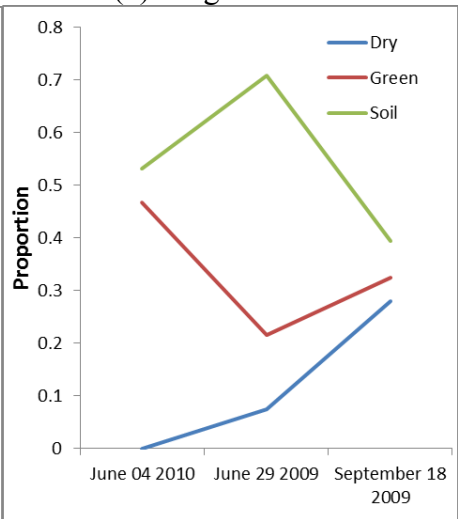


(a). June 16 2010

(b). August 09 2011



(c). Time series Spectrum



(d). Fraction Cover

Figure 34. Photo of Brome Grass Patch at three dates a-b); and c) patch spectra collected at four times in 2001; and d) fractional cover of green, dry and bare soil for the image pixel corresponding to this location.

The fractional cover estimates show that fraction of bare soil is low at Oakville most of the time because of the thick cover of litter on the prairie area. The greenness of native grasses is comparatively low in May, and increases as the growing season progresses. The relative fraction of green cover and dry cover in patches of cord grass and wheat grass reaches a plateau around August. The greenness of forbs (Figure 33) is high at May but decreases later growing season which may be caused by flowering. The dry fraction, however, usually declines with increasing greenness. The smooth brome grass at Woodworth, on the other hand, is distinctive. Soil proportion is always high at

Woodworth which may mainly represent the different background from Oakville Prairie. Some smooth brome grass sample sites were close to road compared with 30 meters image resolution so this may have contaminated these sites. However, in general, the Woodworth smooth brome grass stands may accumulate substantial litter loads since they are not grazed or mown in order to protect breeding habitat for birds. The trend of greenness, however, is distinctive. It starts with a high proportion in early June then decreases as the growing season progresses, but then rises again late in the growing season. The dry proportion keeps increasing compared with Oakville Prairie.

Based on the above analysis, it can be assumed that:

1. Smooth brome grass tends to have high greenness in the early growing season;
2. Some grasses, especially smooth brome grass, tend to become less green later growing season due to flowering behavior.

Thus the fractional cover proportions are also important since signal changes of green grass can indicate differences between species.

However, the fractional cover proportions show the combination of green vegetation, dry grass and soil at 30 by 30 meters scale. Therefore, the results do not represent the exact sample sites, which could result in some disagreement with spectral analysis.

Discussion

The processes applied to the field measurement of this research were carefully documented. Ideally pre-processing and correction of spectra should be done with great care to ensure possibility of use of spectra for other applications and to further the

collective knowledge of the whole hyperspectral community dealing with ecological/vegetation applications (Pfitzner et al. 2006).

The results show substantial variation in spectral profiles over time. Early in the growing season, this variation is mainly caused by changes from litter and senescent vegetation or bare soil to green vegetation. Thus, spectral curves generally represent more vegetation features, like the green peak and red edge, by June and July. The spectral profiles continue to change, but these changes show no consistency among locations. The variation is made up of complex information related both to structural changes among the species present, phenological changes associated with flowering, and growth of new species, especially forbs and herbs, which grow out in the patches.

The collection of field spectra involves a multitude of challenges. In this study, weather and light conditions and personnel schedules meant that it was not possible to sample as frequently as was desirable in order to fully capture temporal variation. In addition, the decision was made to take field-of-view spectra rather than pure green leaf spectra due to the logistics involved in such pure measurements. With relatively large pixels and relatively modest SNR for Hyperion images, it was considered to be more important to capture spectra representative of patches rather than spectra of pure green leaves.

The fractional cover results show some consistent change patterns among site locations at Oakville. For example, most native grasses trend to higher greenness along growing season because of increasing green leaves; but there are exceptions to this trend such as June grass. There was a distinct spectral response pattern, for ASD sites at

Woodworth, since smooth brome grass flowered earlier than most native grasses, and therefore showed less greenness later in the growing season.

Given that the pixel resolution of Hyperion imagery results in mostly mixed pixels (mixtures of species and cover types) in these grasslands, the next chapter applies spectral matching methods using the field measured spectra in order to define specific combinations of species and cover fractions that may be indicative of grassland naturalness.

CHAPTER V

SPECTRUM MATCHING

Introduction

This chapter describes three stages of analysis designed to create spatial data layers that describe spectral properties of the grassland that could be used to model naturalness – the continuum from native to introduced grassland. The stages involve:

1. Spectral matching involving comparison of a range of methods and selection of results from the best of these.
2. Examination of the relative extent to which the spectral match is dominant by generation of two measures – level of dominance and band variance
3. Examination of the spatial pattern of spectral matches using textural co-occurrence methods – i.e. determining if there are larger patches and regions characterized by difference combinations and levels of spectral matching.

The analysis is presented in three sections and at the end, a set of data layers that could be most discriminatory for distinguishing between native and introduced grassland is defined. These layers are used in naturalness modeling in Chapter 6.

Spectral Library

The spectral library was first built based on field measurements for both native and introduced species. As spatial resolution of Hyperion image is 30m, sparse species

distribution is not detectable in sensor response. Thus only the major species that can provide enough signal are included in the spectral library for native grassland, such as June grass, cord grass, wheat grass, wild rye, and common forbs like Maximilian sunflower, thistle, sage, and sage willow. Since the native prairie is usually covered by litter, particularly in early spring due to senescence, freezing and shattering of the growth from the previous season, the dry grass signal can comprehensively affect the image spectrum especially at early growing season. Therefore, the dry grass spectra are an essential component of the spectral library. The major introduced species in this analysis are smooth brome grass and Kentucky blue grass. Figure 1 shows changes in the appearance and phenology of the major species over the growing season. June grass and wild rye flower in early July, but by late August June grass inflorescences have dried off and wild rye inflorescences have shattered. Smooth brome grass and Kentucky blue grass have already started flowering in June. By September, however, Kentucky blue grass has completely dried off and smooth brome grass displays mixed dry and green patches. Cord grass and wheat grass change little through the middle of growing season. Forbs like Maximilian sunflower, sage and sage willow present mainly a leafy appearance early in the growing season, but appear less leafy and sparse later on. When Maximilian sunflower starts flowering at late August, significant yellow color is evident in the grassland. The thistle begins flowering reasonably early, and the flowers became more dense later in the growing season.

As the vegetation spectrum varies during the entire growing season, from a spectrum dominated by dry grasses very early in the season, to a spectrum made up of diverse vegetation with flowering later in the season, separate spectrum libraries are created for

early (May to middle August, Figure 36) and later growing seasons (middle August to later September, Figure 37). Based on visual assessment (Figure 35), separate spectra for early and late growing season are used for June grass, wild rye, Maximilian sunflower, sage and sage willow. For Cord grass and wheat grass, the same spectra were used in early and later growing season (cord grass changes very little, and suitable wheat grass spectra were not collected for the early growing season period). Introduced species include green smooth brome grass and Kentucky blue grass in early growing season. For later growing season, both green and flowering smooth brome grass spectra are used. Kentucky blue grass, however, is excluded since it is already dry out and was not distinguishable from the non-photosynthetic litter and senescent grass spectra collected.

In order to simulate Hyperion data, ASD reflectance is resampled to Hyperion bands. The function is provided by ENVI which assumes critical sampling and uses a Gaussian model with a full width at half maximum (FWHM) spacing.















			
Junegrass July-07-2011	Junegrass August-25-2011	Cordgrass July-07-2011	Wheatgrass August-25-2011
			
Maximillian Sunflower July-07-2011	Maximillianb Sunflower August-25-2011	Wildrye July-07-2011	Wildrye August-25-2011
			
Sage Willow August-09-2011	Sage Willow September-8-2011	Thistle August-09-2011	Thistle Flowering September-8-2011
			
Sage August-09-2011	Sage September-8-2011	Bromegrass June-16-2010	Bromegrass Flowering September-8-2011
			
Kentucky Blue Grass June-16-2010	Drygrass May-16-2011		

Figure 35. Field Condition of Spectral Library

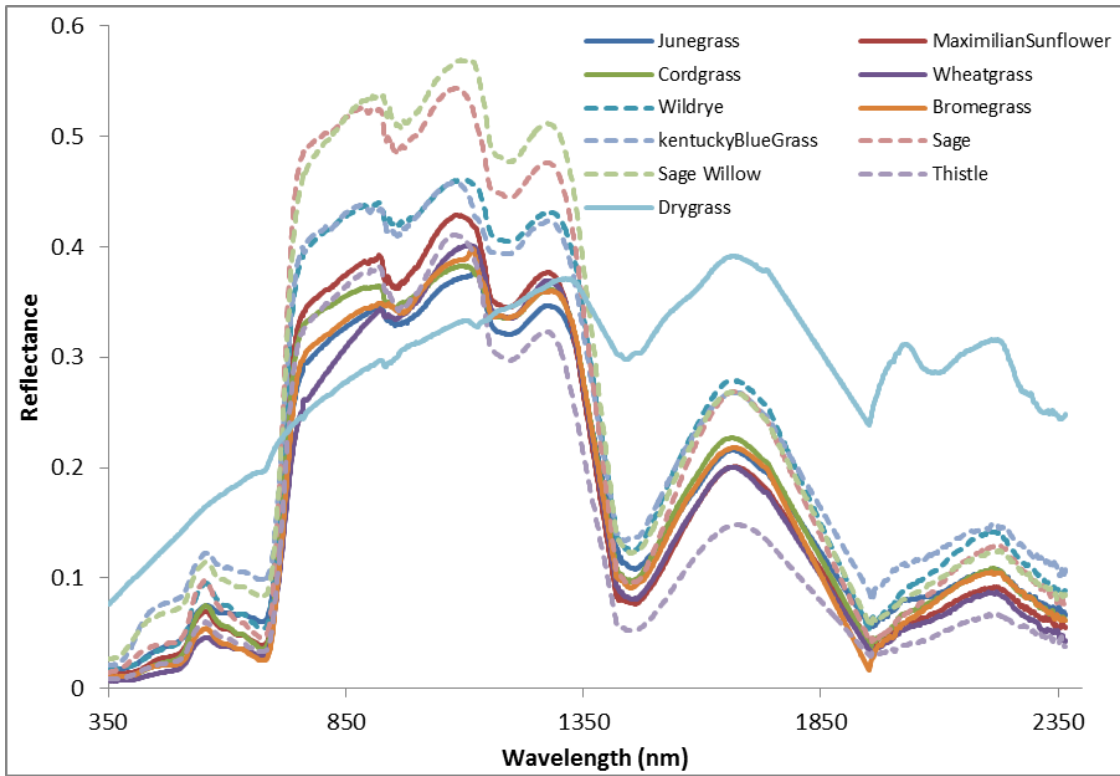


Figure 36 Early Growing Season Spectral Library

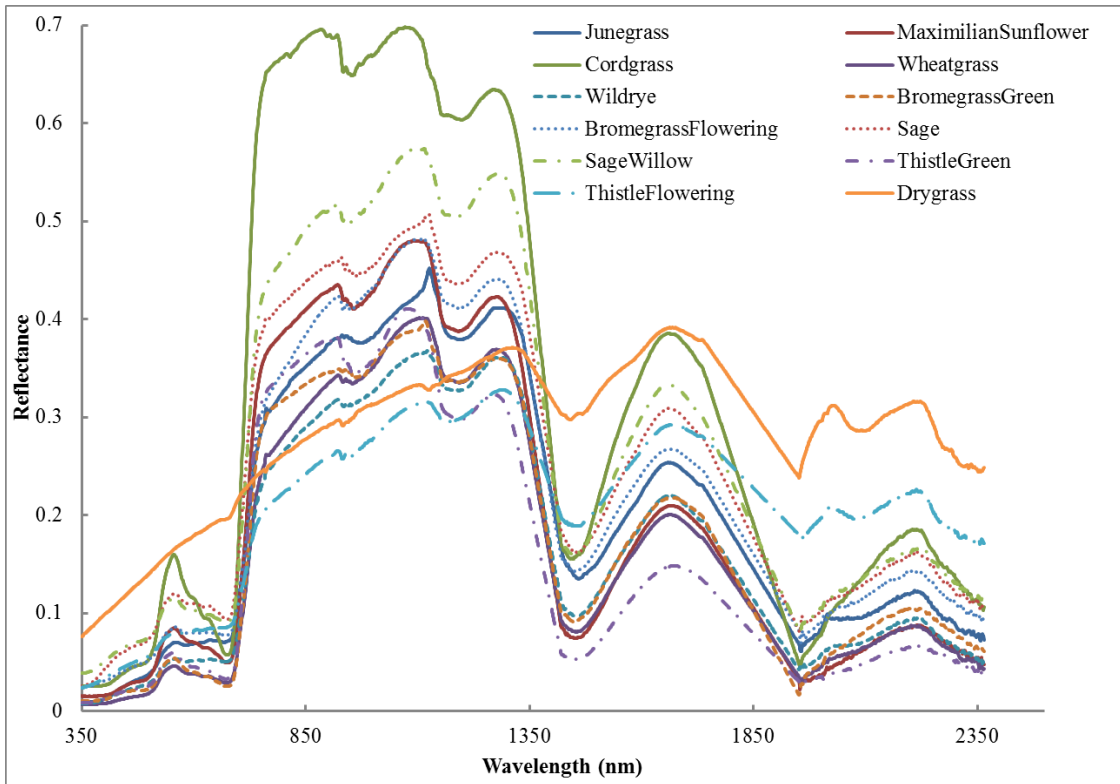


Figure 37 Late Growing Season Spectra Library

As Figure 36 and Figure 37 illustrate, all vegetation spectra are highly correlated, and some parts of wavelength regions have weak responses for vegetation. Therefore, the data were transformed using continuum removal to decrease dimensionality and increase discrimination in critical wavelength regions. As different vegetation types may have various physical and biochemical structures, in a spectrum these differences may be represented in terms of different absorption features (Figure 38, Figure 39). Five known chemical absorption features were selected for this study. The first feature is related to chlorophyll absorption in the visible domain (R550 – 750), which have been found to be related to nitrogen concentration and other bio chemicals on fresh standing canopies (Mutanga et al., 2002, Mutanga et al., 2003). Another chlorophyll absorption feature (R470 – 518) is not used because signal in this region in Hyperion image is noisy due to atmosphere effects. Short wave absorption features (R1116 – 1284, R1634 – 1786, R2006 – 2196 and R2222 – 2378) are also introduced since these have previously been related to characteristics of both fresh standing plant and dried ground plant materials. Then band normalized areas of the absorption features were calculated and were then used in the target detection methods (Figure 40, Figure 41).

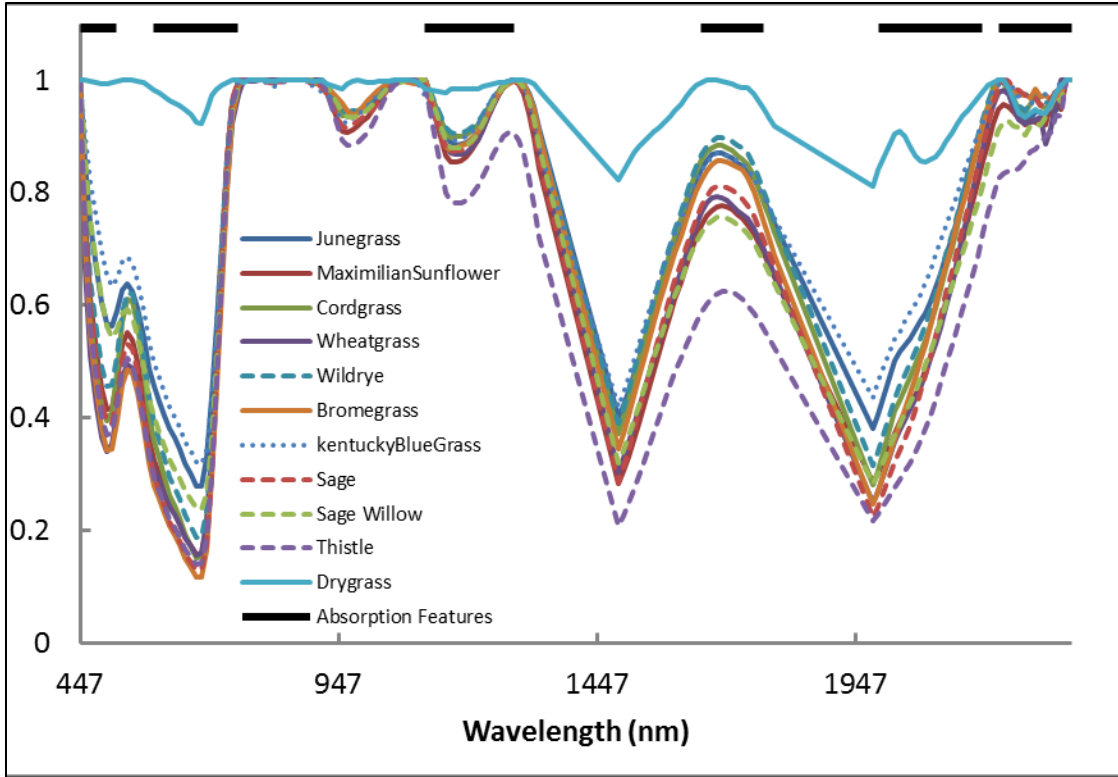


Figure 38 Early Growing Season Spectral Library Continuum Removal

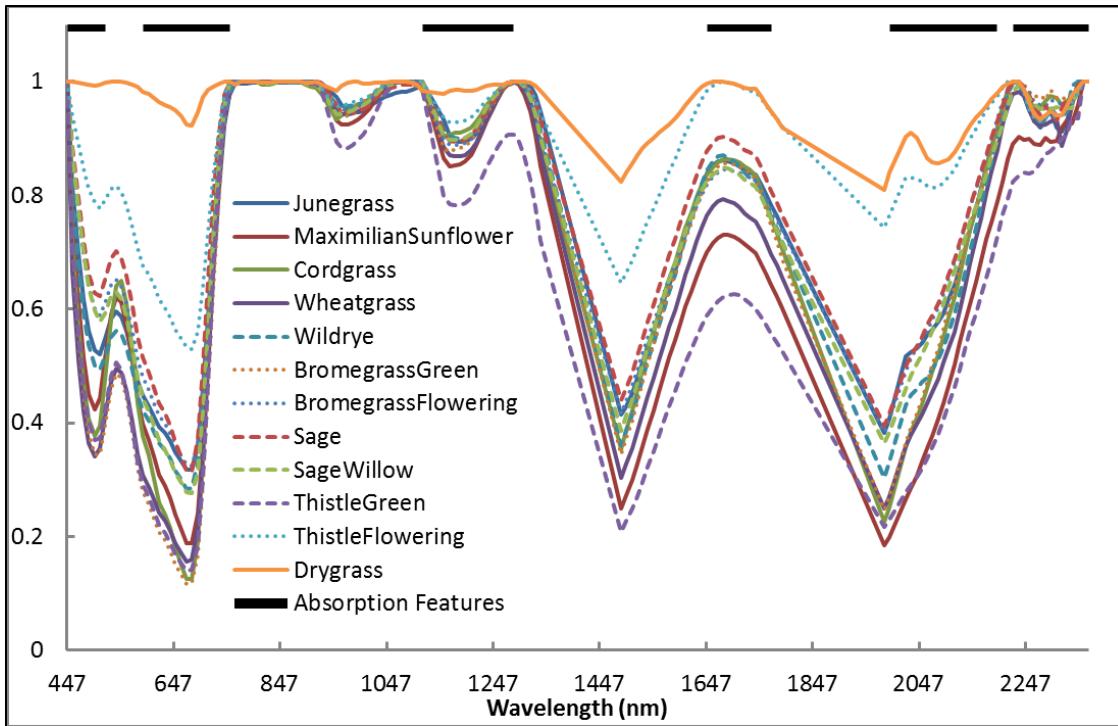


Figure 39 Late Growing Season Spectra Library Continuum Removal

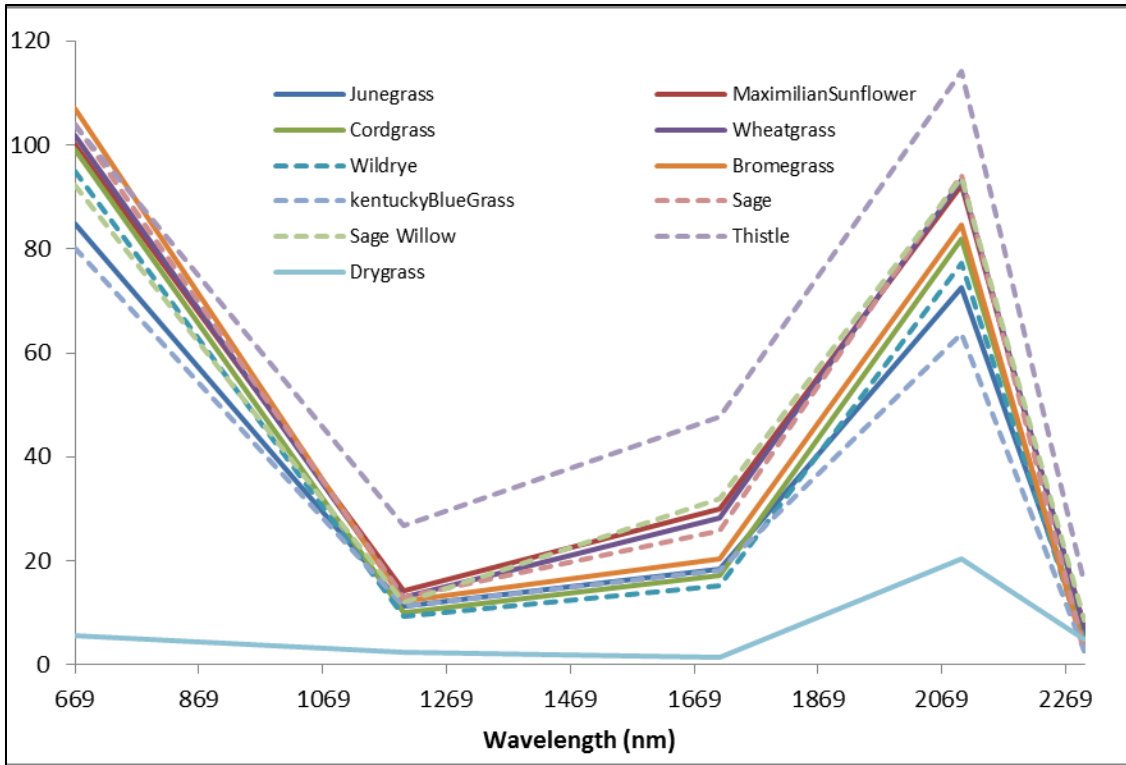


Figure 40 Early Growing Season Spectral Library Area of Absorption Features

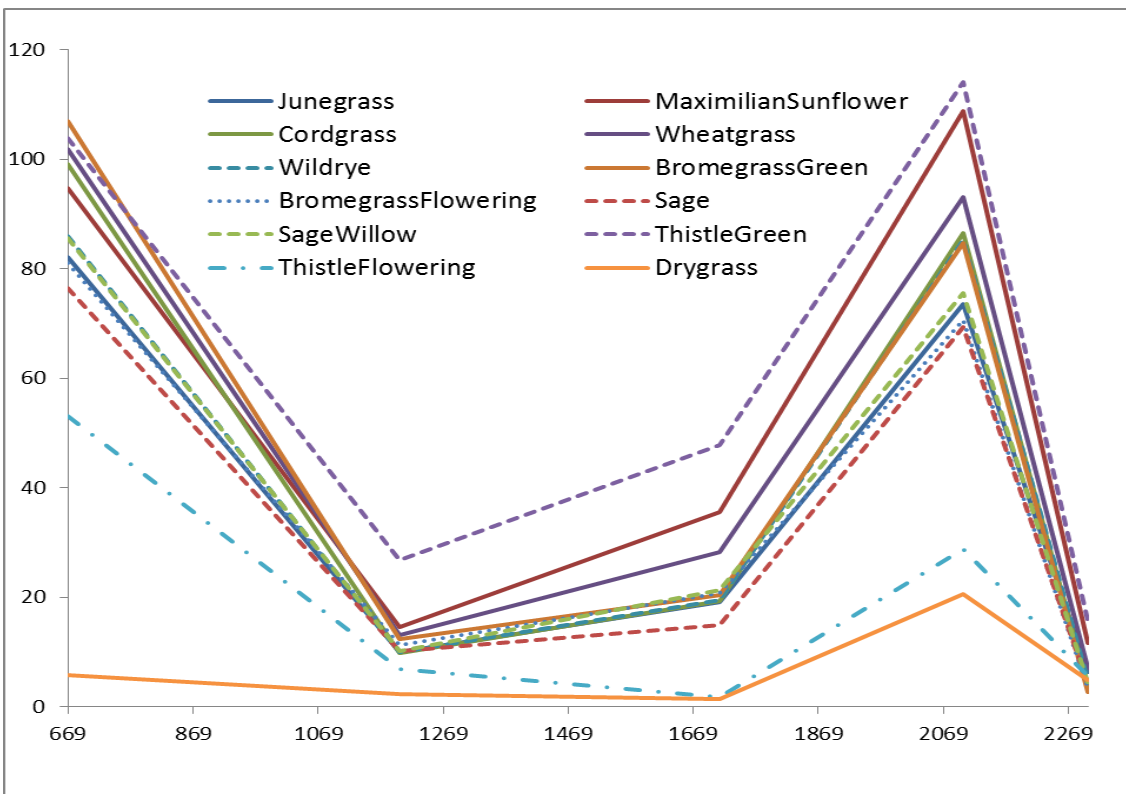


Figure 41 Later Growing Season Spectral Library Area of Absorption Features

Methods

Matching Methods

A class of techniques called target detecting technologies can be used to measure similarity between an unknown pixel and a reference spectral library (Homayouni 2004). There are generally two groups of methods for the analysis of hyperspectral data (Homayouni 2004). The first group of methods is based on binary hypothesis testing (Manolakis, 2002). The other methods, on the contrary, measure the similarity (Homayouni 2004). These techniques provide the basis for the spectral matching approach that is applied to the image and spectral library data in this study to discriminate between native and introduced grassland.

There are eight methods provided by ENVI target detection module (ENVI Help):

1. Adaptive Coherence Estimator (ACE)
2. Constrained Energy Minimization (CEM)
3. Matched Filtering (MF)
4. Mixture Tuned Matched Filtering (MTMF)
5. Orthogonal Subspace Projection (OSP)
6. Spectral Angle Mapper (SAM)
7. Target-Constrained Interference-Minimized Filter (TCIMF)
8. Mixture Tuned Target-Constrained Interference-Minimized Filter (MTTCIMF):

All eight methods were tested, and the spectral match results were rescaled to greater than 0 and summed equal to 1 with the aim of subsequently comparing the distributions in the spatial dimension. A description of the ACE method is given in the next section as an example of the matching methodology involved. This method was eventually selected for the matching analysis. The basis for this selection is discussed in the Results section.

Adaptive Coherence Estimator (ACE)

According to Manolakis (2002), the ACE is calculated as follows:

$$\mathbf{D}_{ACE}(\mathbf{x}) = \frac{\mathbf{x}^T \hat{\Gamma}^{-1} \mathbf{S} (\mathbf{S}^T \hat{\Gamma}^{-1} \mathbf{S})^{-1} \mathbf{S}^T \hat{\Gamma}^{-1} \mathbf{x}}{\mathbf{x}^T \hat{\Gamma}^{-1} \mathbf{x}} \quad (5)$$

Where \mathbf{x} is the Hyper-spectral image pixel, $\hat{\Gamma}$ is the covariance estimation of \mathbf{x} , \mathbf{S} is the species spectrum template (Farrell, et al., 2005). If an adaptive whitening transformation is applied $\tilde{\mathbf{x}} \triangleq \hat{\Gamma}^{1/2} \mathbf{x}$, where $\hat{\Gamma} \triangleq \hat{\Gamma}^{1/2} \hat{\Gamma}^{1/2}$, the ACE can be expressed as (Manolakis, 2002)

$$\mathbf{D}_{ACE}(\mathbf{x}) = \frac{\tilde{\mathbf{x}}^T \tilde{\mathbf{S}} (\tilde{\mathbf{S}}^T \tilde{\mathbf{S}})^{-1} \tilde{\mathbf{S}}^T \tilde{\mathbf{x}}}{\tilde{\mathbf{x}}^T \tilde{\mathbf{x}}} = \frac{\tilde{\mathbf{x}}^T \mathbf{P}_{\tilde{\mathbf{S}}} \tilde{\mathbf{x}}}{\tilde{\mathbf{x}}^T \tilde{\mathbf{x}}} \quad (6)$$

Where $\tilde{\mathbf{S}} \triangleq \hat{\Gamma}^{-1/2} \mathbf{S}$ and $\mathbf{P}_{\tilde{\mathbf{S}}} \triangleq \tilde{\mathbf{S}} (\tilde{\mathbf{S}}^T \tilde{\mathbf{S}})^{-1} \tilde{\mathbf{S}}^T$ is the projection of estimated species spectrum $\tilde{\mathbf{S}}$. Since $\mathbf{P}_{\tilde{\mathbf{S}}}^2 = \mathbf{P}_{\tilde{\mathbf{S}}}$, The ACE can be written as (Manolakis, 2002)

$$\mathbf{D}_{ACE}(\mathbf{x}) = \frac{\|\mathbf{P}_{\tilde{\mathbf{S}}} \tilde{\mathbf{x}}\|^2}{\|\tilde{\mathbf{x}}\|^2} = \mathbf{cos}^2 \theta \quad (7)$$

Which shows that $\mathbf{D}_{ACE}(\mathbf{x})$ is equal to the square cosine of the angle between the hyperion pixel and the species spectrum subspace into the whitened coordinate space (Figure 42) (Manolakis, 2002).

As dry grass dominant the research area at most of the growing season, abundance of vegetation is relatively low and variation among species is also depressed. With the purpose of species abundance comparison, conditional probabilities of individual species are calculated:

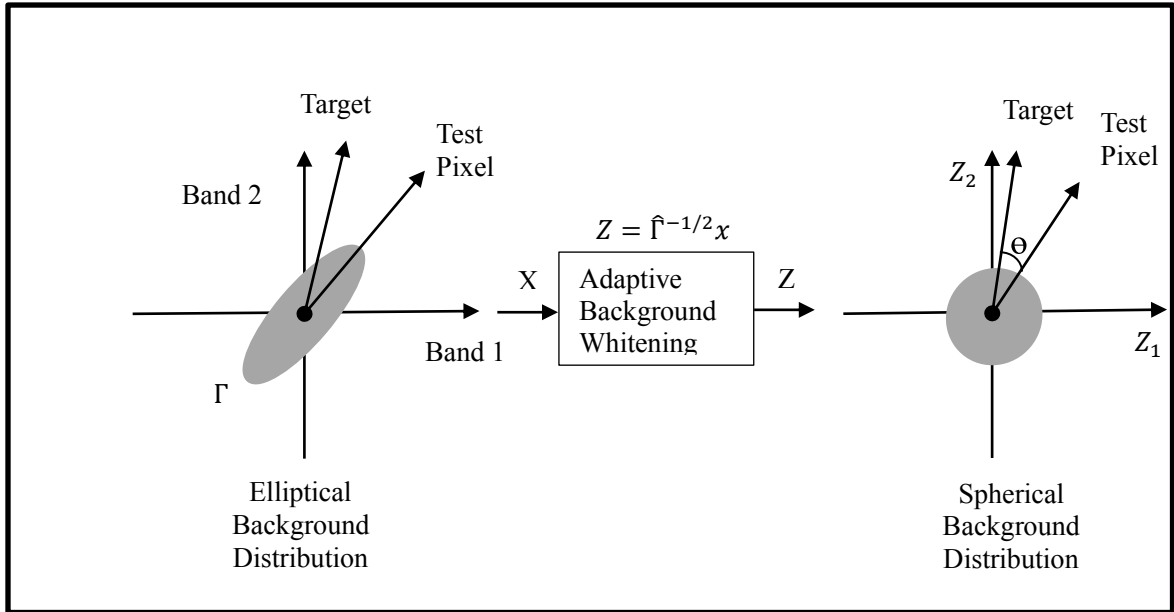


Figure 42 Illustration of ACE detector (Manolakis, 2002)

$$P(\mathbf{S}_i | \neg \mathbf{D}) = \frac{P(\mathbf{S}_i)}{1 - P(\mathbf{D})} \quad (8)$$

Dominance Analysis

The conditional probabilities suggested relative proportion among species. However, all species in spectral library are assigned a score which suggests that it is possible for every species to appear in each pixel. This is partly because of correlation between species spectrum as well as some limitations of the algorithm. As a result, it is valuable to estimate if the pixel spectrum is very close to single species spectrum, in other words, if there is a dominate species within the pixel area. Therefore, another two parameters were derived for measuring dominance. “Level of Dominance” calculates the difference

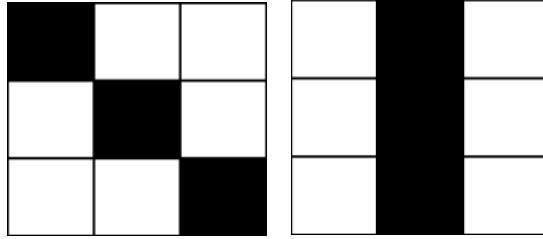
between the highest proportion and the average of the rest of the proportions. “Band Variance” is the variance of all proportions within each pixel. A high “level of dominance” or a high “band variance” is an indicator of pixels with a more dominant spectral identity associated with a single species.

Texture Co-occurrence Measurements: Spatial Grain

Once the species combination is estimated within a pixel, additional information may be gained from analyzing the spatial relationships of species combinations and dominance for the wider region, since this integrates among individual pixels and shows more information about grassland structure like the patch distribution. The analysis is based on the following assumption:

1. Native Prairie is more likely to be multispecies mixed, thus “Level of Dominance” and “Band variance” are supposed to be low.
2. Disturbed area is more likely to be dominated by invasive species like smooth brome grass, thus “Level of Dominance” and “Band variance” are supposed to be high

Texture co-occurrence measurements are the important characteristics, which have been widely used in identifying objects or regions of interest in an image (Haralick 1973). Textural features contain information about the spatial distribution of tonal variations within an image (Figure 43) (Haralick 1973). The concept of tone is based on the varying shades of gray of resolution cells in an image (Haralick 1973). Four angular (0 degrees, 45 degrees, 90 degrees, 135 degrees) are most commonly used based on the nearest-neighbor gray-tone (Figure 44).



a) Texture example 1 b) texture example 2
Figure 43 Example of image texture

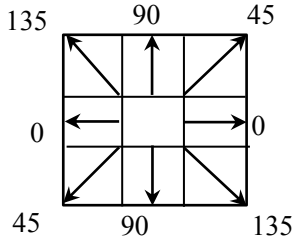


Figure 44 Illustration of four nearest-neighbor (distance is 1 pixel) directions

It is first assumed that the texture features is specified by the grey-level co-occurrence matrices (GLCM's) P_{ij} which counts frequencies of two neighboring cells separated by distance d within given window, one with gray-level i and the other with gray-level j . Thus the location in GLCM indicates level of differences and the value counts times of the differences appeared in distance d . Figure 45 illustrates the gray-tone spatial-dependence matrix in all four distance 1.

0	0	1	1
0	0	1	1
0	2	2	2
2	2	3	3

(a)

		Grey Tone			
		0	1	2	3
Grey Tone	0	(0,0)	(0,1), (1,0)	(0,2),(2,0)	(0,3),(3,0)
	1	(0,1), (1,0)	(1,1)	(1,2),(2,1)	(1,3),(3,1)
	2	(0,2),(2,0)	(1,2),(2,1)	(2,2)	(2,3),(3,2)
	3	(0,3),(3,0)	(1,3),(3,1)	(2,3),(3,2)	(3,3)

(b)

$$P_H = \begin{pmatrix} 4 & 2 & 1 & 0 \\ 2 & 4 & 0 & 0 \\ 1 & 0 & 6 & 1 \\ 0 & 0 & 1 & 2 \end{pmatrix} \quad P_V = \begin{pmatrix} 6 & 0 & 2 & 0 \\ 0 & 4 & 2 & 0 \\ 2 & 2 & 2 & 2 \\ 0 & 0 & 2 & 0 \end{pmatrix}$$

(c) (d)

$$P_{LD} = \begin{pmatrix} 2 & 1 & 3 & 0 \\ 1 & 2 & 1 & 0 \\ 3 & 1 & 0 & 2 \\ 0 & 0 & 2 & 0 \end{pmatrix} \quad P_{RD} = \begin{pmatrix} 4 & 1 & 0 & 0 \\ 1 & 2 & 2 & 0 \\ 0 & 2 & 4 & 1 \\ 0 & 0 & 1 & 0 \end{pmatrix}$$

(e) (f)

Figure 45 (a) 4 by 4 image with four gray-tone values 0-3; (b) General form of any gray-tone spatial-dependence matrix for image with gray-tone values 0-3; (c)-(f) Calculation of all four distance 1 gray-tone spatial-dependence matrices.

Then seven common grey-level texture features (Table 3) are tested in this study. These statistics extract two fundamental characteristics from the spatial-dependence matrix (Clausi et al., 1998): the degree of smoothness of the image in certain directions, such as dissimilarity, contrast and homogeneity; the uniformity of the image, such as second moment and entropy.

Scale determination is the first task for spatial exploring. In this case, since section is the fundamental unit of land management, three sub section scales are tested: 90X90m (3X3 pixels, about 1/18X1/18 miles); 270X270m (9X9 pixels, about 1/6X1/6 miles); 810X810m (27X27 pixels, about 1/2X1/2 miles – this is approximately a quarter section). Only late growing season images are tested because of more abundant patches information at this period and just zero degree directional factors are processed at this stage.

Table 3 Texture Statistics defined i, j are row and column

Mean	$\mu_i = \sum_{i,j=0}^{N-1} i(P_{i,j})$	$\mu_j = \sum_{i,j=0}^{N-1} j(P_{i,j})$
Variance	$\sigma_i^2 = \sum_{i,j=0}^{N-1} P_{i,j}(i - \mu_i)^2$	
Homogeneity	$\sigma_i^2 = \sum_{i,j=0}^{N-1} P_{i,j}(i - \mu_i)^2$	
Contrast	$\sum_{i,j=0}^{N-1} \frac{P_{i,j}}{1 + (i - j)^2}$	
Dissimilarity	$\sum_{i,j=0}^{N-1} P_{i,j}(i - j)^2$	
Entropy	$\sum_{i,j=0}^{N-1} P_{i,j} i - j $	
Second Moment	$\sum_{i,j=0}^{N-1} P_{i,j}(-\ln P_{i,j})$	
	$\sum_{i,j=0}^{N-1} (P_{i,j})^2$	

Results

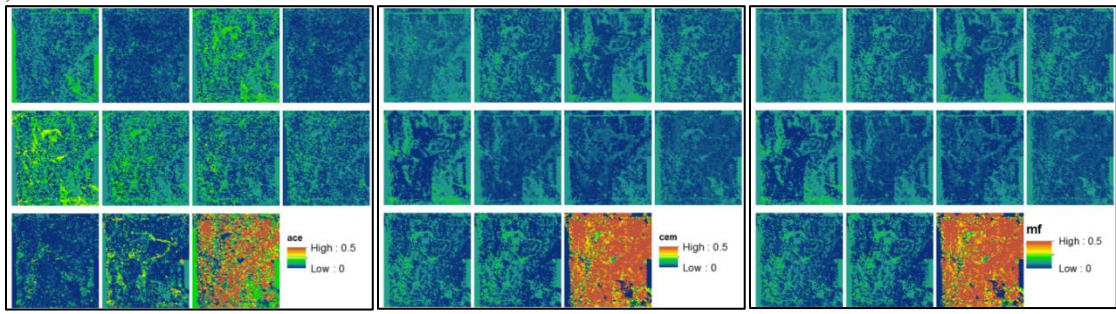
Matching

The first criteria of method selection is based on the assumption that in the early growing season, most green grass has not grown in May and prairie is mainly covered by dry grass. Among the methods, OSP, however, provides a high score for June grass, as do TCIMF and MTTCIMF for sage for May 20 2010 (Figure 46). The TCIMF and MTTCIMF methods failed to detect dry grass as highest score (Figure 47). The CEM, MF and MTMF methods, on the other hand, detect little difference in species distribution information for May 24 2009 (Figure 47). Many species are growing vigorously in August and some patches become very distinct at this stage of growing season. The ACE, CEM, MF, MTMF and SAM methods all identify similar patch information, with

especially ACE and MTMF detecting more variation (Figure 48). Early in the growing season, the most fractional cover component in the grassland at Woodworth is supposed to be dry grass. Only the ACE, CEM, MF and MTMF methods provided reasonable results (Figure 49; Figure 50). From the early growing season analysis, two methods, ACE and MTMF, gave the best discrimination.

When comparing matching approaches later in the growing season, a method with higher sensitivity to individual species spectra is required. The ACE method identified more variation within a single match image, and more variation among species maps (Figure 51; Figure 52). Conversely, the CEM, SAM, TCIMF, MTTCIMF and MF showed little variation among species possibility for Maximilian Sunflower, cord grass, and wheat grass, for example (Figure 51, Figure 52). This suggested that CEM and MF were not effective at detecting any patches containing these species. Although the MTMF method identifies variation within each possibility map, the pattern of this variation is very similar between species maps (Figure 51, Figure 52). Hence, MTMF method is barely distinguishing species from each other. The OSP method in both Oakville and Woodworth (Figure 51, Figure 52), and the TCIMF and MTTCIMF methods at Woodworth (Figure 52) predict a wide distribution of certain native species like June grass or sage willow, which is not agreement with field observation. As a result, it was clear that the ACE method was the most sensitive method available, and the results of the ACE analysis were used in the subsequent work.

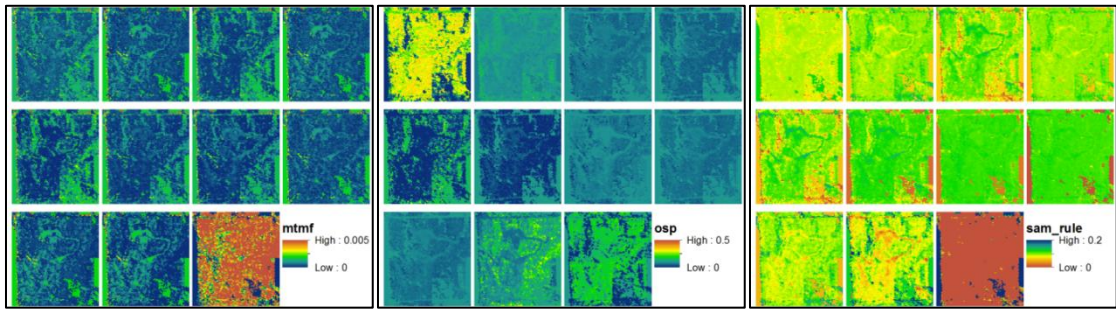
A)



a ACE

b CEM

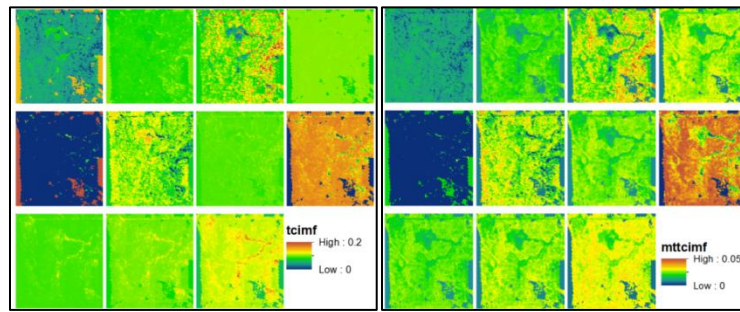
c MF



d MTMF

e OSP

f SAM



g TCIMF

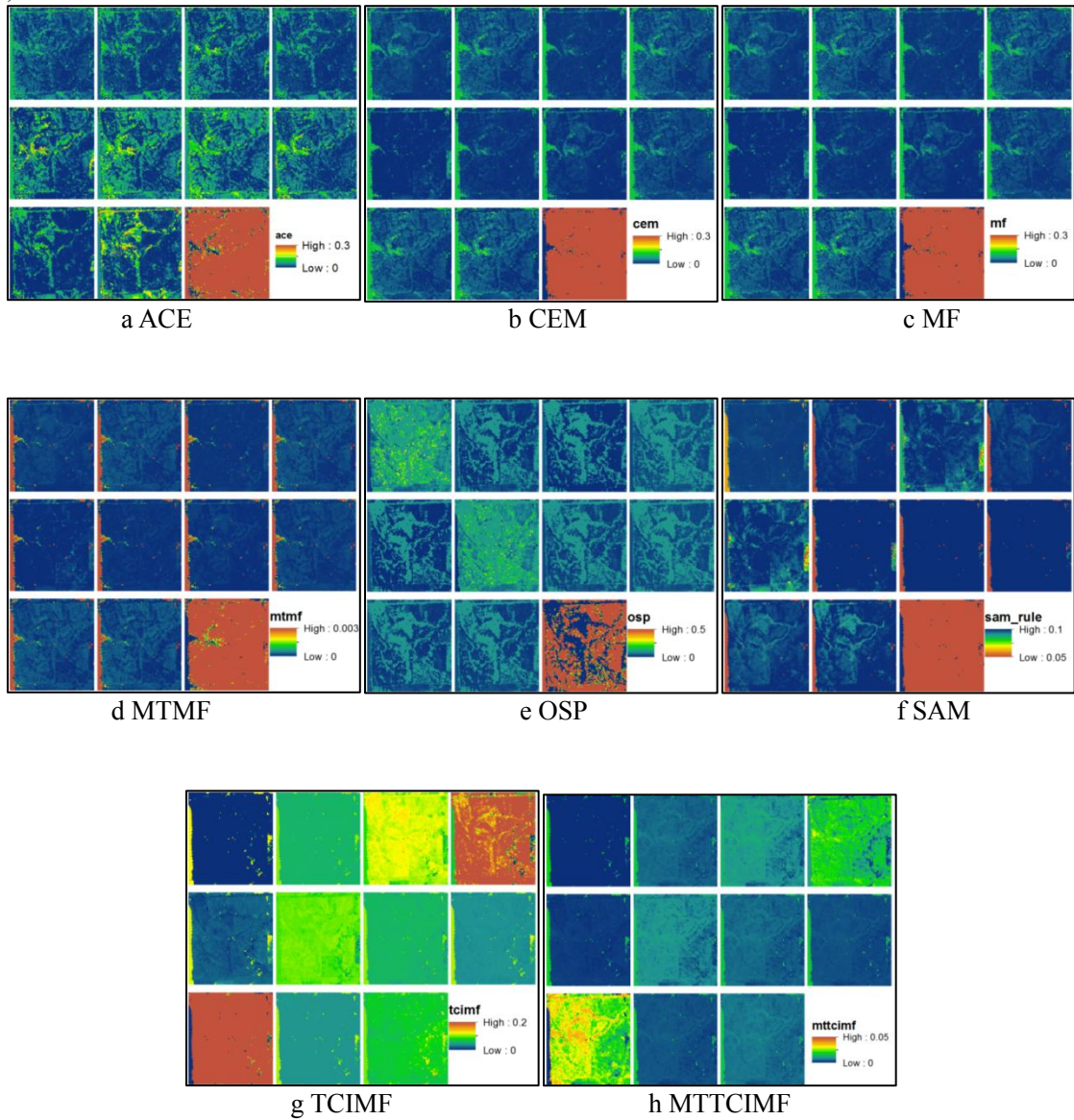
h MTTTCIMF

June Grass	Maximilian Sunflower	Cord Grass	Wheat Grass
Wild rye	Brome Grass	Kentucky Blue Grass	Sage
Sage Willow	Thistle	Dry Grass	

B)

Figure 46 A) Methods test of Oakville May 20 2010. For each method, 11 endmembers are included. B) Legend for data layers.

A)

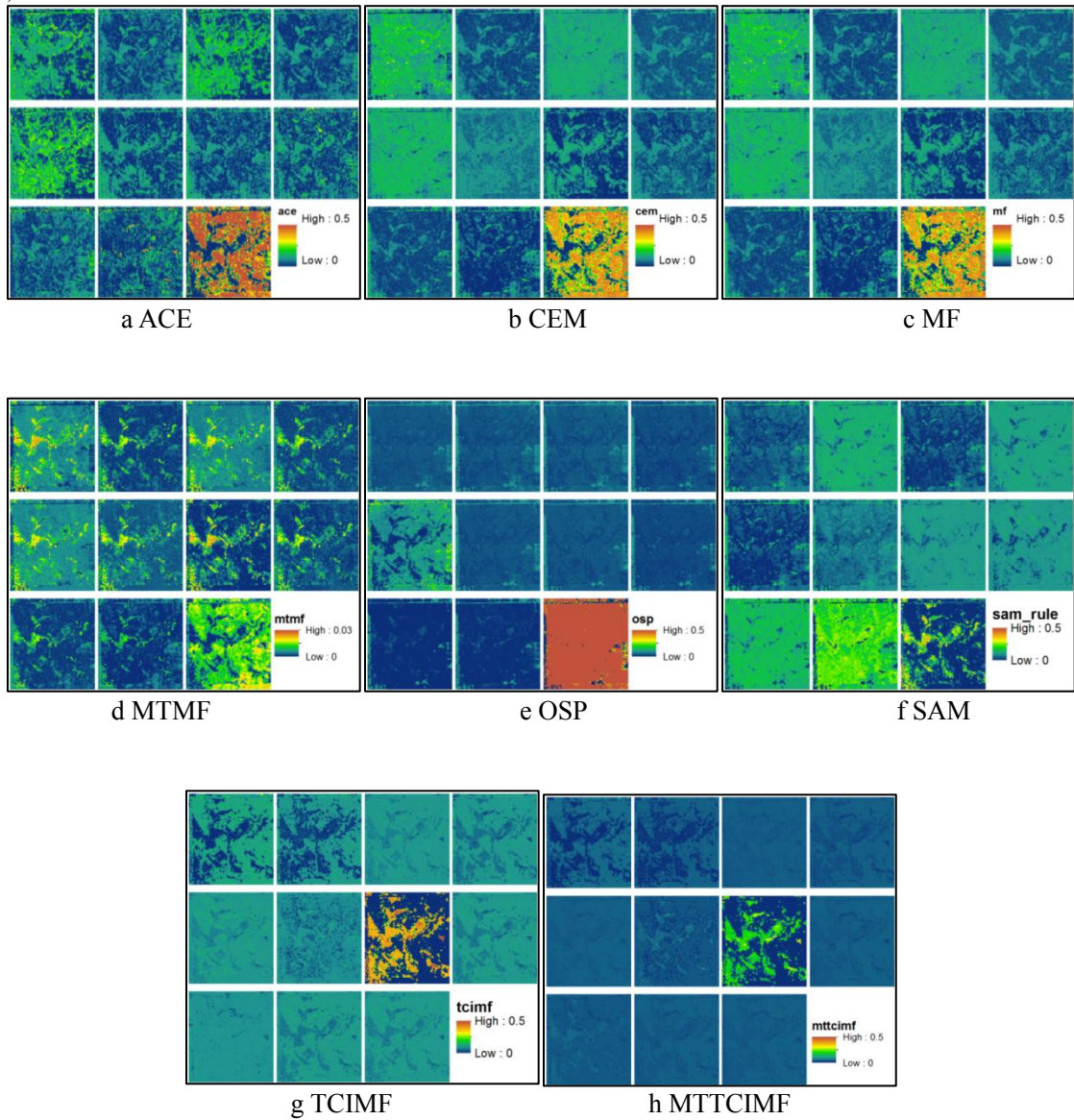


June Grass	Maximilian Sunflower	Cord Grass	Wheat Grass
Wild rye	Brome Grass	Kentucky Blue Grass	Sage
Sage Willow	Thistle	Dry Grass	

B)

Figure 47 A) Methods test of Oakville May 24 2009. For each method, 11 endmembers are included. B) Legend for data layers.

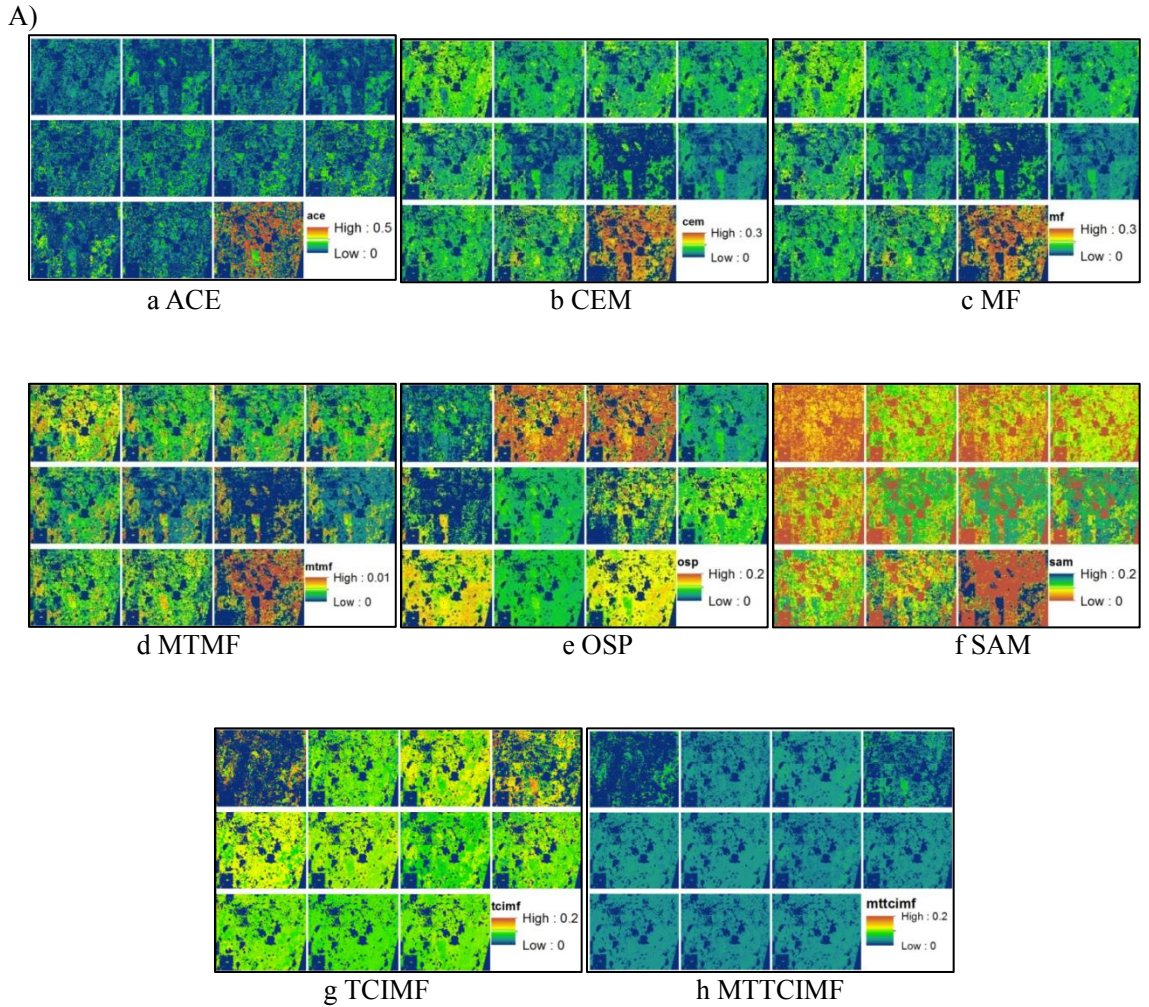
A)



June Grass	Maximilian Sunflower	Cord Grass	Wheat Grass
Wild rye	Brome Grass	Kentucky Blue Grass	Sage
Sage Willow	Thistle	Dry Grass	

B)

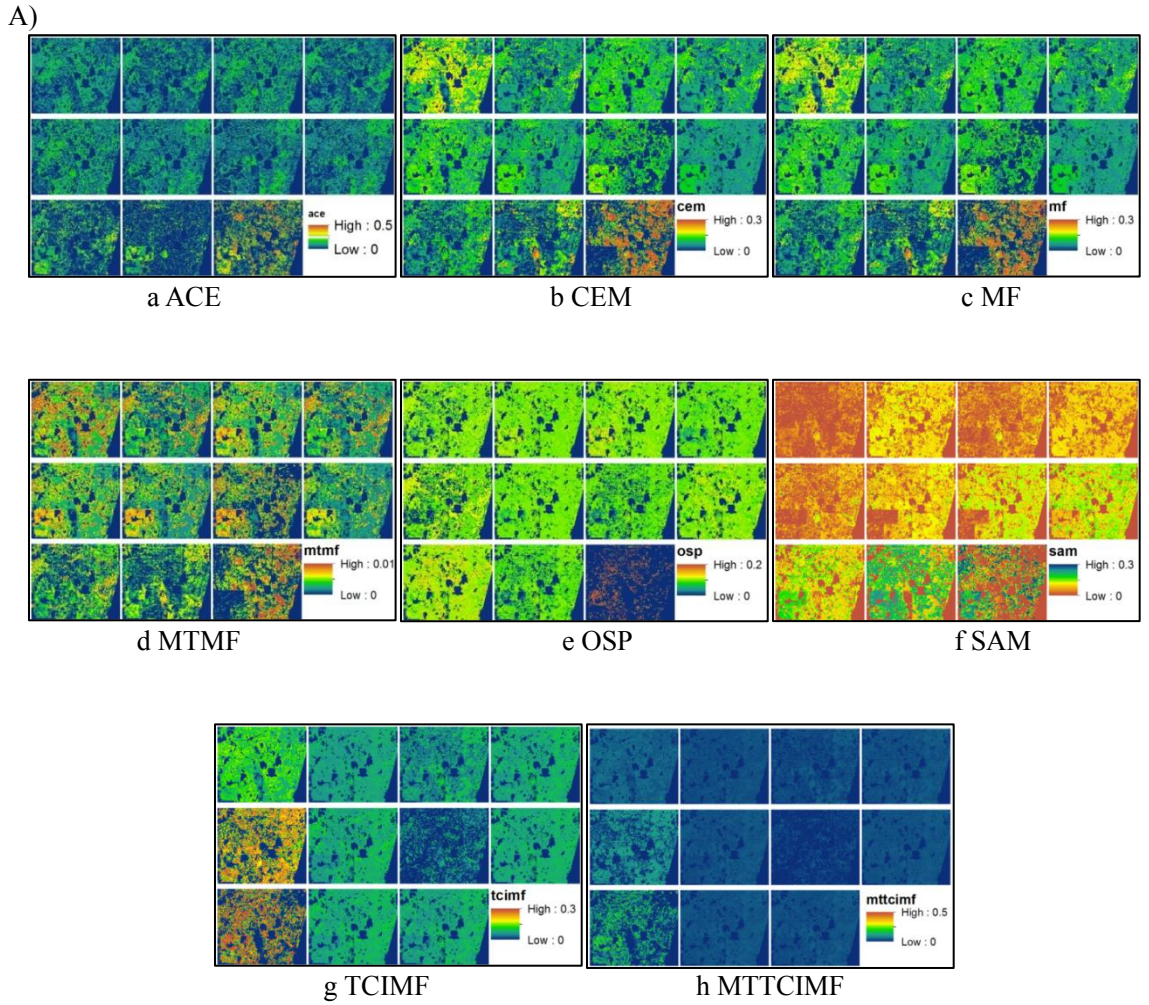
Figure 48 A) Methods test of Oakville August 08 2010. For each method, 11 endmembers are included. B) Legend for data layers.



June Grass	Maximilian Sunflower	Cord Grass	Wheat Grass
Wild rye	Brome Grass	Kentucky Blue Grass	Sage
Sage Willow	Thistle	Dry Grass	

B)

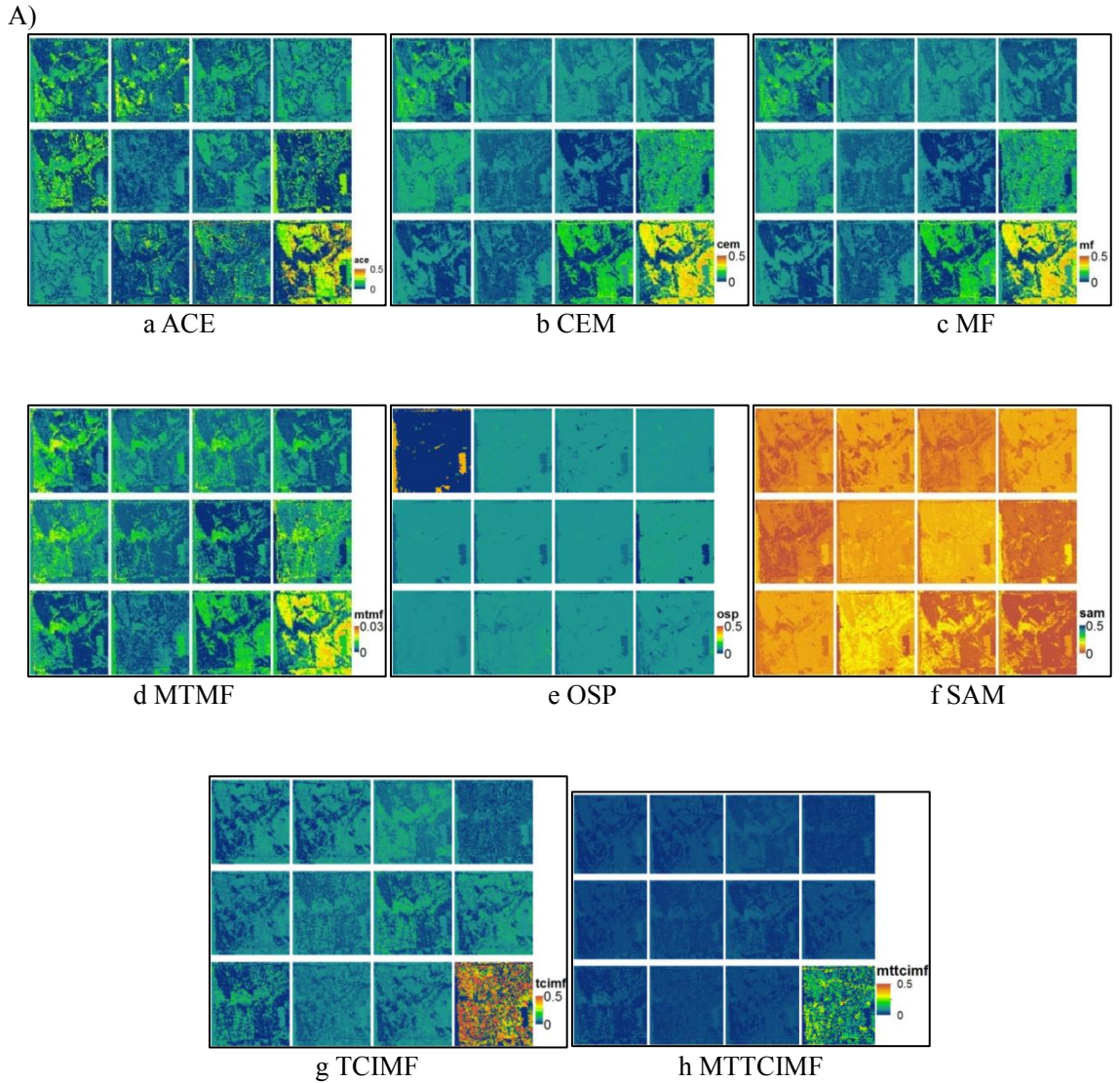
Figure 49 A) Methods test of Woodworth June 04 2010. For each method, 11 endmembers are included. B) Legend for data layers.



June Grass	Maximilian Sunflower	Cord Grass	Wheat Grass
Wild rye	Brome Grass	Kentucky Blue Grass	Sage
Sage Willow	Thistle	Dry Grass	

B)

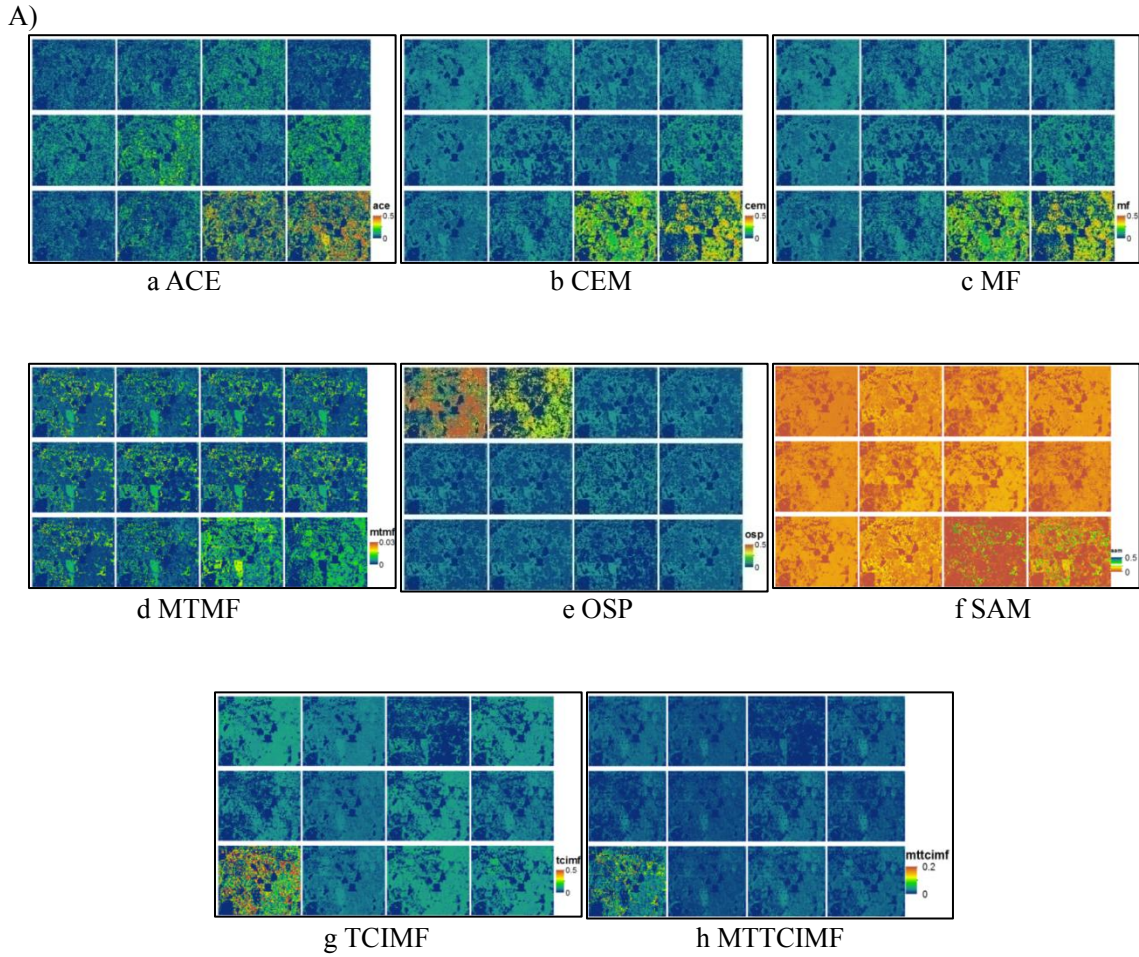
Figure 50 A) Methods test of Woodworth June 29 2009. For each method, 11 endmembers are included. B) Legend for data layers.



June Grass	Maximilian Sunflower	Cord Grass	Wheat Grass
Wild rye	Brome Grass Green	Brome Grass Flowering	Sage
Sage Willow	Thistle Green	Thistle Flowering	Dry Grass

B)

Figure 51 A) Methods test of Oakville September 01 2009. For each method, 12 endmembers are included. B) Legend for data layers.



June Grass	Maximilian Sunflower	Cord Grass	Wheat Grass
Wild rye	Brome Grass Green	Brome Grass Flowering	Sage
Sage Willow	Thistle Green	Thistle Flowering	Dry Grass

B)

Figure 52 A) Methods test of Woodward September 18 2009. For each method, 12 endmembers are included. B) Legend for data layers.

Level of Dominance and Band Variance

Early in the growing season, both “Level of Dominance” and “Band Variance” show little difference across Oakville Prairie and the surrounding area (Figure 57, Figure 58). However, by August and September, the saline grassland areas of Oakville Prairie showed noticeably lower “level of dominance” than the other areas (Figure 57, Figure 58). A high score of “level of Dominance” was obtained for the School Trust Land area at Oakville (Figure 57, Figure 58). At the Woodworth site, including the restored area, the “Level of Dominance” showed highly score throughout the whole growing season (Figure 57). The indicator “Band Variance” was somewhat less sensitive than “Level of Dominance”. However, “Band Variance” did show less spatial variation of score in the restored area compared with other places of Woodworth (Figure 58).

Scatter plots of “Level of Dominance” versus “Band Variance”(Figure 59) show some degree of correlation, but also a high degree of scatter at higher values, and a curvilinear trend that reveals a very high level of variation in “Band Variance” for a given “Level of Dominance” value.. “Band Variance” has lower value range, but shows more detailed information on high dominant area and less information on less dominant area compared with “Level of Dominance”.

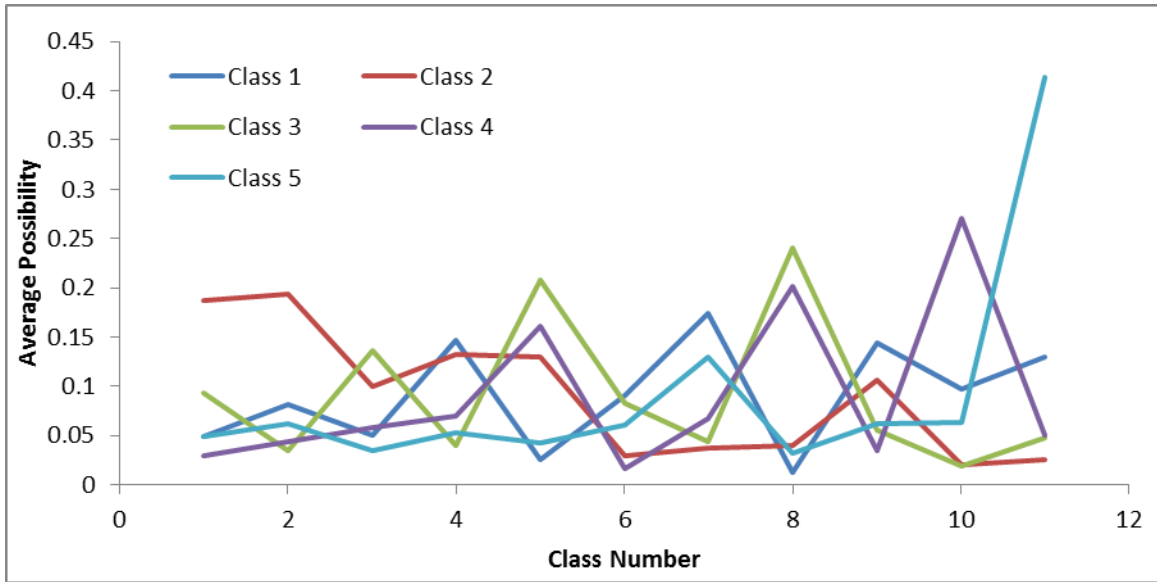


Figure 53 Mean Possibility of Species in Oakville September 01 2009. (X axis from 1 to 11 are June grass; Maximilian Sunflower; Cord grass; Wheat grass; Wild rye; Brome grass green; Brome grass flowering; Sage; Sage Willow; Thistle green; Thistle flowering)

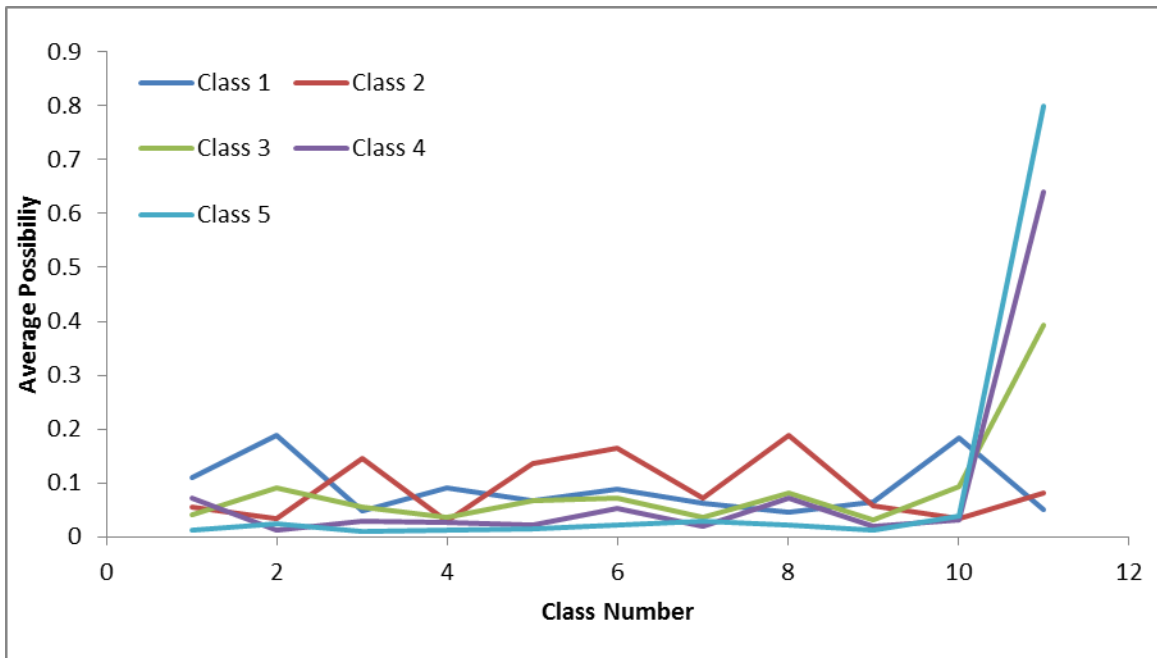


Figure 54 Mean Possibility of Species in Woodworth September 18 2009. (X axis from 1 to 11 are June grass; Maximilian Sunflower; Cord grass; Wheat grass; Wild rye; Brome grass green; Brome grass)

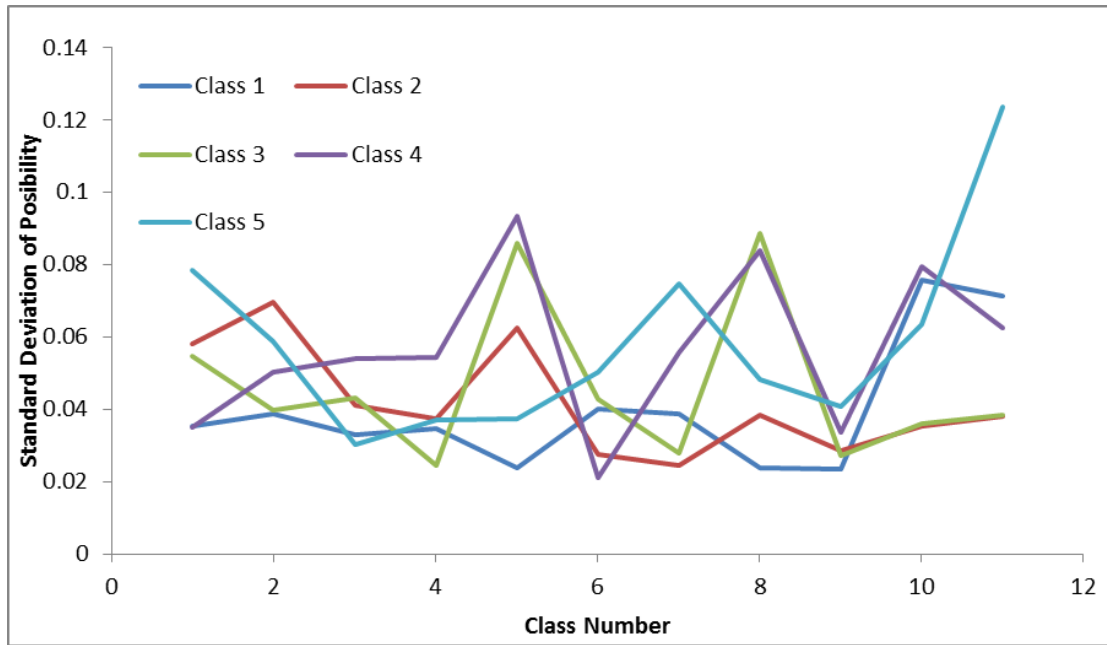


Figure 55 Possibility Standard Deviation of Species in Oakville September 01 2009. (X axis from 1 to 11 are June grass; Maximilian Sunflower; Cord grass; Wheat grass; Wild rye; Brome grass green; Brome grass flowering; Sage; Sage Willow; Thistle green; Thistle flowering)

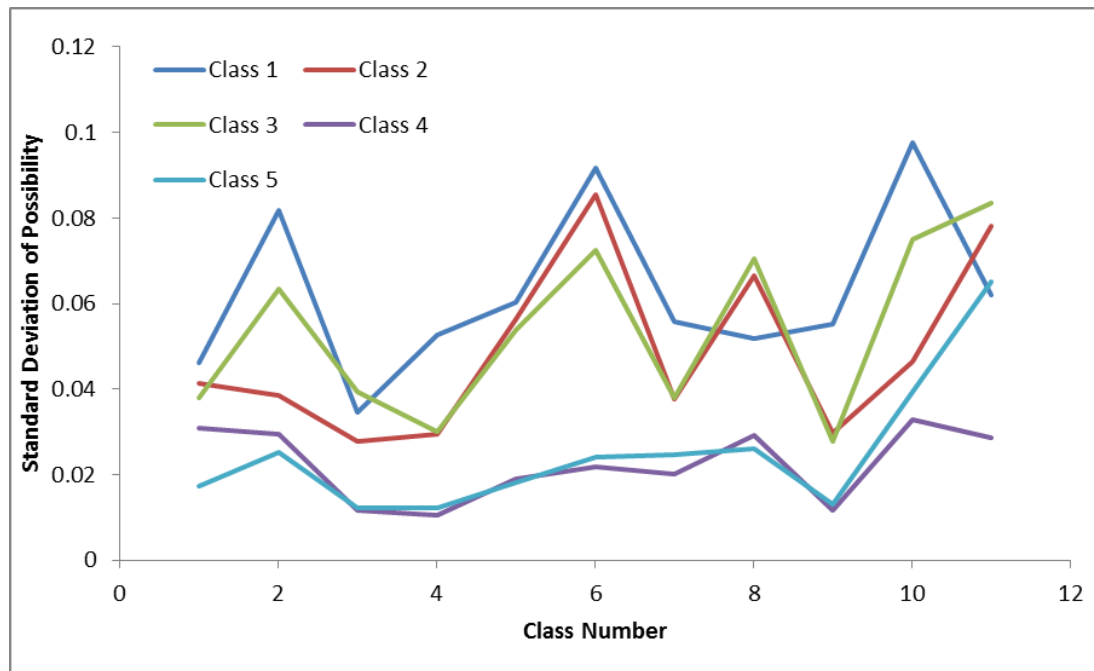
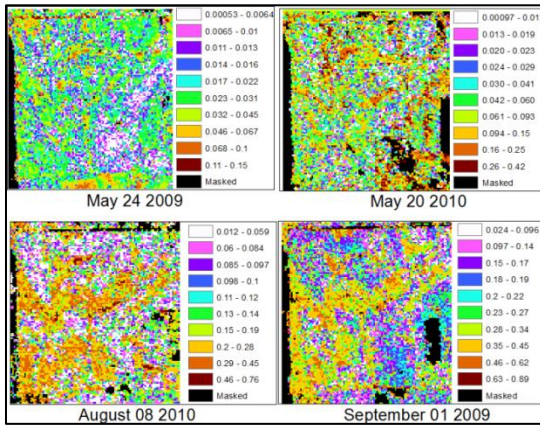
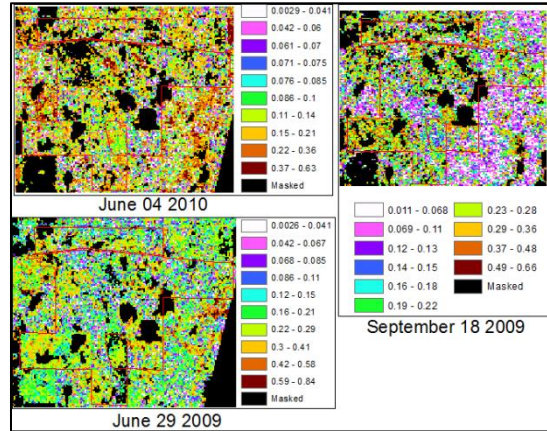


Figure 56 Possibility Standard Deviation of Species in Woodworth September 18 2009. (X axis from 1 to 11 are June grass; Maximilian Sunflower; Cord grass; Wheat grass; Wild rye; Brome grass green; Brome grass flowering; Sage; Sage Willow; Thistle green; Thistle flowering)

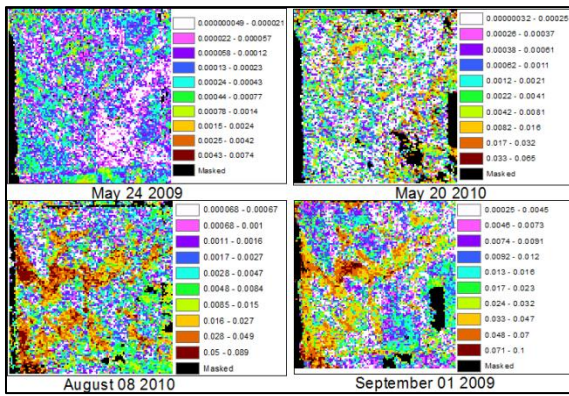
Dominance



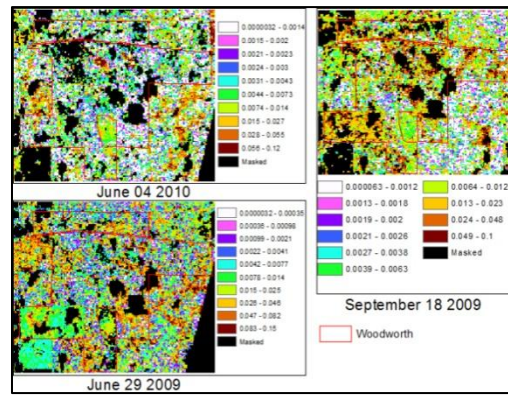
a Oakville
Figure 57 Level of Dominance



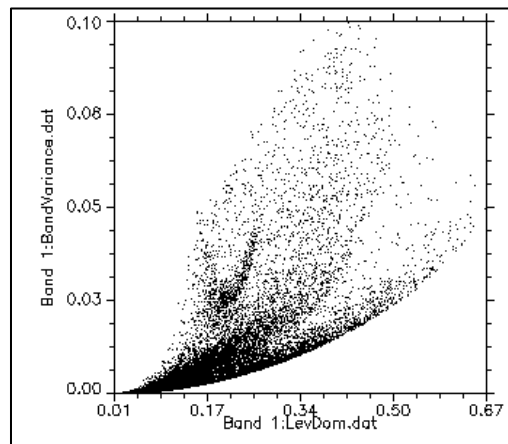
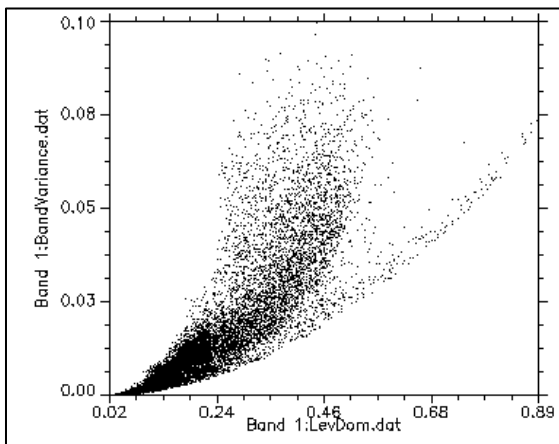
b Woodworth



a Oakville
Figure 58 Band Variance



b Woodworth



Oakville (September 01 2009) Woodworth (September 18 2009)
Figure 59 Scatter Plot of Band Variance and Level of Dominance in Oakville and Woodworth

Texture Co-Occurrence

The texture co-occurrence analysis shows (Figure 60) that the images from the 90x90m scale analysis contain many small patches and do not provide sufficient generalization of spatial patterns and barely any variation in other factors. The textural analysis at 810x810m scale, however, removes all patch information. The 270x270m scale, by contrast, extracted spatial patterns with reasonable detail in the “Mean” statistics and also revealed variation in other factors (e.g., variance, contrast and dissimilarity). Therefore, the texture layers at 270x270m scale were selected for further analysis. Based on a further comparison among texture features at the 270x270m scale, four properties (Mean, Variance, Dissimilarity, and Contrast) were selected based on value range and patches sensitivity.

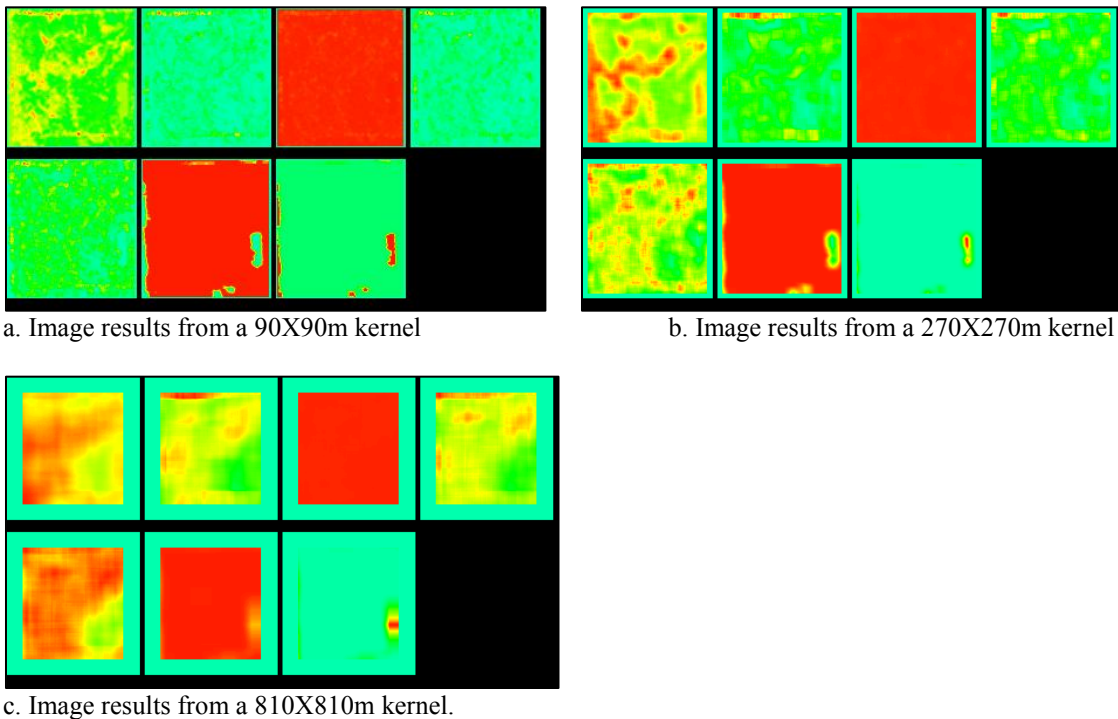
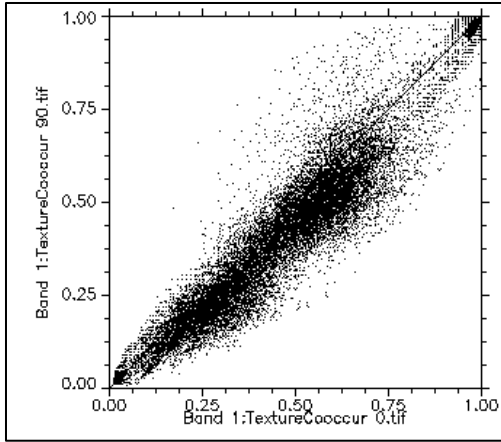
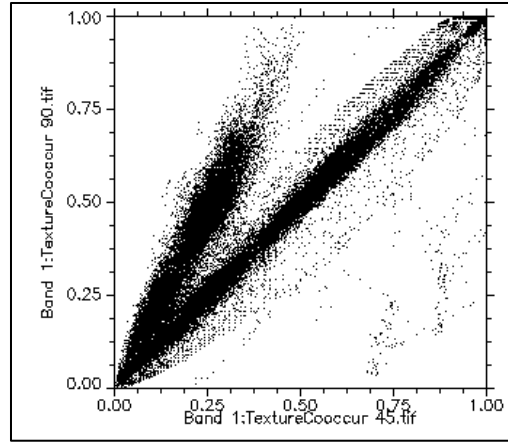


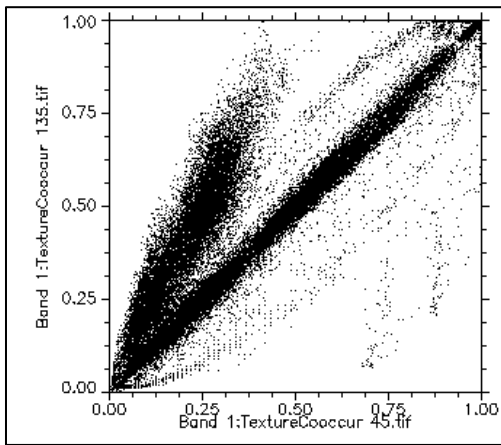
Figure 60 Texture Co-occurrence measurements of level dominance in Oakville September 01 2009 (Upper from left to right: mean, variance, homogeneity, contrast; Bottom from left to right: dissimilarity, entropy, second moment)



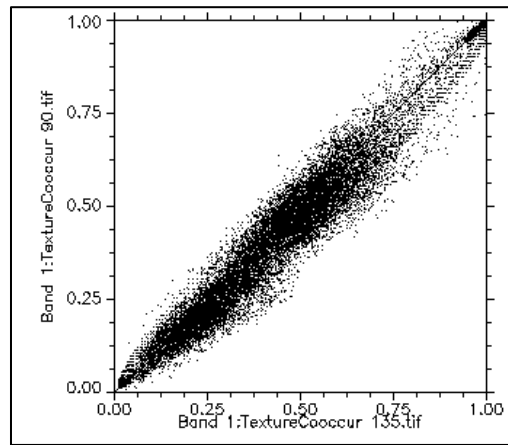
a 0 degree versus 90 degree texture features



b 45 degree versus 90 degree texture features



c 45 degree versus 135 degree texture features

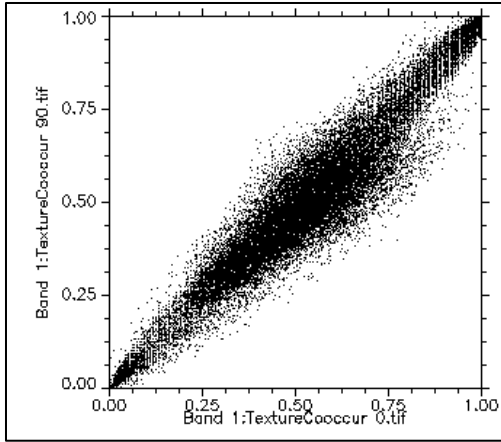


d 135 degree versus 90 degree texture features

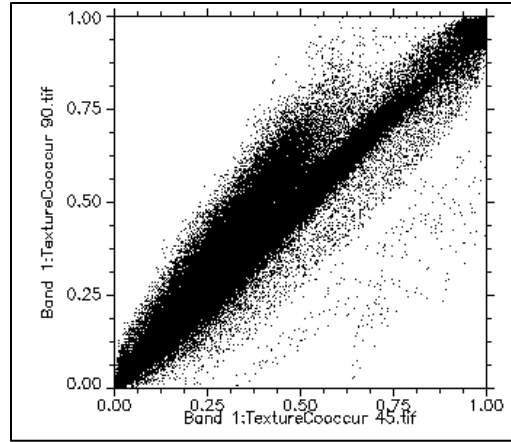
Figure 61 Scatter plot of Texture co-occurrence measurements in multi directions for level dominance in Oakville for September 1, 2009.

As mentioned above, texture co-occurrence can estimate spatial relationships in different directions. In this case, four main directions were tested and plotted in order to examine if there were any significant differences due to directional features.

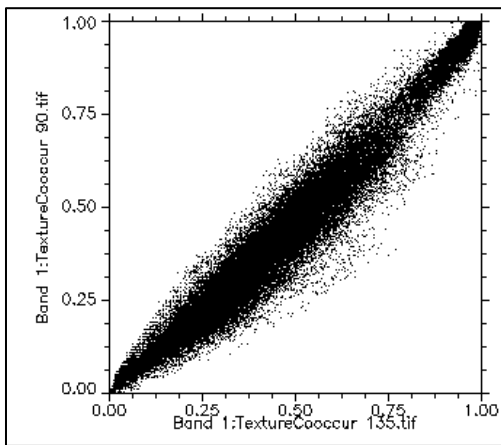
The texture co-occurrence measurements were linearly distributed in three directions (0, 90, 135; Figure 61, Figure 62). This means that all those three direction show similar spatial patterns, but there are some disagreements for the 45 degree direction. Based on



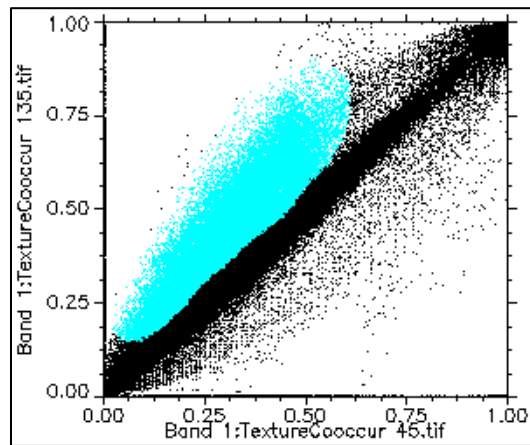
a 0 degree versus 90 degree texture features



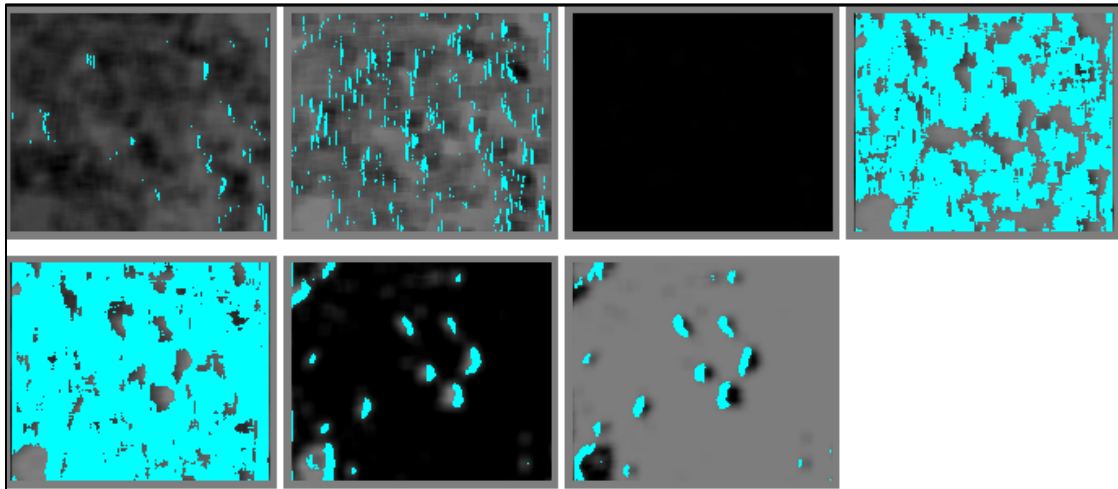
b 45 degree versus 90 degree texture features



c 135 degree versus 90 degree texture features



d 45 degree versus 135 degree texture features.



e Texture Co-occurrence measurements at 45 degrees.

Figure 62. Scatter plot of texture co-occurrence measurements in multi directions for level dominance in Woodward September 18 2009. The cyan area suggests disagreements between 45 degree and 135 degree measurements.

the classification result (Figure 62 e), the disagreement mainly comes from ‘contrast’ and ‘dissimilarity’ measurements which show an overall low value in 45 degree direction in both Oakville and Woodworth. This disagreement may come from landscape differences, and thus is treated as background information and not be considered in the subsequent analysis. In order to minimize the background effect, the 135 degree texture features were used in the following analysis.

Discussion

Eight spectral matching methods were tested. The matching results were relatively poor for most of the methods. The high correlation between species spectra (Andrew & Ustin, 2008) the relatively low spatial resolution (Underwood et al., 2007), and modest SNR of the Hyperion sensor all contribute to the poor matching results. Based on a visual examination of the sensitivity of the methods, in terms of both discrimination within a matching image for a single species, and discrimination between species images, the ACE method was selected as the best method for detecting differences in grassland composition.

The ACE method estimates the possibility of occurrence of each species from the spectral library in each pixel in the image. The classification of species match images provided very different class signatures for possibility values within a pixel between native grassland (Oakville Prairie) and introduced grassland (Woodworth). At Oakville, there is high complexity since there are a lot of different multispecies combinations due to the small, but pure patch structure relative to the pixel resolution (e.g. Andrew & Ustin, 2008). As a result, the algorithm failed to identify high possibilities for individual species and instead assigned similar scores to all species. At Woodworth, most of the area

is dominated by one or a few species. Therefore, the site complexity is relatively low, and the ACE method assigned significantly higher possibility scores to single species.

Using the classification results, the two parameters, “Level of Dominance” and “Band Variance”, were calculated to provide a spectrally derived metric to indicate if the pixel is dominated by a single species. Although the resulting images hardly show any distinctive signatures early in the growing season at both Oakville Prairie and Woodworth, the dominance measures are more useful later in the growing season. At Oakville, in September, a low dominance score is observed on the grass-dominated area where there are many small pure patches of native grasses widely distributed. By contrast, for the southern part of the Oakville Prairie site, there is a large area where the dominance score is much higher. At Woodworth, the whole area, excluding the replanted area, shows generally high dominance score, but with some significant spatial variation.

The spatial texture co-occurrence analysis showed generally low score of “Mean” and “Dissimilarity” at Oakville Prairie, which indicated the grassland is mixture of various grasses at 270 meter scale and none single species dominance. The forb dominated area at south of Oakville Prairie, in contrast, showed high score of “Mean”, which indicate that the grassland is highly dominated by single species. Similar analysis were also performed and presented at the next chapter in order to extract the brome grass dominated area.

CHAPTER VI

NATURALNESS MODELING

In the preceding chapters, image processing, and spectral analysis and matching, have identified a number of image layers that capture various characteristics of the grassland sites. In Chapter 3, fractional cover of green vegetation (NPV), dead or dry vegetation (NPV) and bare soil (BS) were estimated using the methods of (Guerschman et al., 2009). In Chapter 5, field spectral libraries and Hyperion images were used for spectral matching to extract a series of data layers that represent the likelihood of a spectral match for each major species. In addition, data layers were derived that describe the spectral variance and level of dominance of spectral matches. Then finally, data layers describing spatial properties of these spectral match data layers were derived using texture co-occurrence measures.

In this chapter the potential of using these spectral and spatial measures for estimating disturbance of native grassland by introduced species, a measure of grassland naturalness is examined using a spatially-explicit Multi-Criteria Analysis Shell (MCAS-S). The modeling is based on the assumption that Oakville Prairie is completely native i.e. a naturalness level of 100% and that Woodworth is mainly dominated by introduced smooth brome grass i.e. a naturalness level of 0-10%. However, one section of the Woodworth property had been recently replanted with a prairie grassland mixture dominated by native grasses and forbs.

MCAS-S - Multi-Criteria Analysis Shell for Spatial Decision Support

The multi-criteria analysis measures and aggregates a variety of property layers of research area for estimating complex effects in spatial dimension (Lesslie et al., 2008). A multi-criteria analysis provided by MCAS-S is performed in this research. The MCAS-S integrates actual map and cognitive mapping into one workspace window with live update when primary layers are changed (Hill et al., 2005). The MCAS-S provides a histogram based classification which supports up to 10 classes with equal interval, equal area or custom criteria (Hill et al., 2005). There are three functions available for map aggregating: “Composite”, “Two-way”, “Multi-way” (Hill et al., 2005). The Composite function combines layers of interest with different weights. Two-way analysis allows users to explore the association of two classified maps and highlight particular value combinations of the two maps (Hill et al., 2005). The multi-way function rescales input layers into the range of 0 and 1 before combination. Then a grey scale map is created to represent “distance” from a target envelope of values in the input layers (Hill et al., 2005). The MCAS-S is flexible and easy-to-use for land management decision making (Lesslie et al., 2008). For example, MCAS-S has been used to assess development pressures on greenbelts in two North American cities (Hill et al., 2009).

Summary of Potential Input Data Layers for Modeling

A list of previous results is first presented (Figure 63 to Figure 66) and analyzed in order to select the best layers to use in MCAS-S modeling. Several models are then developed based on different concepts. Based on a qualitative assessment, a final modeling approach is chosen. The ability of this model to provide some assessment of grassland naturalness is then tested at an independent field site (Mekinock).

Figure 63 to Figure 66 summarize the spatial data layers (factors) derived from the previous analysis that are available for modeling at Oakville and Woodworth for both early and late in the growing season. Since the data layers usually have different data ranges, each image is first rescaled to 0 to 1 and then stretched to ensure that low values are displayed. Thus, the figures are designed to illustrate variation within images only.

Figure 63 shows the factors derived for Oakville for May 20, 2010. Level of dominance and band variance factors indicate that the area is not dominated by any single species. The majority of layers show little if any patch structure early in the growing season. This is because few species are actively growing at this stage of the year, and the density of green cover is low. The fractional cover of dry grass is very high, while soil fraction is generally low. The green vegetation fraction indicates that part of the area has started to grow. The area of Oakville Prairie is hard to distinguish at this time, while the texture layers show low overall values on northern part of Oakville Prairie, and adjacent school trust land. The low texture values suggest a lack of dominance and high spatial similarity in spectral properties.

Figure 64 shows factors derived for Oakville for September 01, 2009. The level of dominance and band variance factors indicate that there is a relatively high level of spectral diversity on Oakville Prairie and it is not dominated by any single species. There is a spectrally distinct patch located between the Oakville Prairie and School trust land to the south, which is mostly dominated by forbs – it shows a strong match with Maximillian sunflower. The fractional cover layers show high proportions of both dry and green fractions at this latestage of the growing season. Both the ACE spectral matching results and the texture analysis layers show distinct areas of grass-dominated

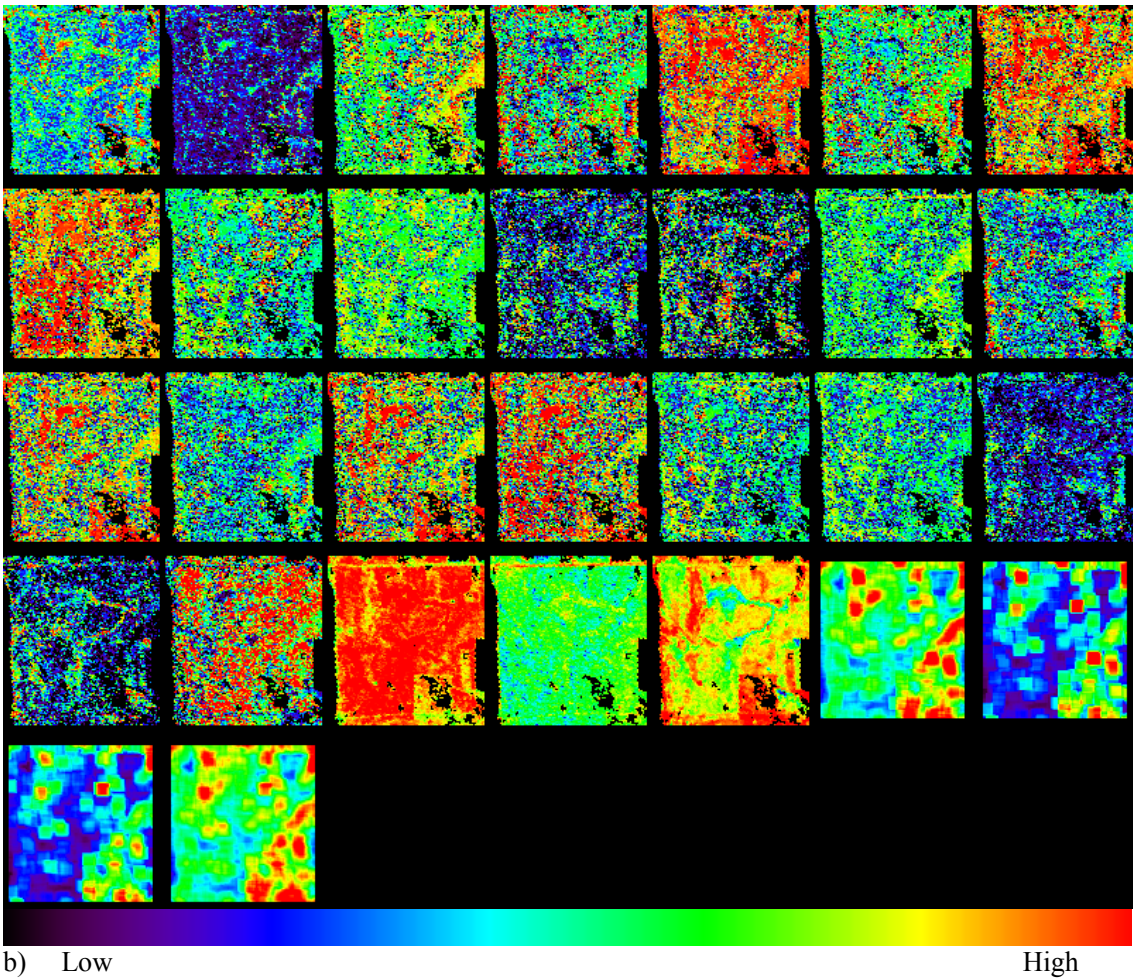
native prairie, an area dominated by forbs and herbs, and the area of School Trust land to the south. Low values in the texture analysis layers for the native prairie area suggest evenly mixed grass and no single species dominates the whole prairie compared with the area apparently dominated by forbs.

Figure 65 shows the factors derived for Woodworth for June 4 2010. Level of dominance and band variance strongly indicate that the area is not dominated by any single species, and the replanted area shows little difference with other areas in Woodworth. The ACE spectral matching results show that the replanted area has more sunflower and wheatgrass and less dry litter, which agrees with the fractional cover analysis: high fraction of green vegetation cover and low fractional cover of dry grass. The texture layers, including contrast and dissimilarity, show little variation within the Woodworth area.

Figure 66 shows the factors derived for Woodworth for September 18, 2010. Level of dominance and band variance show that there is no dominant spectral signature and the replanted area is hardly distinguishable from other parts of Woodworth. The ACE spectral matching results identify a significant match with sunflowers which is consistent with the early growing season ACE result (Figure 65). Unlike the result early in the growing season, the match results for wheatgrass do not highlight the restored area (Figure 66). However, similar to the early season (Figure 65), green fractional cover is high and dry fractional cover is low on the replanted area. The texture layers show low values on the replanted area compared with other area of Woodworth.

Level of Dominance	Variance	Junegrass w/o Dry Grass (DG)	Maximilian Sunflower w/o DG	Cordgrass w/o DG	Wheatgrass w/o DG	Wildrye w/o DG
Bromegrass w/o DG	Kentucky BlueGrass w/o DG	Sage w/o DG	Sage Willow w/o DG	Thistle w/o DG	Junegrass	Maximilian Sunflower
Cordgrass	Wheatgrass	Wildrye	Bromegrass	Kentucky BlueGrass	Sage	Sage Willow
Thistle	Dry grass	Dry grass (Fractional Cover)	Soil	Vegetation	Mean Bandvariance	Variance Bandvariance
Contrast BandVariance	Dissimilarity BandVariance					

a)



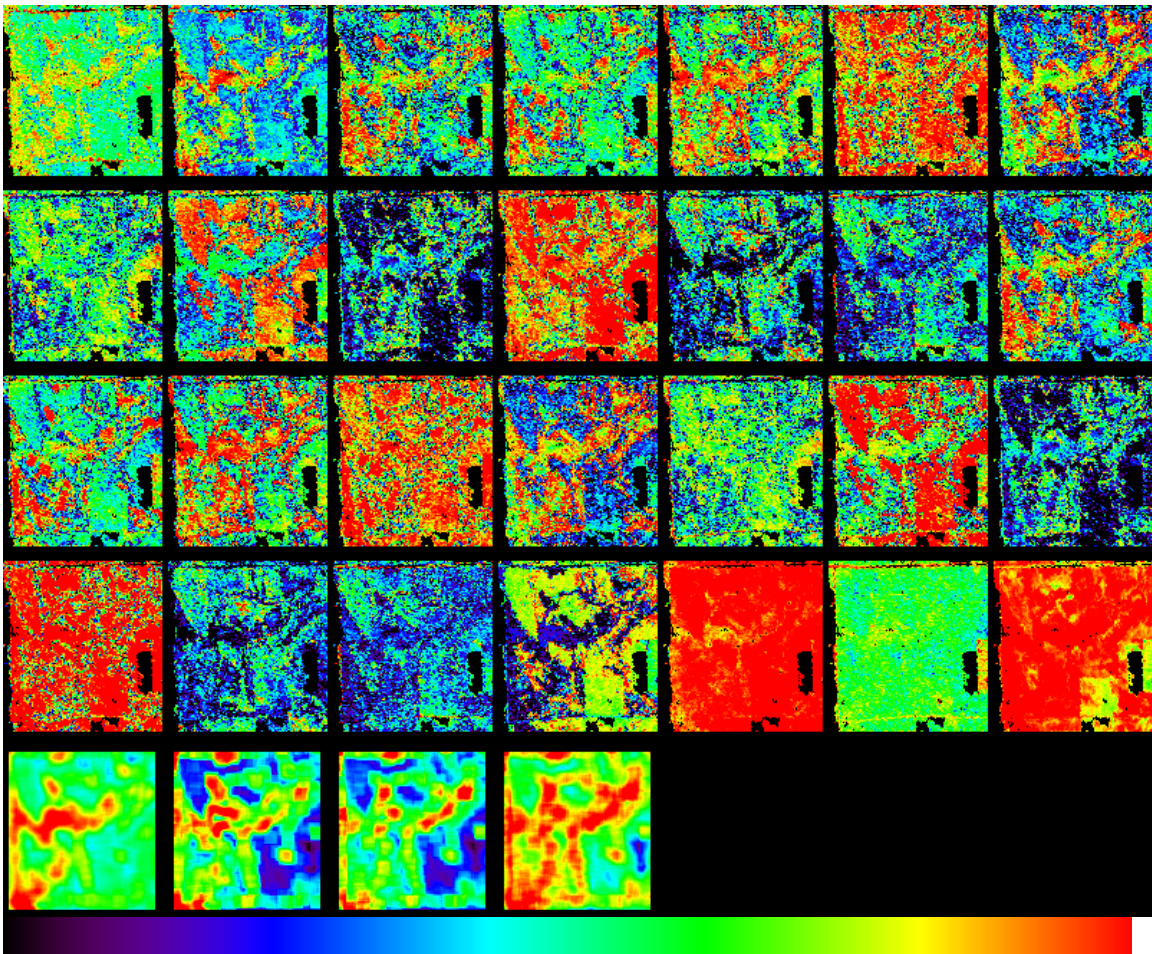
b) Low

High

Figure 63 a) Legend for data layers b) Data layers derived for Oakville site May 20 2010 (Early Growing Season).

Level of Dominance	Band Variance	Junegrass w/o DG	Maximilian Sunflower w/o DG	Cordgrass w/o DG	Wheatgrass w/o DG	Wildrye w/o DG
Brome Grass w/o DG	Brome Grass Flowering w/o DG	Sage w/o DG	Sage Willow w/o DG	Thistle Green w/o DG	Thistle Flowering w/o DG	Junegrass
Maximilian Sunflower	Cordgrass	Wheatgrass	Wildrye	Brome Grass	Brome Grass Flowering	Sage
Sage Willow	Thistle Green	Thistle Flowering	Dry grass	Dry grass (Fractional Cover)	Soil	Vegetation
Mean Bandvariance	Variance Bandvariance	Contrast BandVariance	Dissimilarity BandVariance			

a)



b) Low

High

Figure 64 a) Legend for data layers; b) Data layers derived for Oakville site September 01 2009 (Later Growing Season).

Level of Dominance	Variance	Junegrass w/o Dry Grass (DG)	Maximilian Sunflower w/o DG	Cordgrass w/o DG	Wheatgrass w/o DG	Wildrye w/o DG
Bromegrass w/o DG	Kentucky BlueGrass w/o DG	Sage w/o DG	Sage Willow w/o DG	Thistle w/o DG	Junegrass	Maximilian Sunflower
Cordgrass	Wheatgrass	Wildrye	Bromegrass	Kentucky Blue Grass	Sage	Sage Willow
Thistle	Dry grass	Dry grass (Fractional Cover)	Soil	Vegetation	Mean Bandvariance	Variance Bandvariance
Contrast BandVariance	Dissimilarity BandVariance					

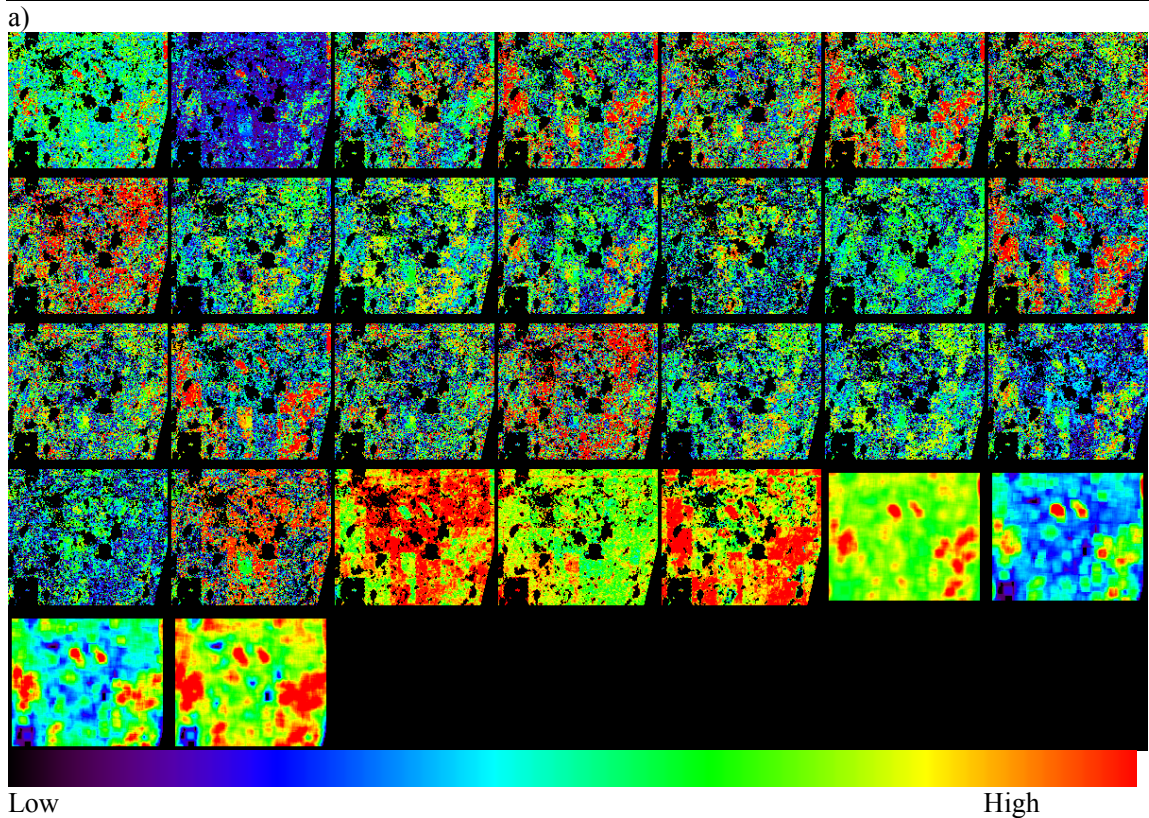


Figure 65 a) Legend for data layers. b) Data layers derived for Woodward site June 04 2010(Early Growing Season).

Level of Dominance	Band Variance	Junegrass w/o DG	Maximilian Sunflower w/o DG	Cordgrass w/o DG	Wheatgrass w/o DG	Wildrye w/o DG
Brome Grass w/o DG	Brome Grass Flowering w/o DG	Sage w/o DG	Sage Willow w/o DG	Thistle Green w/o DG	Thistle Flowering w/o DG	Junegrass
Maximilian Sunflower	Cordgrass	Wheatgrass	Wildrye	Brome Grass	Brome Grass Flowering	Sage
Sage Willow	Thistle Green	Thistle Flowering	Dry grass	Dry grass (Fractional Cover)	Soil	Vegetation
Mean Bandvariance	Variance Bandvariance	Contrast BandVariance	Dissimilarity BandVariance			

a)

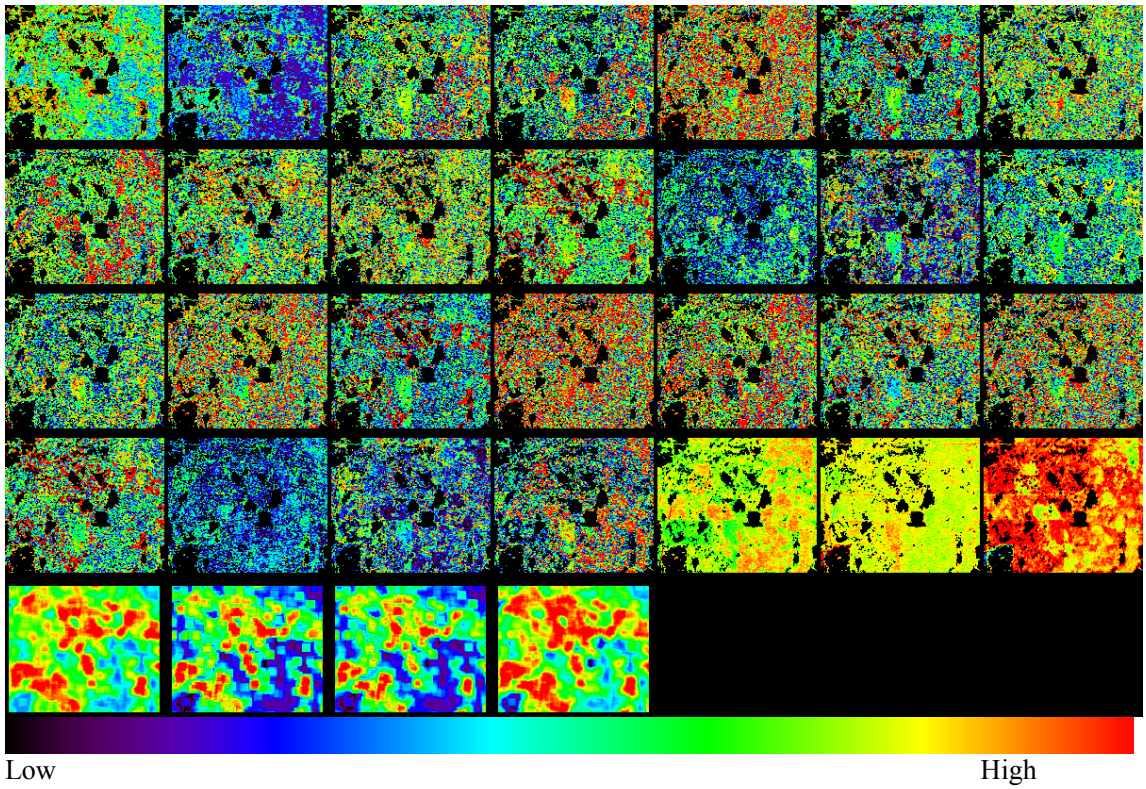


Figure 66. a) Legend for data layers; b) Data layers derived for Woodworth site September 18 2009 (Later Growing Season).

Based on above analysis, a range of factors and layers representing indicator species for native or introduced grassland are selected (Table 4) to identify disturbance and naturalness. Three models are then tested based on the parameters in MCAS. The software automatically rescales input layer to 0 and 1 and all models are based on rescaled results.

Table 4: Factors response at early growing season and later growing season

Parameters	Early Growing Season	Later Growing Season
Wheat Grass	High as indicator Species of Native Grassland	High as indicator Species of Native Grassland
Wildrye	High as indicator Species of Native Grassland	High as indicator Species of Native Grassland
Cord Grass	High as indicator Species of Native Grassland	High as indicator Species of Native Grassland
June Grass	High as indicator Species of Native Grassland	High as indicator Species of Native Grassland
Sunflower	Indicator Species of Forbs	Indicator Species of Forbs
Thistle	Indicator Species of Forbs	NA
Thistle Green	NA	Indicator Species of Forbs
Thistle Flowering	NA	Indicator Species of Forbs
Sage Willow	Indicator Species of Forbs	
Brome Grass	Low as introduced Species	NA
Brome Green	NA	Low as introduced Species
Brome Flowering	NA	Low as introduced Species
Kentucky Blue Grass	Low as introduced Species	NA
Dry Grass	High due to Litter at Native Grassland	High due to Litter and dry out grasses
Dry (Proportion)	High due to Litter at Native Grassland	High due to Litter and dry out grasses
Vegetation (Proportion)	Low based on C3 grass signature	High at forb domain area but low at native grassland because of haying off
Band Variance	Low indicate low dominance	Low indicate low dominance
Level of Dominant	Low indicate low dominance	Low indicate low dominance
Mean of Band Variance	Low indicate generally low dominance	Low indicate generally low dominance
Dissimilarity of Band Variance	The score suggests variation of spatial dominant. Low score means similar level of dominance in spatial dimension	The score suggests variation of spatial dominant. Low score means similar level of dominance in spatial dimension

Model 1: Introduced Grass Model

The Introduced Grass Model is based on the following assumptions:

1. Introduced grass like Kentucky blue grass, smooth brome grass should be present and at high density
2. Greenness should be higher than for native prairie, because smooth brome grass starts growing earlier than most native species.
3. Native species like Wheat grass, Wild rye and Cord grass and June grass should be less likely to be present.
4. As a disturbed area is more likely to be dominated by introduced grasses, Band Variance, Level of Dominance, Mean of Band Variance (BvMean) and Dissimilarity of Band Variance (Bvdis) should be high.

In addition, some other signatures such as Thistle are also used (Figure 67) to indicate disturbed areas. The Introduced Grass Model was applied to analysis of Oakville and Woodworth for early and late growing season data.

Introduced Grass Model applied to Oakville Prairie

For Oakville Prairie, the native prairie areas and school trust lands are barely distinguishable from other land early in the growing season (Figure 68), because most of the land is mainly covered by dry grasses, while vegetation has just started growing. Similarly in the histogram (Figure 71), the scores at this period are close to a normal distribution indicating that the model is any better than chance or random.

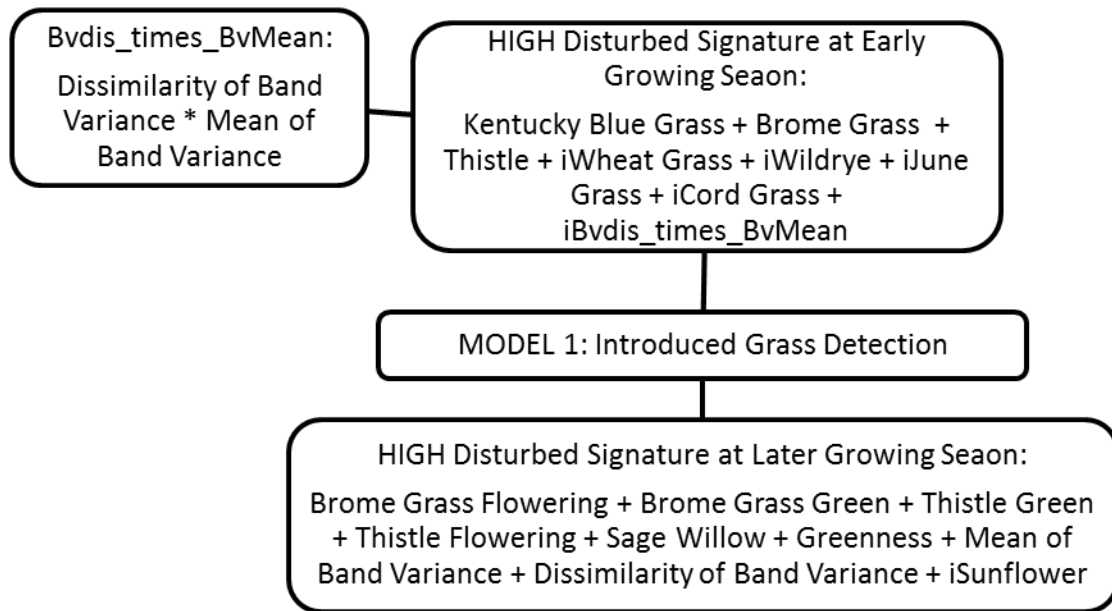


Figure 67. Introduced Grass Detection Model. The character “i” before parameters means inverse, which inverted maximum value to 0 and minimum to 1.

For the later growing season data at Oakville Prairie, (Figure 69), the Introduced Grass Model gives a high score in part of Oakville Prairie and part of the School Trust land, which would suggest significant presence of smooth brome grass. The histogram of pixel values from the final model prediction layer shows score on the native prairie area of Oakville Prairie between 0.5 and 0.8 (Figure 71). The high values for the model in this area gives a false result because spectral matching assigned high likelihood of smooth brome grass (“brome flower”) and Thistle (“thistle green”, “thistle flower”) presence in the native prairie. A time series model is then created by using both early growing season and later growing season results. As a result, the combined time series model also failed to identify native grassland from others (Figure 70).

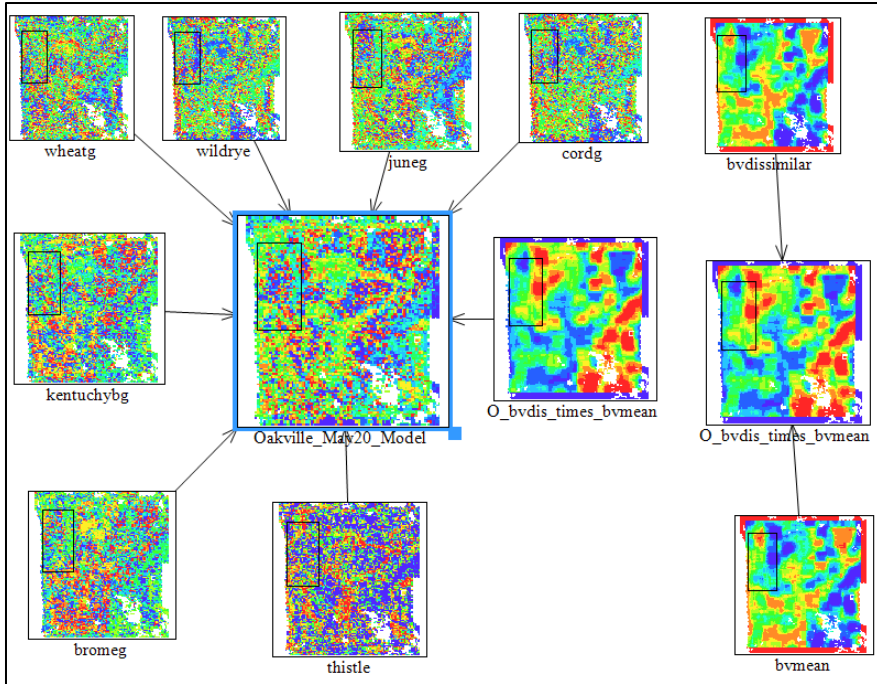


Figure 68 Oakville Early Growing Season Model. Color from blue to red indicates value or model score from low to high

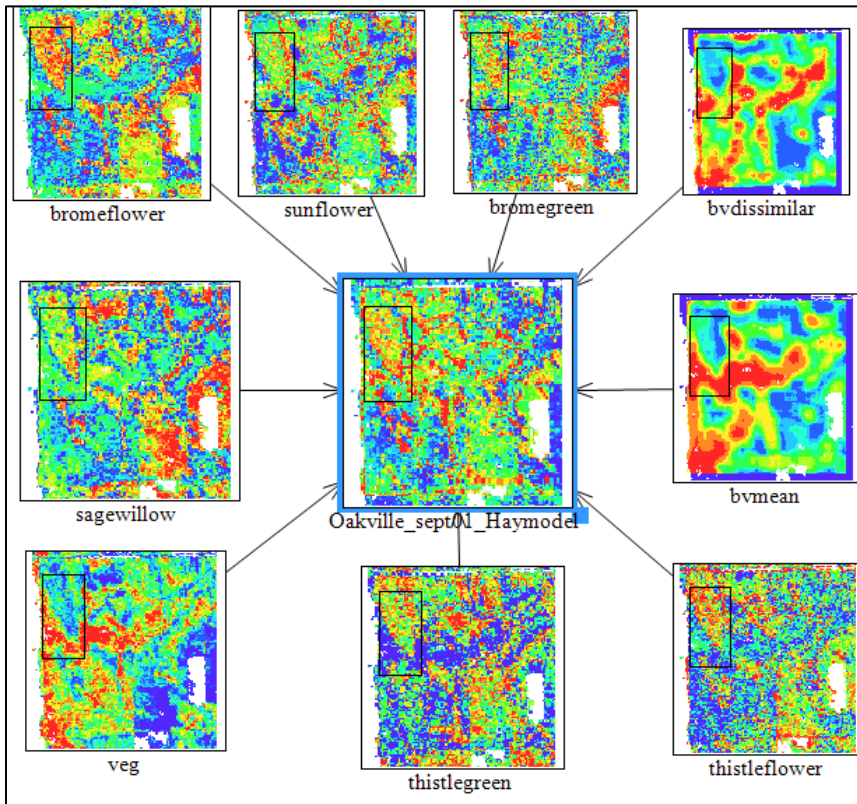


Figure 69 Oakville Later Growing Season Model. Color from blue to red indicates value or model score from low to high

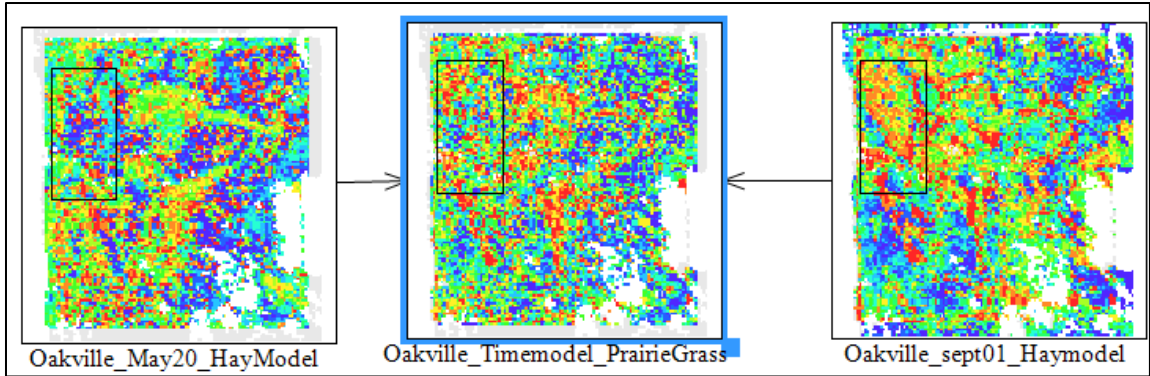


Figure 70 Combined Time Series Model of Oakville Prairie Grass. Color from blue to red indicates value or model score from low to high

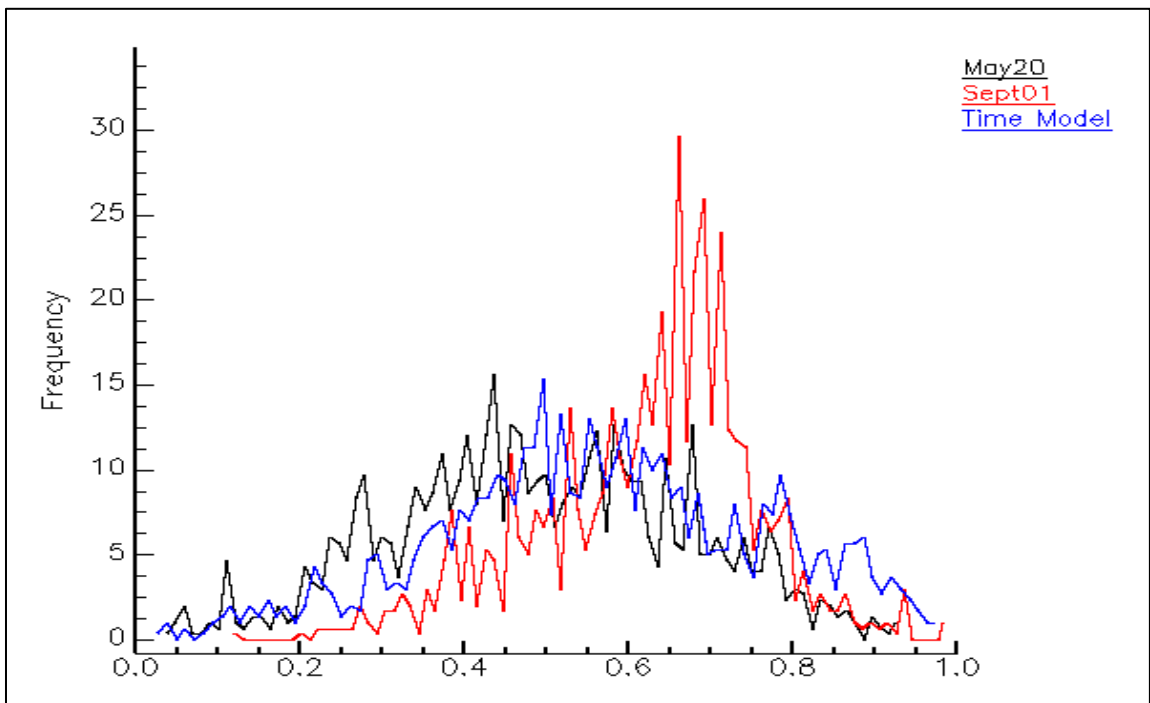


Figure 71 Histogram of Oakville Prairie. Color from blue to red indicates value or model score from low to high

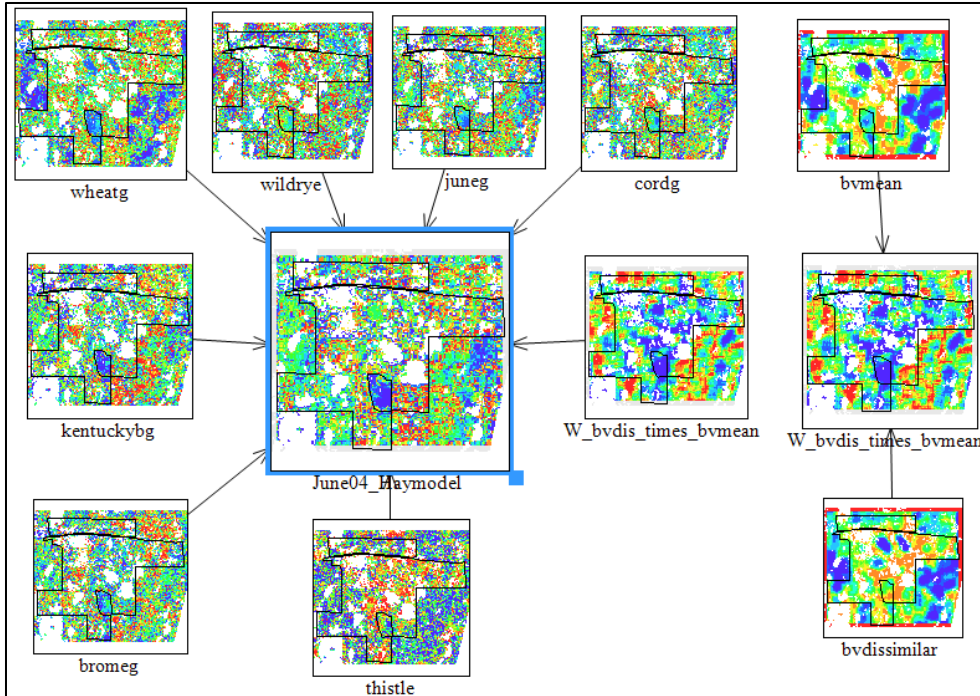


Figure 72 Woodworth Early Growing Season Model. Color from blue to red indicates value or model score from low to high

Introduced Grass Model applied to Woodworth

When the Introduced Grass Model was applied to the Woodworth site (Figure 72 and 67) most of the area shows a higher score compared with the replanted area, which is known to contain mostly native vegetation, for both the early (Figure 66) and late season (Figure 67) data sets. The combined model using the early and late season model result (Figure 74) clearly defines the the Woodworth property and provides an even clearer distinction between the replanted area and the rest.

The Introduced Grass Model appears to work well at the Woodworth site. However at the Oakville site, the model failed to exclude native prairie areas and provided confused results. The main reason, as observed from Figure 69, is that the ACE spectral matching analysis failed to distinguish between estimate brome grass and thistle on the one hand and native grassland on the other at the Oakville site. As shown in Chapter 5,

vegetation spectra for introduced and native grasses were highly correlated with each other, and showed substantial overlap in magnitude and pattern. Thus some of the native species' spectra, alone or in combination, may also resemble spectra of absent species like smooth brome grass, which causes the model to give confused results. Another factor is that early growing season is not helpful in discrimination because most of land is mainly covered by dry grasses and vegetation has only just started growing at that time.

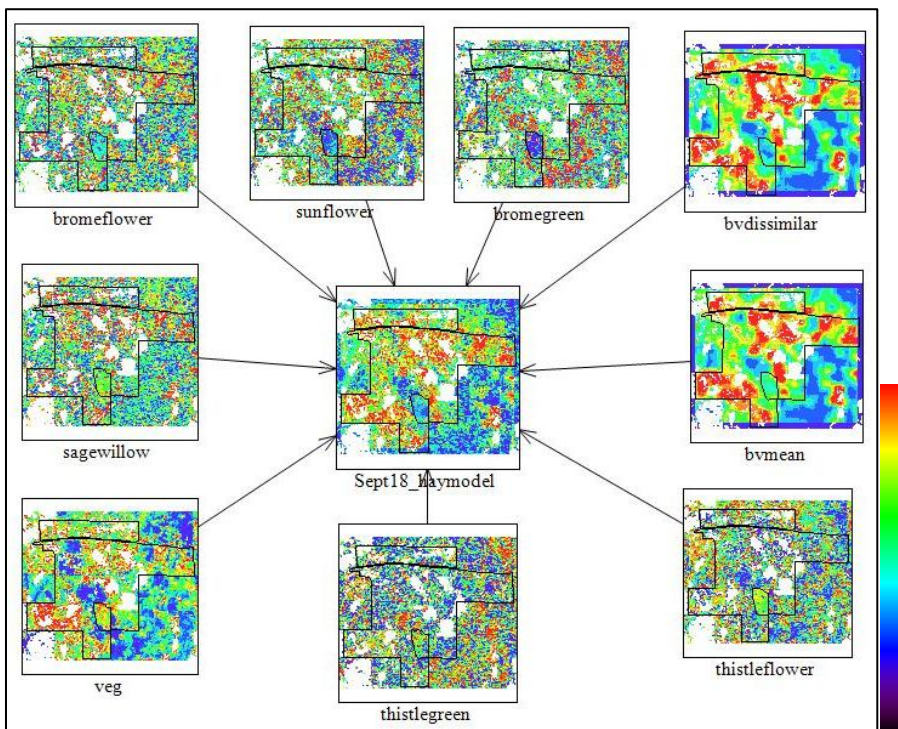


Figure 73 Woodworth Later Growing Season Model. Color from blue to red indicate value or model score from low to high

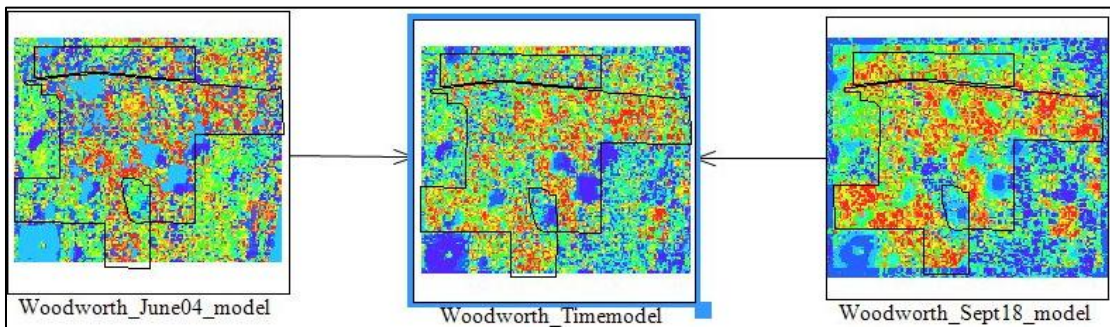


Figure 74 Combined Time Series Model of Woodworth Grass. Color from blue to red indicate value or model score from low to high

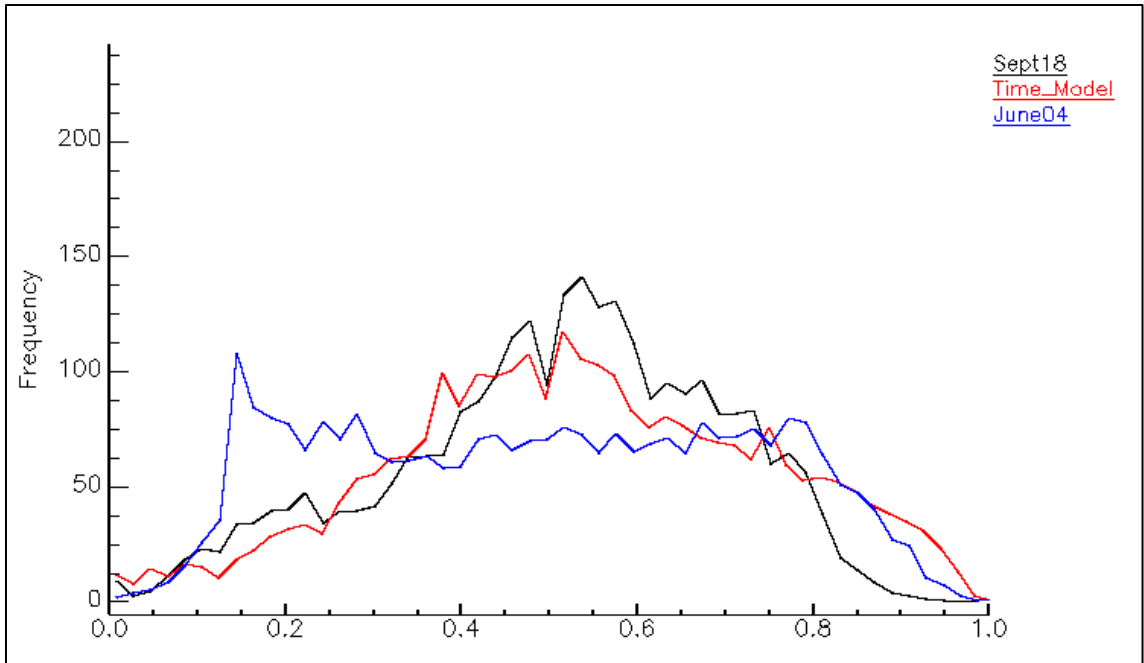


Figure 75 Histogram of disturbed area at Woodworth. Color from blue to red indicate value or model score from low to high

Model 2: Native Grass Model

The Native Grass Model is based on the following assumption (Figure 76):

1. Due to the thick litter background, native prairie has high dry grass signature compared with a disturbed area with introduced species
2. Fractional cover of green vegetation should be lower on native grassland than on disturbed areas with introduced grasses, because native grasses are slower to start growing than smooth brome grass.
3. Indicator species like wheat grass, wild rye and cord grass (at later growing season) are likely to be present.
4. As native prairie is usually made up of numerous several species, Band Variance, Level of Dominance, Mean of Band Variance and Dissimilarity of Band Variance should be lower on native areas.

In the application of the Native Grass Model (Figure 70), it was necessary to make a specific adjustment to account for a big patch of forbs at Oakville Prairie, which may be mis-identified as non-native grasses due to the similarity of spectra between indicator plants such as Maximilian sunflower and smooth brome grass. Therefore, these pure forb areas were excluded from the model by using an index of forbs presence (based on a high match for Maximilian sunflower), and the assumption that the leaf density of forbs is higher than brome grass later in the growing season.

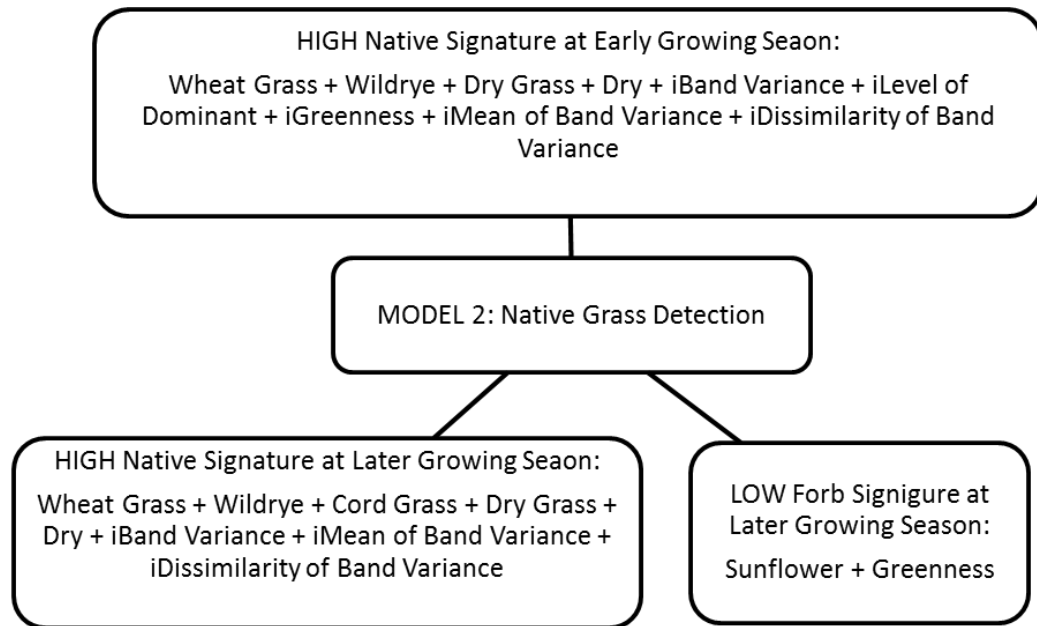


Figure 76 Native Grass Detection Model. The character “i” before parameters means inverse, which inverted maximum value to 0 and minimum to 1.

Native Grass Model Applied To Oakville Prairie

When the Native Grass Model was applied to the early growing season data at Oakville Prairie, (Figure 77) high scores were obtained on many parts of the area and on the School Trust Land. As most of land was mainly covered by dry grasses early in the growing season, the model did not distinguish between native prairie and other land (Figure 80). When the Native Grass Model was applied to the late growing season data

(Figure 78), high scores were obtained for native grass areas. In addition, the sunflower match data identified the forb area. When the distribution of scores was examined in a histogram (Figure 80), the native grass model showed a broad peak for high scores, matching the native grassland, and a sharp peak for low scores, corresponding to a model prediction of native grassland in the forb-dominated area. When the model results from early and late growing season were combined, including the model that identified forb areas, the native grassland (corresponding to the mid-to-late season period) was highlighted (Figure 79).

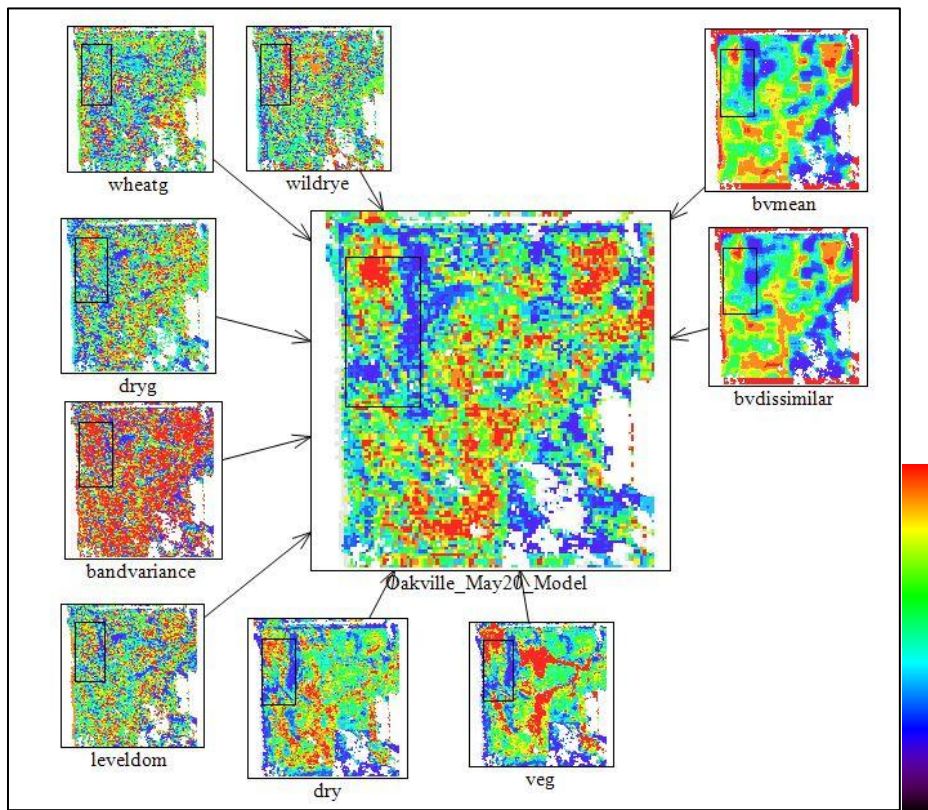


Figure 77 Oakville Early Growing Season Model. Color from blue to red indicates value or model score from low to high

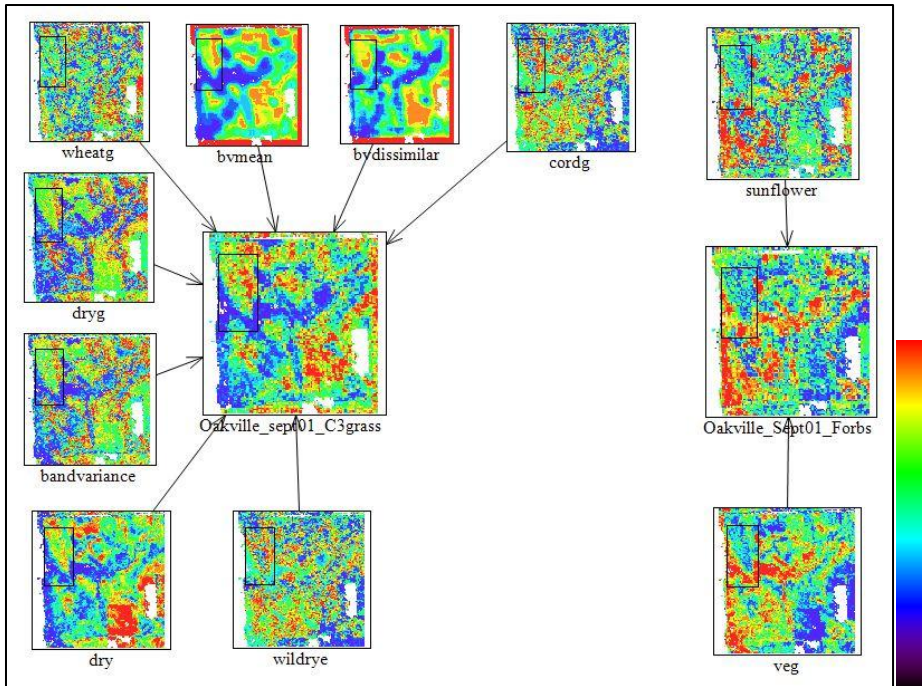


Figure 78 Oakville Later Growing Season Model. Color from blue to red indicates value or model score from low to high

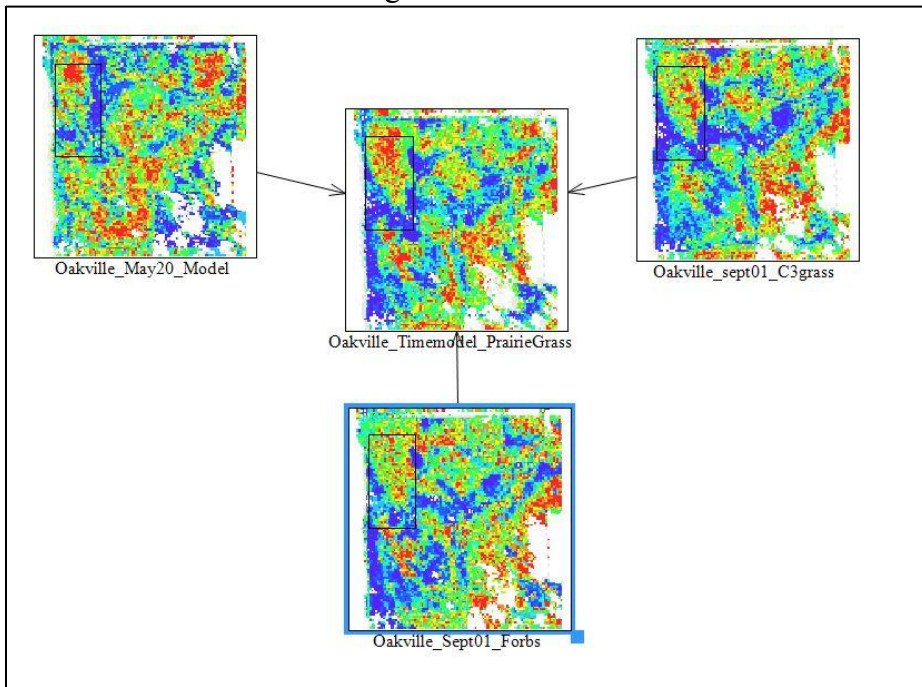


Figure 79 Combined Time Series Model of Oakville Prairie Grass. Color from blue to red indicates value or model score from low to high

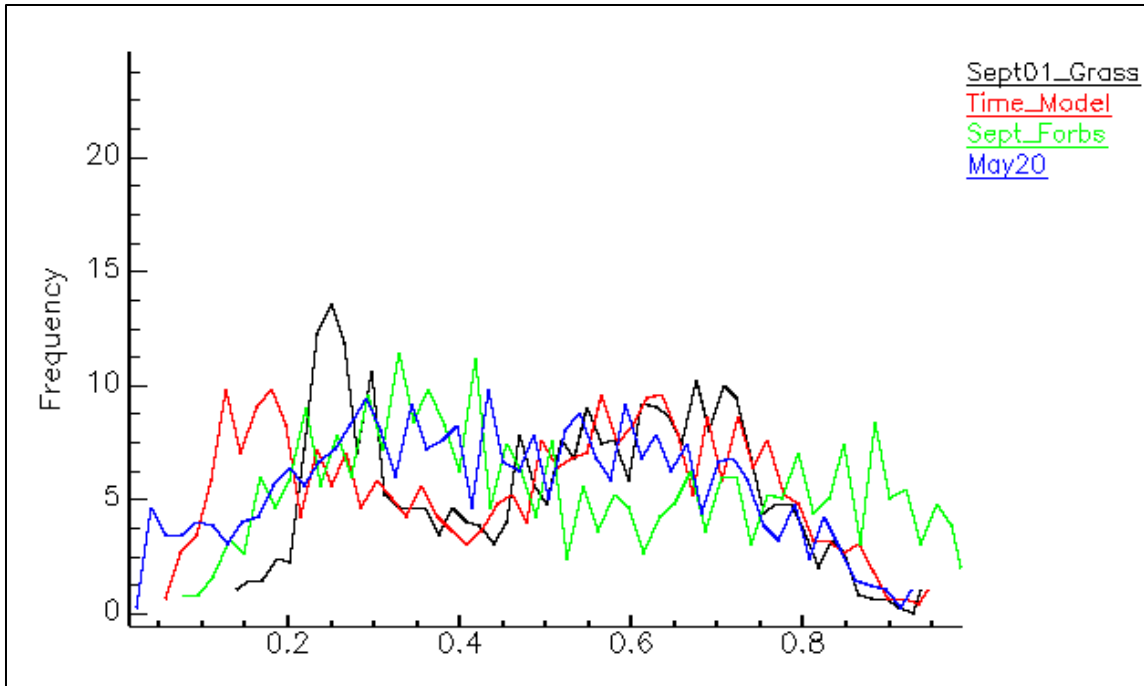


Figure 80 Histogram of left half section above school trust land including Oakville Prairie and part of forb area. Color from blue to red indicates value or model score from low to high

Native Grass Model Applied on Woodworth

Figure 81 shows the native grass model applied at the Woodworth site for the early growing season period. The result shows that the replanted area gets a low score, and the remainder of the property gets a relatively high score (Figure 81). This means that the native grass model is identifying the smooth brome grass areas on Woodworth, and not detecting the replanted area. Later in the growing season (Figure 82), the replanted area gets a moderate score in the model, while the rest of the property gets a low score. This means that the model is doing a better job, not getting confused between native grassland and smooth brome grass. At this time of the year, the replanted area had a high density of forbs, such as sunflower and other broadleaf species. This results in a spectral signature that is closer to smooth brome grass and less like native grasses, which explains why the

model score is only moderate. When the model results for early and late growing season are combined, the model (Figure 77) result is poorer since the early season response counteracts the better result from the late growing season model.

The native grass model does not work very well at the replanted area in Woodworth because the species structure is different with Oakville Prairie. For example, indicator species like wheat grass and wild rye are not common in replanted area, which contains some tall grasses, but is more dominated by a lot of forbs like Maximilian sunflower. In addition, due to the high density of forbs, the replanted area shows more greenness and higher dominance than disturbed area early in the growing season.

Based on above analysis, we can conclude that the early growing season is less helpful for modeling, because vegetation signatures are not strong at this stage, and different combinations of species can cause misleading results. In addition, the ACE spectral matching results are less useful for discriminating species directly, because of the relatively unstable and equivocal match scores.

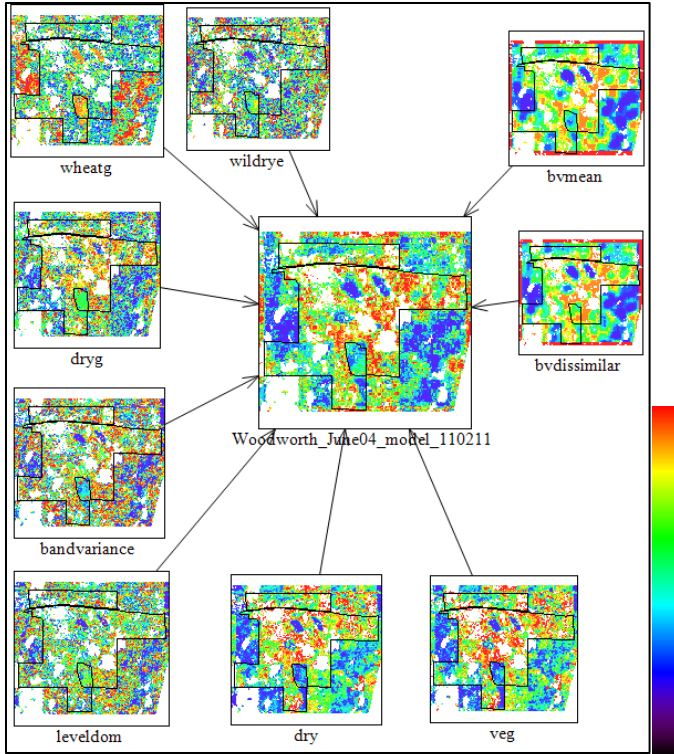


Figure 81 Woodworth Early Growing Season Model. Color from blue to red indicates value or model score from low to high

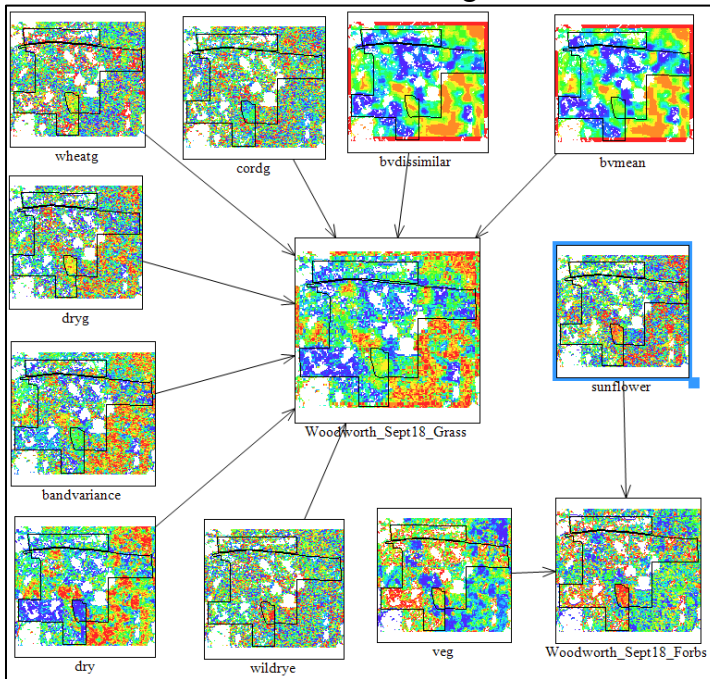


Figure 82 Woodworth Later Growing Season Model. Color from blue to red indicates value or model score from low to high

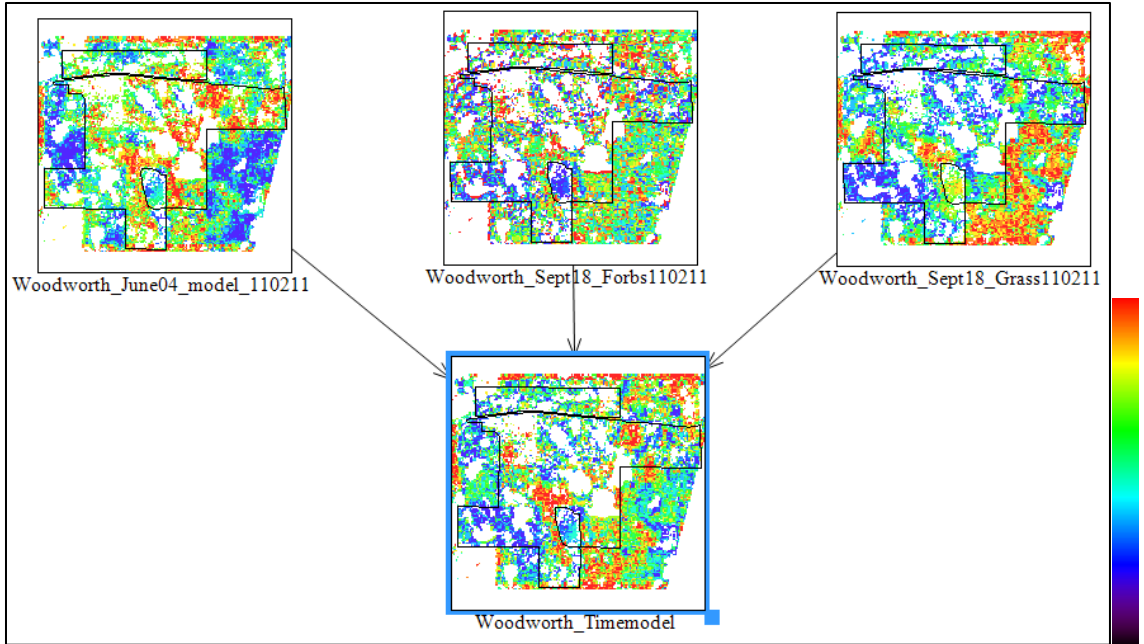


Figure 83 Combined Time Series Model of Woodward Grass. Color from blue to red indicates value or model score from low to high

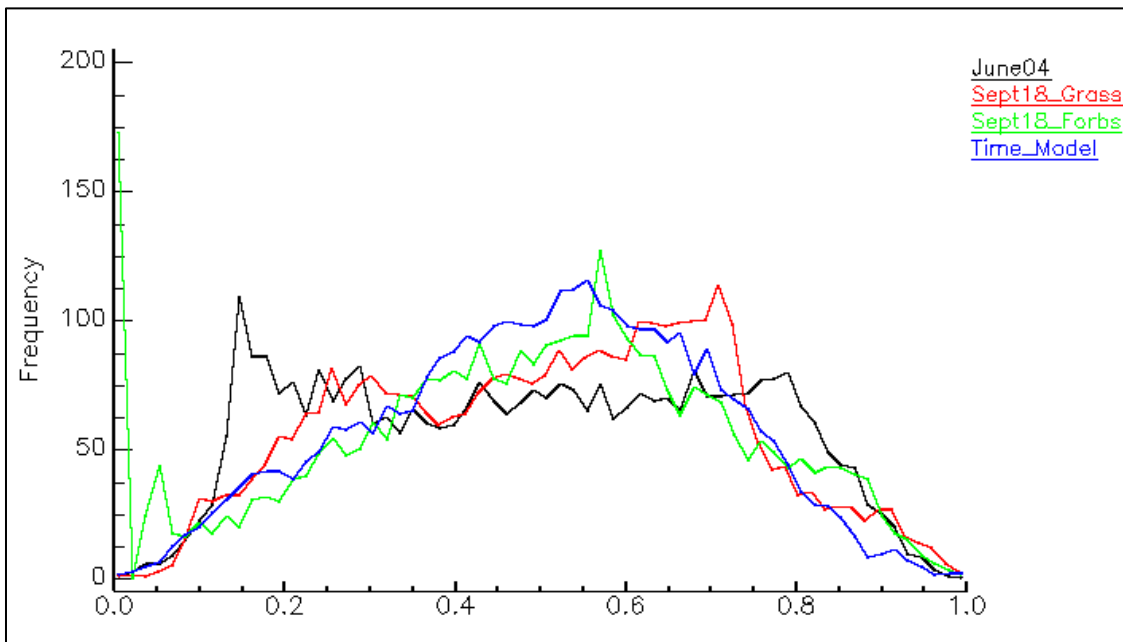


Figure 84 Histogram of Woodward disturbed area. The replanted area has been removed from statistic. Color from blue to red indicates value or model score from low to high

Model 3: Decision Tree (Based on later growing Season)

The spectral matching analysis based on the ACE method may be not very effective when grassland is made up of well mixed combinations of many species, since the combined spectra of indicator native species may be similar too and overlapping with the spectra of introduced species. However, it is reasonable to assume that the combined spectrum of indicator native species is still highly indicative of the native species present in the target field and in some mixtures, but does not exactly match the spectra of the introduced species from which they should be distinguished. As a result, the ACE analysis may assign similar likelihoods to species actually present and species that are actually absent. Since none of species are supposed to have very high scores in ACE result when the grassland is a mixture of many species, the spatial factors, “BV_Mean” and “BV_Dissimilarity”, should be low. On the other hand, if the grassland is dominated by single species, the ACE analysis values for indicator species should be much higher than for the rest of the possible species. When a patch is dominated by a single species, the ACE analysis provides more trustworthy results. Therefore, the score obtained for matches with smooth brome grass can be used to identify if the patch is highly dominated by smooth brome grass. Based on above analysis, grassland is first defined as following types:

1. Mixed Area (Several types of grasses are evenly mixed)
2. Pure Area (Dominated by single type of grass)
 - 1) Native
 - 2) Forbs

3) Brome Grass

Figure 85 shows processing flow to identify grassland conditions. For the test area, grassland is first divided into Mixed Native Grassland and single-species-dominant grassland by using “BV_Mean” and “BV_Dissimilarity” maps. For the single-species-dominant grassland, smooth brome grass is further discriminated from other plants by using the ACE possibility of “Brome Green” and “Brome Flowering” layers.

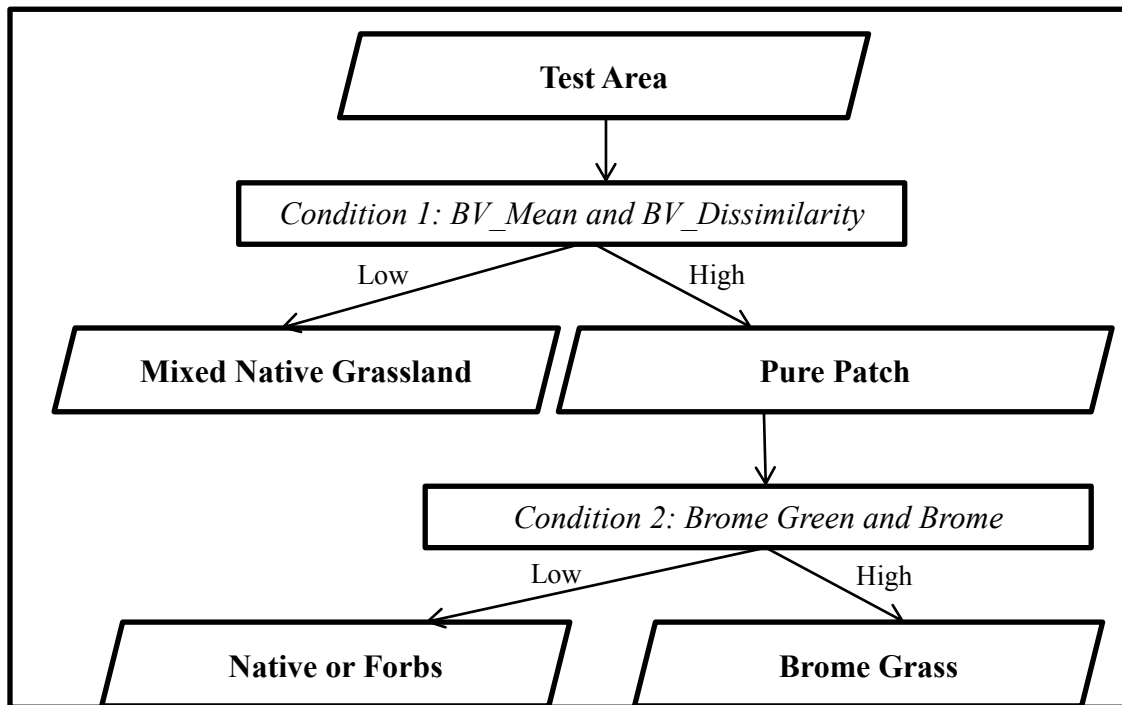


Figure 85 Decision tree to identify brome grass patches from native grassland.

The Figure 86 shows implementation of the Decision Tree Model for Oakville Prairie. The native grassland areas on Oakville Prairie are well detected, as these areas are mostly made up of native grasses mixed at 30 meters pixel scale. Most of the School Trust Land as well as part of forb-dominated area are identified as “Mixed Forbs and Grasses”, while some of the forb-dominated area is misclassified as brome grass-dominated patches.

The Figure 87 shows the implementation of the Decision Tree Model for Woodworth. The replanted area is correctly identified, as the area is mostly forbs and grasses mixed at 30 by 30 meters pixel scale. Most of the Woodworth grassland is identified as “Pure Brome Grass Patch”, while some fragments of the area are misclassified as “Native or Forb” patches.

The native and replanted areas are well identified in the decision tree model. Thus the model is then selected as the final approach. But the model is only sensitive to the presence of non-native grassland if smooth brome grass is the dominant species with high abundance. The “Pure Patch” area, however, is still hard to definitively classify as smooth brome grass and may be confused as either native or introduced grasses.

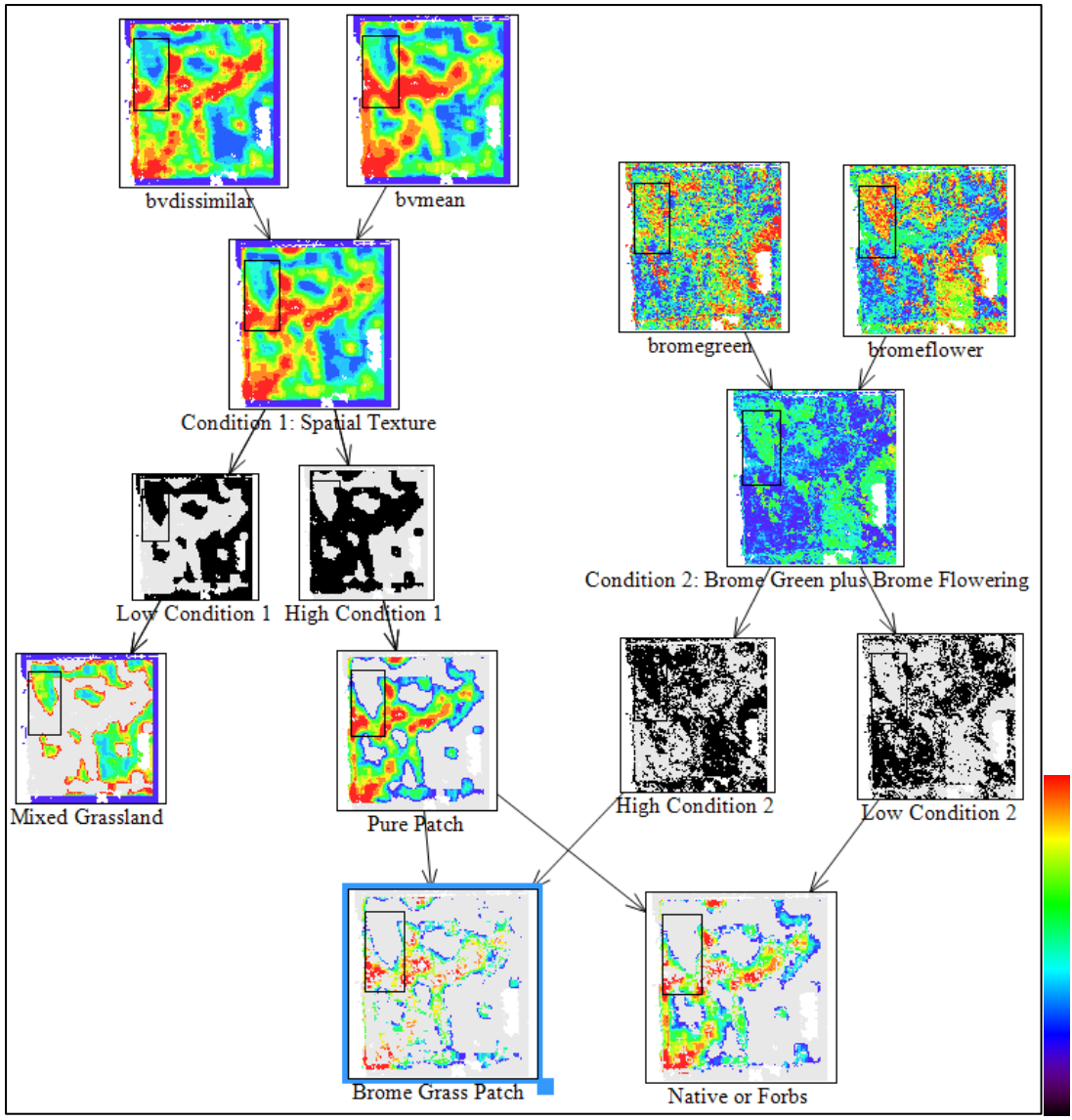


Figure 86. Decision tree applied on Oakville site. Color from blue to red indicate value or model score from low to high

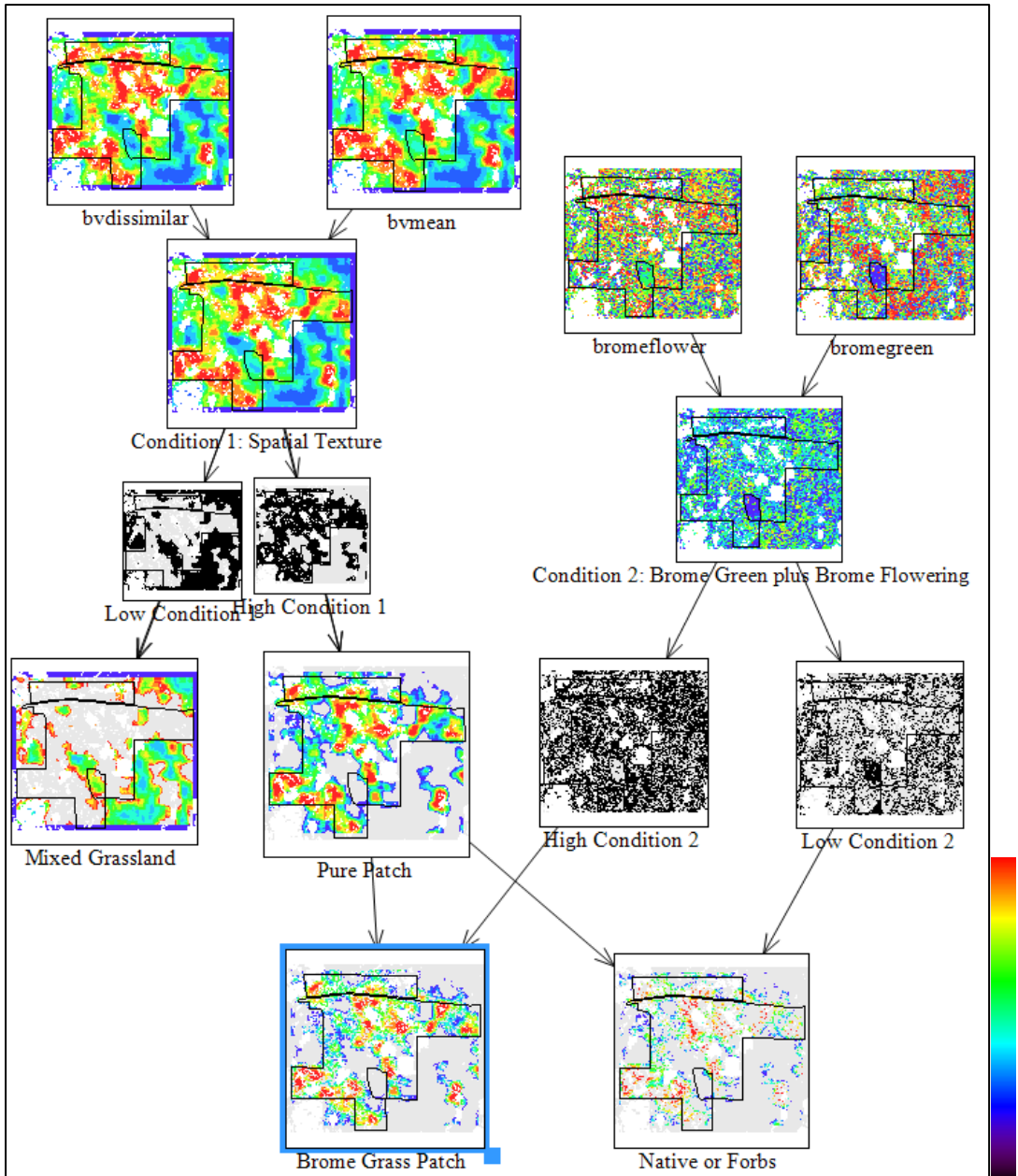


Figure 87. Decision Tree applied on Woodworth site. Color from blue to red indicate value or model score from low to high

Final Model Assessment at an Independent Field Site

In order to determine if the final model is site specific, or can be utilized at other locations, the model is tested on the Mekinock Prairie Chicken Wildlife Management Area under the jurisdiction of the North Dakota Game and Fish Department (Figure 88). This area is a relatively pristine native prairie (Chapter 3) but has been partly disturbed, and contains substantial patches of *Typha* spp, and smooth brome grass at low plant density except in isolated locations.. The area was randomly surveyed (Figure 88) to determine the predominant grassland types present. Figure 89 shows the grassland at each point location mapped in Figure 88. Based on a general assessment of in situ observations and the photographs, the sites were grouped into three broad grassland categories: Mixed Native Grassland; Mixed Forbs and Grasses; and Pure Brome Grass Patches. These points were then used to assess the effectiveness of the final naturalness model applied to an independent study site.

Figure 90 suggests that most of the western part of Mekinock is native grassland, while the eastern part has been partly disturbed. The model results at sample locations are then extracted and compared with survey data (Table 5).

The accuracy of the model predictions for Mekinock is described in Table 5 and Figure 91. The model made correct predictions of grassland type at 10 Mixed Native Grassland locations. Three “Mixed Native Grassland” samples were misclassified into “Pure Brome Grassland” and two were misclassified into “Mixed Forbs and Grasses”. The only Brome grass patch was classified as “Mixed Native Grassland”. One “Pure Native or Forb” point was classified into “Mixed Native Grassland” and five were classified as “Pure Brome Grassland”. Only three “Pure Native or Forb” samples were correctly classified.

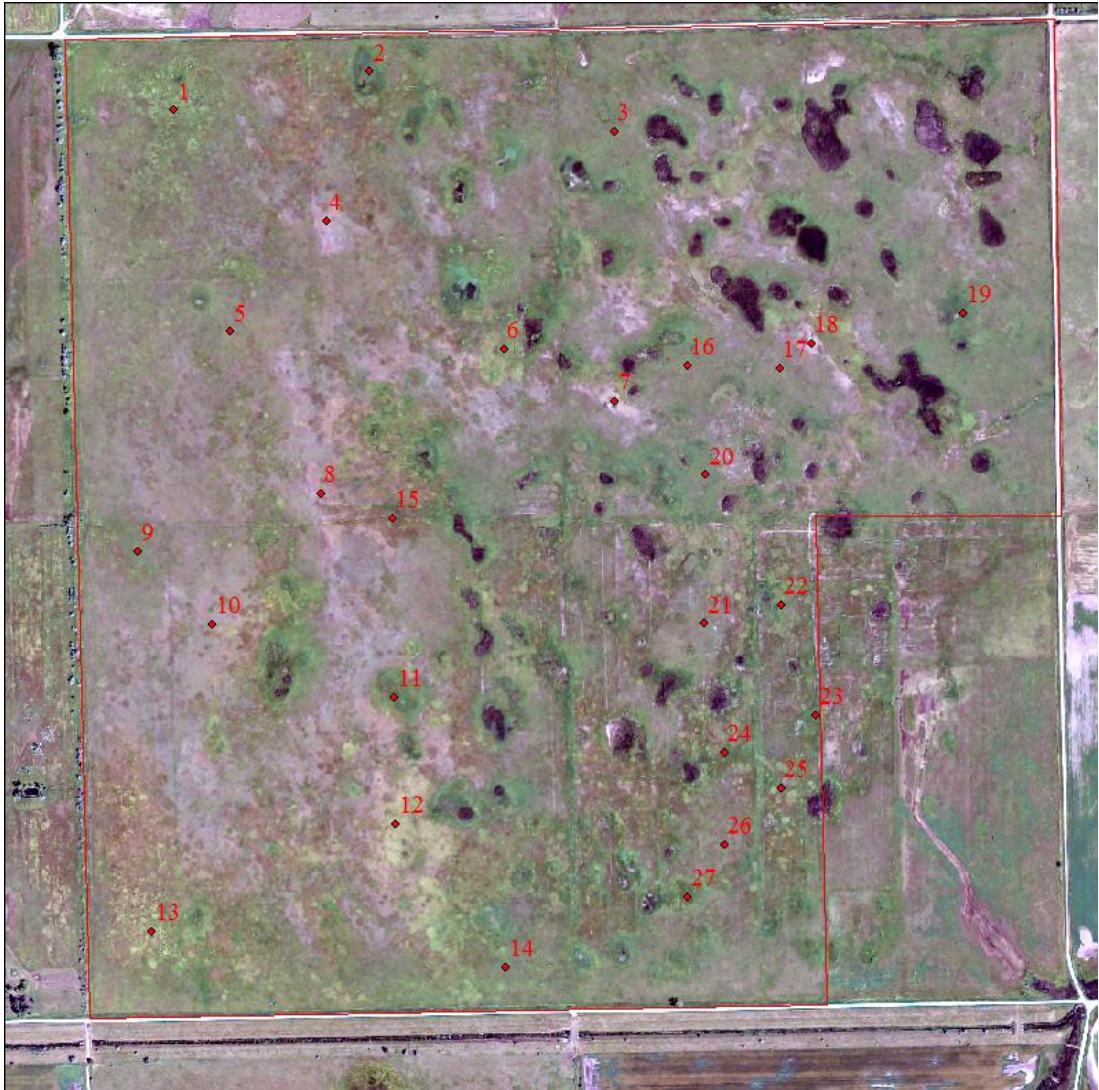


Figure 88 Mekinock Survey at August 26 2010





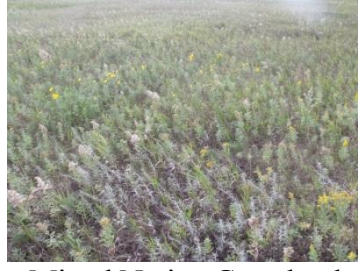










		
1 Pure Brome Grass Patches	2 Mixed Native Grassland	3 Pure Native or Forb
		
4 Mixed Native Grassland	5 Mixed Native Grassland	6 Mixed Native Grassland
		
7 Pure Native or Forb	8 Mixed Native Grassland	9 Mixed Native Grassland
		
10 Mixed Native Grassland	11 Mixed Native Grassland	12 Pure Native or Forb
		
13 Mixed Native Grassland	14 Mixed Native Grassland	15 Pure Native or Forb

Figure 89 Grassland combinations of 27 sample points. All points are classified into three groups: Mixed Native Grassland, Pure Native or Forb and Pure Brome Grass Patch

Figure 89 Cont.



16 Pure Native or Forb



17 Mixed Native Grassland



18 Mixed Native Grassland



19 Mixed Native Grassland



20 Pure Native or Forb



21 Mixed Native Grassland



22 Pure Native or Forb



23 Mixed Native Grassland



24 Pure Native or Forb



25 Mixed Native Grassland



26 Mixed Native Grassland



27 Pure Native or Forb

“Mixed Native Grassland” was most successfully classified (Table 5; Figure 85). But the accuracy of “Pure Brome Grassland” and “Mixed Forbs and Grasses” is relatively low. This is partly because of highly correlation between species spectrum (Andrew & Ustin, 2008) as well as limitation of ACE method. On the other hand, the sample size for some grassland types, such as pure smooth brome grass, is too small; only one smooth brome grass patch was identified in the test area. However, Mekinock does represent an intermediate case between pure native grassland and an introduced grass field, so some mixed results might be expected.

Table 5 Confusion Matrix of Decision Tree Model

		Point Category			Point Category (Percentage)		
		Mixed Native Grassland	Pure Brome Grassland	Mixed Forbs and Grasses	Mixed Native Grassland	Pure Brome Grassland	Mixed Forbs and Grasses
Model Result	Mixed Native Grassland	10	1	1	83.33%	8.33%	8.33%
	Pure Brome Grassland	3	0	5	37.5%	0.00%	62.5%
	Mixed Forbs and Grasses	2	0	3	40.00%	0.00%	60.00%

Table 6 Grassland Condition Distribution of Three Sites: Oakville Prairie in a half section; Woodworth without the replanted area and Mekinock

	Oakville Prairie	Woodworth	Mekinock
Mixed Native Grassland (Number of Pixel)	626	2859	1243
Pure Native or Forb (Number of Pixel)	427	3615	531
Pure Brome Grass (Number of Pixel)	398	5043	677
Total	1451	11517	2451
Mix Grassland (%)	43.14%	24.82%	50.71%
Pure Native or Forb (%)	29.43%	31.39%	21.66%
Pure Brome Grass (%)	27.43%	43.79%	27.62%

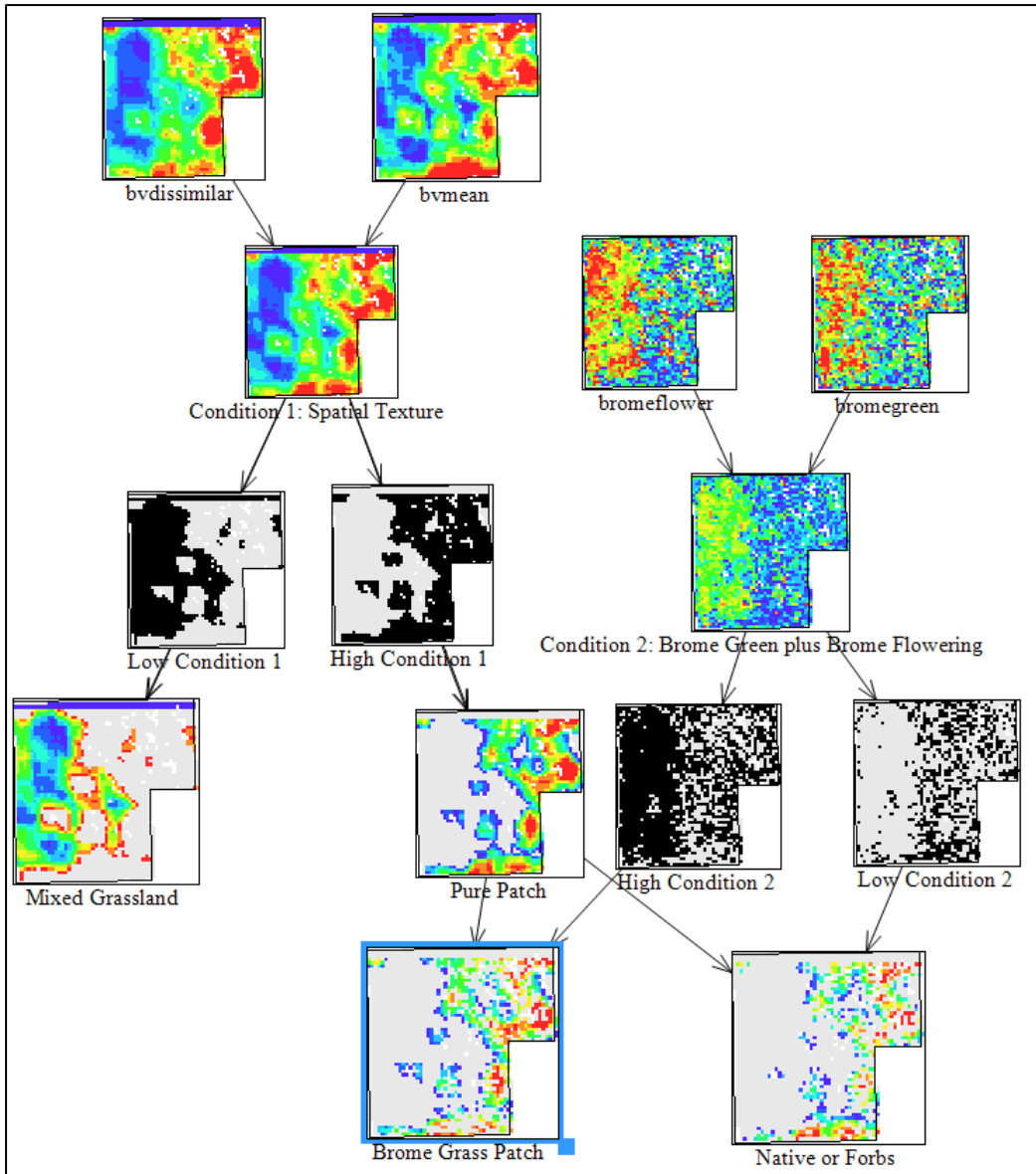


Figure 90. Decision Tree applied on Mekinock site. Color from blue to red indicate value or model score from low to high

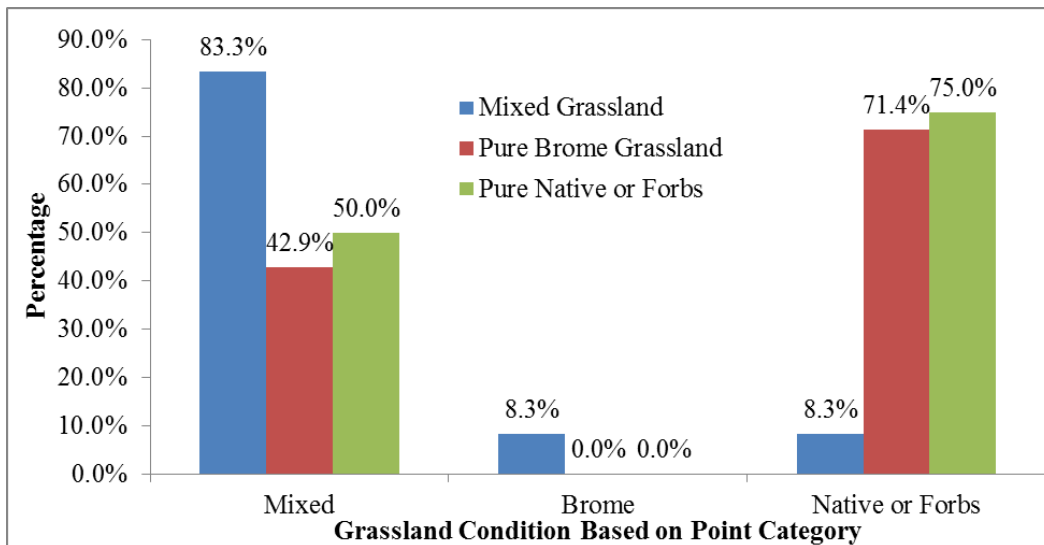


Figure 91 Decision Tree Model results distribution based on Field Survey Points

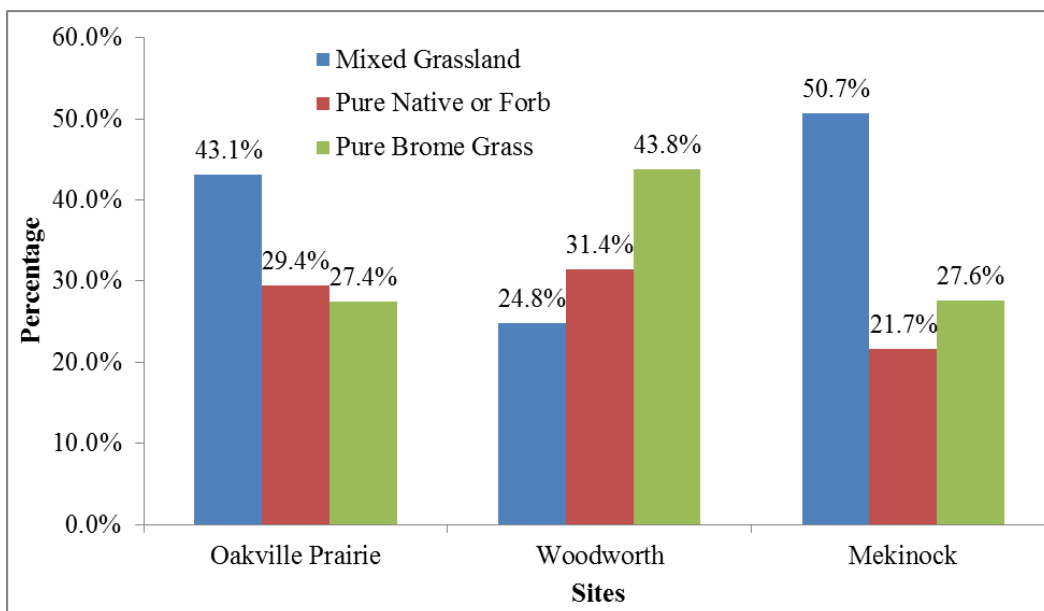


Figure 92 Land Cover Proportion of Three Sites: Oakville Prairie in a half section; Woodworth without the replanted area and Mekinock

Table 6 and Figure 92 suggest the proportion of three types of land cover in all sites. Oakville Prairie and Mekinock are mostly “Mixed Native Grassland”. Woodworth, however, is dominated by Brome Grass.

Discussion and Conclusion

Based on the analysis carried out in the previous chapters, some key spectral and other data layers required for modeling can be defined:

1. Indicator species that distinct native grassland or replanted area like wheat grass, wild rye, cord grass, June grass and forbs like Maximilian sunflower, Thistle and sage willow.
2. Introduced species like smooth brome grass and Kentucky blue grass
3. Fractional cover including dry litters and vegetation
4. Dominance indicators: “level of Dominance” and “band variance”
5. Spatial structures: “Mean of Band Variance” and “Dissimilarity of Band Variance”

Three models were created. The Introduced Grass Model successfully identified smooth brome grass at the Woodworth site, but failed when mapping native prairie at Oakville site. One of the reasons is that ACE algorithm is not robust enough to clearly distinguish species that are highly correlated. Another reason is that early growing season is not suitable for species discrimination as there are not enough distinct signatures developed at this stage of growing season.

The Native Grass Model failed to identify the replanted area at the Woodworth site mainly because of the major differences in species mixtures between that site and Oakville grassland. For example, Woodworth replanted area is more dominated by forbs like Maximilian sunflower, thus lack of native grass indicator species like wheat grass and wild rye leads to some poor prediction.

The Decision Tree Model first focused on spatial structure of grassland, represented by the textural analysis of the spectral variation and spectral dominance measures later in the growing season. Though native grassland has patch structures, it still is detected as evenly mixed. This may because those patches are mixed within themselves or pure native patches are not big enough at 30m scale. On the other hand,

as smooth brome grass is aggressively competitive with other species (Sedivec et al. 2009), and therefore it is more likely to form highly dominant patches. Therefore, from this analysis native grassland is generally well mixed (low “BV_Mean” and low “BV_Dissimilarity”), while disturbed area contain more grasslands with higher dominance measures (high “BV_Mean” and high “BV_Dissimilarity”). However, forb-dominated area has similar dominance characteristics to the smooth brome grass areas, thus ACE possibility of smooth brome grass is used to separate forbs and brome grasses. The final model well identified native grassland, however, it is still confusion at brome grass and forb dominated area. The area based statistic (Figure 92), instead, is more reasonable and shows more agreement with site conditions.

CHAPTER VII

CONCLUSION, LIMITATION AND FUTURE WORK FOR THE STUDY

Conclusion and Discussion

This thesis sought to assess grassland naturalness by mapping grassland composition based on spectral signatures and, in particular, by identifying areas occupied by smooth brome grass (*Bromus inermis*), an introduced hay crop. Smooth brome grass is an effective weed, and therefore can compete with native grasses and forbs when natural grassland is disturbed (Whitman & Barker 1994). As a result, biodiversity of natural grassland could be decreased. Plant diversity in prairie grasslands supports a wide range of pollinating insects (Franzén & Nilsson, 2008), is strongly related to ecosystem productivity (Bullock et al., 2007), and makes the ecosystem potentially more resilient under environmental disturbance (Hooper & Vitousek, 1997).

This study has a number of major findings.

1. Spectral matching analysis plus assessment of spatial patterns and spectral variation could distinguish between smooth brome grass and pure native grasslands.
2. However, there was a high correlation and similarity of absorption features between smooth brome grass dominant stands and natural grassland dominated by forbs which limited discrimination between these stands.

3. There was a strong effect of background litter and dry grass spectral responses at Oakville Prairie, and it was necessary to compensate for this strong signature in spectral matching analysis.
4. There were major differences in fractional cover of PV and NPV between native grassland and smooth brome grass areas at different times during the growing season; however this was not always definitive.
5. There was significant variation in field spectral signatures across the growing season, which made selective of definitive signatures for matching difficult.
6. The high variability in spectral signatures within image pixels and moderate SNR and low spatial resolution (30 m) of Hyperion data placed limitation on discrimination between grassland types. Especially in view of the small differences in spectral signatures and high correlation of spectral patterns.
7. Since spectral differences were not definitive to grassland types, relatively simple decision tree models utilizing the most discriminatory spectral and spatial layers ultimately proved to be the best approach for assessing naturalness.

The Oakville Prairie, representing undisturbed native grassland, contains variety of native grasses as well as thick dry grass litter accumulated historically. The Woodworth site, on the other hand, is largely sown grassland dominated and managed as a breeding environment for water birds. The site is mostly dominated by brome grass with less litter background compared with Oakville Prairie.

The imagery data used in this research was acquired from the Hyperion imager on the EO-1 satellite. The Hyperion LIR data was pre-processed to remove bad pixels, de-stripping, bad bands removing, atmosphere correction, spectrum smoothing and geo-correction. However, the moderate SNR of Hyperion sensor (around 160:1 in the

visible and NIR, and 40:1 in the short wave infrared), relatively large differences in spectral signatures may be needed for distinguishing between cover types. Any noise effect adds to the uncertainties when identifying invasive species, particularly for analysis involving mostly mixed image pixels.

Some researchers have mapped invasive species by using common techniques like supervised classification (Underwood et al., 2003; Underwood et al., 2007; Yang et al. 2009) or statistical unmixing approaches (Andrew & Ustin, 2008; Miao et al., 2006). Generally, mapping accuracy decreases when site complexity increases (Andrew & Ustin, 2008). In other words, the mapping accuracy depends on species spectrum complexity within a pixel: higher correlation between species spectra leads to lower mapping accuracy. In addition, higher spectral and spatial resolution generates higher accuracy in unmixing results (Underwood et al., 2007). This is because high spectral resolution enables extraction of more detailed biophysical information about the vegetation (Gianelle & Guastella 2007), which increases the possibility of discriminating species. High spatial resolution decreases the likelihood of species complexity within pixels and increases the likelihood of having pure (single species) pixels. Given the complex species mixtures in the native grasslands of Oakville Prairie (including diverse broadleaf forbs), and the highly correlated spectra among species, and sample sites in the study area, simple spectral unmixing techniques proved to be insufficient to provide discrimination on their own.

Field spectra were collected during growing season and pre-processed (chapter 4) for the later use of species detection. As the overall spectra charts show (Figure 36, Figure 37), most species spectra are highly correlated and the smooth brome grass spectrum is not distinctive when compared with many of the other spectra. In addition, the reflectance at certain wavelengths shows relatively low variation and is of little

use for distinguishing between photosynthetically active herbaceous plants and vegetation swards. Therefore, in order to reduce dimensionality of the data, and concentrate analysis on wavelengths with high variation among species spectra, absorption features were extracted (Thulin, 2009). Although this magnified some of the differences among species, absorption feature curves were still similar and highly correlated (Figure 40, Figure 41).

The spectrum matching approach (ACE; chapter 5), applied to estimate the proportional presence in the grassland of each species in the spectral library initially highlighted the domination of a dry grass signature at all sites early in the growing season. Later in the growing season, a mosaic of patches of grassland dominated by green leaves and stems developed, and more diversity in spectral responses was evident. However, the ACE spectral matching analysis showed some false detection results, in particular, a relatively high likelihood of smooth brome grass presence at Oakville Prairie. This seemed to occur because of non-unique spectral signatures for smooth brome grass and native grasses, complex species combinations within a single pixel, and a generally high correlation among spectra of many species. This problem has been reported in other studies. For example, Andrew and Ustin (2008), found that the accuracy of identification of invasive species decreased with increasing site complexity. In addition, it is clear that the 30m pixel resolution limited the identification accuracy (e.g., Underwood et al. 2007), since a single 30 x 30 m pixel almost always contained multiple patches of grassland with different dominant species.

Nevertheless, the combination species likelihoods within pixels were significantly different between Oakville Prairie and Woodworth. Although the Oakville Prairie is a complex mosaic of species and patches, and the ACE result was

not definitive, the likelihoods for species presence tend to be evenly distributed among all tested species. At Woodworth, on the other hand, the results clearly showed a high likelihood of presence for one species (smooth brome grass) and a low likelihood for native grasses. Since Oakville Prairie is a mixture of various species at the 30m pixel scale; the combined spectrum also tends to be the average spectrum of all of the native species, and tends to fall in the middle of the spectral range. At Woodworth, the spectrum from a 30 m pixel is more likely to be dominated by a single species, and the pixel spectrum tends to correspond more closely to that of one dominant species such as smooth brome grass. The two indexes that were developed to capture this level of spectral variability within a pixel, “Level of Dominance” and “Band variance”, indicate the extent to which any area is dominated by a single species. Differences in dominance mainly occur later in the growing season. Both “Level of Dominance” and “Band variance” show relatively low scores at Oakville Prairie and a high score with wide spatial variation at Woodworth.

Texture co-occurrence analysis suggests that native prairie has generally low “Level of Dominance” and “Band variance” (“Mean”) as well as low spatial dissimilarity (“Dissimilarity”). The two factors clearly identified native prairie and the restored area in Woodworth. This may be because the native species have evolved in a diverse and compatible association, and tend to mix with each other at the 30m spatial scale. On the other hand, smooth brome grass is not very compatible with other species (Sedivec et al. 2009) and it is more likely to dominate sown and disturbed areas, and to aggressively spread where established as a weed.

In general, smooth brome grass begins growing earlier than most native grasses. Based on this, it was hypothesized that the proportion of green vegetation on the brome grass dominant area should be higher than that for the native grassland early in

the growing season. In order to capture test this, proportions of green vegetation, dry vegetation and soil were calculated in chapter 3, using the triangle distribution in NDVI and CAI (Guerschman et al. 2009). Time series of fractional cover were calculated from Hyperion imagery, and extracted from the fractional cover data layers for each of the field measurement locations. In general, the results showed that native grasses tended to exhibit an increase in green fraction with decrease dry fraction from May to early September, while smooth brome grass exhibited a high proportion of green fraction by early June, and then a variable green and dry cover fraction from June to September. The dry cover fraction of brome grass increased from June to September which is a significantly different trend to that of native grasses. However, forbs which had significant levels of abundance on both parts of Oakville Prairie and Woodworth, however, showed similar dry proportion changing patterns with brome grass. As the fractional cover data provided useful additional information for areas dominated by grasses, but was less helpful overall in this study because of the significant presence of forbs.

Since the forbs generally exhibit higher levels of greenness than grasses, the fractional cover analysis did not provide useful information in the identification of brome grass dominant areas when the grassland was also mixed with forbs. In this study, forbs like Maximilian sunflower are widely spread in grassland, making differences in fractional cover proportions unreliable for discrimination between grassland types early in the growing season.

Later growing season, Oakville Prairie e exhibits a higher dry grass proportion with less green vegetation because of a combination of early senescence of some flowering native grasses and continued dry grass and litter effects. The vegetation composition pattern on the more saline drainage line area is distinctive from the rest

of the area at Oakville. At Woodworth, dry grass proportion is lower and green vegetation proportion is higher late in the growing season. . However, the replanted native prairie area with a very high abundance of forbs shows similar fractional cover proportions to the smooth brome grass areas. Thus fractional cover analysis was less helpful to assessment of grassland naturalness than was originally hoped.

The lack of a definitive spectral approach to discriminating between levels of grassland naturalness led to the exploration of a different approach using some simple combinational models and decision tree models (chapter 6). Models based on data from early in the growing season did not work very well because the green vegetation signature was not strong enough at this stage to cause significant difference in Hyperion imagery. A decision tree model based on the data from later in the growing season was finally selected which divided area into “Mixed Native Grassland”, “Mixed Forbs and Grasses” and “Pure Brome Grass Patches”.

This decision tree model successfully identified “Mixed Native Grassland” including Oakville Prairie and the replanted Woodworth area. This is because the Oakville Prairie and the replanted native prairie area at Woodworth area had highly mixed vegetation and corresponding spectral signatures at 30 m pixel scale. As a result, “Level of Dominance” was at Oakville Prairie, and on the replanted area at Woodworth. By contrast, the “Level of Dominance” index was high for large patches of the remainder of Woodworth, indicating that spatial variation in spectral signatures occurred at much greater spatial scale than for the native grassland.. However, the method may not perform very well, when native grassland is invaded by smooth brome grass as a weed, since the “Level of Dominance” would most likely be that same as for pure native stands. Even for those areas that have more pure grassland types, the accuracy of ACE spectral matching method was still limited by the spectral

variability inherent in grassland. Thus even areas that are dominated by native plants or smooth brome grass can be falsely classified at times. The results of the study suggest that for more definitive discrimination of grassland naturalness, hyperspectral data with both higher SNR and higher spatial resolution would be more effective by decreasing the combination and complexity of spectral signatures within pixels (e.g., Underwood et al. 2007).

The final model was tested at Mekinock, an independent site used for prairie chicken breeding and having a mix of native grasses with some smooth brome grass at low abundance. Twenty five sample sites were randomly selected and compared with the model output. The test results suggested highest accuracy at “Mixed Native Grassland” (83%) and then “Mixed Forbs and Grasses” (60%). The “Pure Brome Grass Patches” was failed to be correctly detected because there was only one pure smooth brome grass site and the patch was small relative to the pixel resolution. The result confirmed the assertion above that intermingling of smooth brome grass at low density with native grassland would not be detectable and would be classified as native grassland. However, although the small sample size limited this test of the model, the spatial data output showed a variable likelihood of native, mixed and smooth brome grass categories. . When an area based statistic was also calculated this placed Mekinock in an intermediate state between Oakville Prairie and Woodworth. The result of this area-based statistic for Oakville Prairie indicated that it is mostly “Mixed Native Grassland”, while the result for Woodworth identified that it is broadly dominated by smooth brome grass. The results from the broad area-based statistics are more reasonable and are in better agreement with site conditions.

Limitations of the Study and Future Work

The naturalness estimates based on the models are limited by various factors.

The first limitation is based on the 30m by 30m spatial resolution of Hyperion imagery, combined with a relatively modest SNR. This combination restricts species detection accuracy. Image noise may make it difficult to detect fine differences in spectra between species, and also make the spectral signature unstable for species detection.

Weather had a significant impact on this study in many respects. Firstly, cloudy days restricted field sample frequency to about once a month. However, results showed that rapid changes can occur in spectral signatures for different species as a result of rapid drying or flowering behavior. In addition, weather conditions, especially the rainfall and snowmelt runoff early in the growing season, also affect patch structure and species dominance in the grassland, which creates more variation in species dominance and complexity of composition.

As explained in Chapter 4 and Chapter 5, most field spectra were collected from grassland patches dominated by, but not 100% covered by, single species. Rarely was it possible to collect spectra from absolutely pure single species patches. These slightly mixed signatures may have introduced more variation into species signatures and cause more similarity among species signatures. For the whole spectral library, this limitation can lead to higher correlations among species. In order to avoid this problem, spectra should be collected from more pure patches for at least most dominant species, and/or spectra should be measured for pure samples of each species in the laboratory. Since seasonal changes in spectra were widely observed, and these varied between 2010 and 2011, more frequent measurements through whole growing season are also necessary.

The final validation survey at Mekinock was based on a very limited sample size.

In addition, all Hyperion images were acquired one or two years earlier than the final field survey – it should be noted that these grasslands are not grazed or modified at all, and hence remain relatively stable from year to year.. Considering the effect of phenological variation between species and between years, species combination within each pixel may also disagree with survey result due to changes in dominance from year to year. It is clear that the study would have benefitted from both a wider range of grassland sites for spectral collection, and a much more detailed field survey for validation of the model.

The results also suggest that new hyperspectral sensors with better SNR, and better spatial and temporal coverage could greatly improve detection capability over grasslands. The Hyperspectral Infrared Imager (HysPIRI), planned to launch in 2020, measures the spectrum from 380nm to 2500nm with 10nm spectral resolution. The repeat cycle is 19 days. The proposed instrument would capture the signal from 150km (compared with Hyperion 7.5km) ground swath at 60m spatial resolution (Zhang et al., 2011). This swath coverage would allow the collection and comparison of grassland signatures over a much wider ground range. Another hyperspectral sensor, Environmental Mapping and Analysis Program (EnMAP) is planned to launch in 2015, which captures 30km wide ground strips with 30m spatial resolution. The sensor covers the wavelength range from 420 to 2450nm (20nm spectral sampling) (Stuffer et al., 2007). The repeat cycle is 23 days; however, the 30° across track pointing capability allows revisit within 4 days. Both hyperspectral sensors would provide global survey with repeat cycle less than one month, which would be helpful to detect changes in grasslands through growing season. These sensors could be used to develop the kind of area-based statistics described here for assessment of grassland properties over wider areas of the fragile and threatened global grassland biome.

REFERENCES

- Ač, A., Malenovský, Z., Hanuš, J., Tomášková, I., Urban, O., & Marek, M. V. (2009). Near-distance imaging spectroscopy investigating chlorophyll fluorescence and photosynthetic activity of grassland in the daily course. *Functional Plant Biology*, *36*(11), 1006-1015.
- Adams, J. B., Smith, M. O., & Johnson, P. E. (1986). Spectral mixture modeling: A new analysis of rock and soil types at the viking lander 1 site. *Journal of Geophysical Research*, *91*(B8), 8098-8112.
- Addink, E. A., de Jong, S. M., & Pebesma, E. J. (2007). The importance of scale in object-based mapping of vegetation parameters with hyperspectral imagery. *Photogrammetric Engineering and Remote Sensing*, *73*(8), 905.
- Almeida, T. I. R., & Filho, D. S. (2004). Principal component analysis applied to feature-oriented band ratios of hyperspectral data: A tool for vegetation studies. *International Journal of Remote Sensing*, *25*(22), 5005-5023.
- Andrew, M. E., & Ustin, S. L. (2008). The role of environmental context in mapping invasive plants with hyperspectral image data. *Remote Sensing of Environment*, *112*(12), 4301-4317.
- Apan, A., & Held, A. (2002). In-house workshop on hyperion data processing: Echo-ing the sugarcane project experience. *Black Mountain Laboratories, Canberra: CSIRO Land and Water*,
- Asner, G. P., & Heidebrecht, K. B. (2002). Spectral unmixing of vegetation, soil and dry carbon cover in arid regions: Comparing multispectral and hyperspectral observations. *International Journal of Remote Sensing*, *23*(19), 3939-3958.
- Asner, G. P., & Vitousek, P. M. (2005). Remote analysis of biological invasion and biogeochemical change. *Proceedings of the National Academy of Sciences of the United States of America*, *102*(12), 4383.
- Bergquist, E., Evangelista, P., Stohlgren, T. J., & Alley, N. (2007). Invasive species and coal bed methane development in the powder river basin, wyoming. *Environmental Monitoring and Assessment*, *128*(1), 381-394.

- Bicknell, W. E., Digenis, C. J., Forman, S. E., & Lencioni, D. E. (1999). EO-1 advanced land imager. Paper presented at the *SPIE Conference on Earth Observing Systems IV*, 80-88.
- Biewer, S., Fricke, T., & Wachendorf, M. (2009). Determination of dry matter yield from Legume–Grass swards by field spectroscopy. *Crop Science*, *49*(5), 1927-1936.
- Biewer, S., Fricke, T., & Wachendorf, M. (2009). Development of canopy reflectance models to predict forage quality of Legume–Grass mixtures. *Crop Science*, *49*, 1917.
- Biondini, M. E., Patton, B. D., & Nyren, P. E. (1998). Grazing intensity and ecosystem processes in a northern mixed-grass prairie, USA. *Ecological Applications*, *8*(2), 469-479.
- Biondini, M. E., Patton, B. D., & Nyren, P. E. (2008). Grazing intensity and ecosystem processes in a northern mixed-grass prairie, USA.
- Boardman, J. W., & Kruse, F. (1994). Automated spectral analysis: A geological example using AVIRIS data, north grapevine mountains, nevada. Paper presented at the *Proceedings Of The Thematic Conference On Geologic Remote Sensing*, *1*
- Brand, M. D., Moore, M. M., & Williams, R. P. (1988). Management of North Dakota's school lands. *Rangelands*, *10*
- Bullock, J. M., Pywell, R. F., & Walker, K. J. (2007). Long-term enhancement of agricultural production by restoration of biodiversity. *Journal of Applied Ecology*, *44*(1), 6-12.
- Ceccato, P., Flasse, S., Tarantola, S., Jacquemoud, S., & Grégoire, J. M. (2001). Detecting vegetation leaf water content using reflectance in the optical domain. *Remote Sensing of Environment*, *77*(1), 22-33.
- Chang, C. I. (2005). Orthogonal subspace projection (OSP) revisited: A comprehensive study and analysis. *Geoscience and Remote Sensing, IEEE Transactions on*, *43*(3), 502-518.
- Chen, W., & Henebry, G. M. (2010). Spatio-spectral heterogeneity analysis using EO-1 hyperion imagery. *Computers & Geosciences*, *36*(2), 167-170.
- Cheng, Y. B., Tom, E., & Ustin, S. L. (2007). Mapping an invasive species, kudzu (*pueraria montana*), using hyperspectral imagery in western georgia. *Journal of Applied Remote Sensing*, *1*, 013514.
- Cho, M. A., Skidmore, A., Corsi, F., van Wieren, S. E., & Sobhan, I. (2007). Estimation of green grass/herb biomass from airborne hyperspectral imagery using spectral indices and partial least squares regression. *International Journal of Applied Earth Observation and Geoinformation*, *9*(4), 414-424.

- Cho, M. A., & Skidmore, A. K. (2009). Hyperspectral predictors for monitoring biomass production in mediterranean mountain grasslands: Majella national park, italy. *International Journal of Remote Sensing*, 30(2), 499-515.
- Cho, M., & Skidmore, A. (2009). Hyperspectral predictors for monitoring biomass production in mediterranean mountain grasslands: Majella national park, italy. *International Journal of Remote Sensing*, 30(2), 499-515.
- Chopping, M., Su, L., Laliberte, A., Rango, A., Peters, D. P. C., & Kollikkathara, N. (2006). Mapping shrub abundance in desert grasslands using geometric-optical modeling and multi-angle remote sensing with CHRIS/Proba. *Remote Sensing of Environment*, 104(1), 62-73.
- Clark, M. L., Roberts, D. A., & Clark, D. B. (2005). Hyperspectral discrimination of tropical rain forest tree species at leaf to crown scales. *Remote Sensing of Environment*, 96(3-4), 375-398.
- Clausi, D. A., & Jernigan, M. E. (1998). A fast method to determine co-occurrence texture features. *Geoscience and Remote Sensing, IEEE Transactions on*, 36(1), 298-300.
- Conner, R., Seidl, A., VanTassell, L., & Wilkins, N. (2001). United States grasslands and related resources: An economic and biological trends assessment. *Texas Agricultural Extension Service, Texas A&M University*, pp154
- Corina, J. R., William, E. J., & Kimberly, A. (2008). Grassland bird responses to land management in the largest remaining tallgrass prairie. *Conservation Biology*, 23(2), 420-432.
- D'Urso, G., Dini, L., Vuolo, F., Alonso, L., & Guanter, L. (2004). Retrieval of leaf area index by inverting hyperspectral multiangular CHRIS/PROBA data from SPARC 2003. Paper presented at the *Proceedings of the 2nd CHRIS/PROBA Workshop*, 28-30
- Dadon, A., Ben-Dor, E., Beyth, M., & Karnieli, A. (2011). Examination of spaceborne imaging spectroscopy data utility for stratigraphic and lithologic mapping. *Journal of Applied Remote Sensing*, 5, 053507.
- Darvishzadeh, R., Skidmore, A., Schlerf, M., & Atzberger, C. (2008). Inversion of a radiative transfer model for estimating vegetation LAI and chlorophyll in a heterogeneous grassland. *Remote Sensing of Environment*, 112(5), 2592-2604.
- Datt, B., & Jupp, D. (2004). *Hyperion Data Processing Workshop: Hands-on Processing Instruction*,

- Datt, B., McVicar, T. R., Van Niel, T. G., Jupp, D. L. B., & Pearlman, J. S. (2003). Preprocessing EO-1 hyperion hyperspectral data to support the application of agricultural indexes. *Geoscience and Remote Sensing, IEEE Transactions on*, *41*(6), 1246-1259.
- Daughtry, C. S. T., Doraiswamy, P., & Hunt, E. (2006). Remote sensing of crop residue cover and soil tillage intensity. *Soil and Tillage Research*, *91*(1-2), 101-108.
- Daughtry, C. S. T., McMurtrey, J. E., Chappelle, E. W., Hunter, W. J., & Steiner, J. L. (1996). Measuring crop residue cover using remote sensing techniques. *Theoretical and Applied Climatology*, *54*(1), 17-26.
- Dechant, J. A., Sondreal, M. L., Johnson, D. H., Igl, L. D., Goldade, C. M., Nenneman, M. P., & Euliss, B. R. (2003). Effects of management practices on grassland birds: Chestnut-collared longspur. northern prairie wildlife research center, jamestown, ND. northern prairie wildlife research center online. <http://www.npwrc.usgs.gov/resource/literatr/grasbird/cclo/cclo.htm> (Version 28MAY2004).
- Deering, D. W. (1978). Rangeland reflectance characteristics measured by aircraft and spacecraft sensors. pp316.
- Dobigeon, N., & Tourneret, J. Y. (2009). Library-based linear unmixing for hyperspectral imagery via reversible jump MCMC sampling. Paper presented at the *Aerospace Conference, 2009 IEEE*, 1-6.
- Dorigo, W., Bachmann, M., & Heldens, W. (2006). *ASD toolbox & processing of field spectra*. Institute for Environment and Geo-information Team Imaging Spectroscopy: German Aerospace Center (DLR). pp30.
- Farrell, M., & Mersereau, R. M. (2005). On the impact of covariance contamination for adaptive detection in hyperspectral imaging. *Signal Processing Letters, IEEE*, *12*(9), 649-652.
- Feneman, N. (1931). Physiography of the western united states. *New York, McGraw-Hill Book Co., Inc. Pi*, *1*(1938), 8.
- Foster, B. L., Kindscher, K., Houseman, G. R., & Murphy, C. A. (2009). Effects of hay management and native species sowing on grassland community structure, biomass, and restoration. *Ecological Applications*, *19*(7), 1884-1896.
- Foster, J. R., Townsend, P. A., & Zganjar, C. E. (2008). Spatial and temporal patterns of gap dominance by low-canopy lianas detected using EO-1 hyperion and landsat thematic mapper. *Remote Sensing of Environment*, *112*(5), 2104-2117.

- Franz n, M., & Nilsson, S. G. (2008). How can we preserve and restore species richness of pollinating insects on agricultural land? *Ecography*, 31(6), 698-708.
- Gamon, J. A., Pequeles, J., & Field, C. B. (1992). A narrow-waveband spectral index that tracks diurnal changes in photosynthetic efficiency* 1. *Remote Sensing of Environment*, 41(1), 35-44.
- Gao, B. C. (1995). Normalized difference water index for remote sensing of vegetation liquid water from space. Paper presented at the *Proceedings of SPIE*, , 2480 225.
- Gauthier, D. A., & Wiken, E. B. (1998). The great plains of north america. *Parks*, 8(3), 9-20.
- Gerhard, L. C., Anderson, S. B., & Fischer, D. W. (1990). Petroleum geology of the williston basin. *Interior Cratonic Basins: AAPG Memoir*, 51, 507–559.
- Gianelle, D., & Guastella, F. (2007). Nadir and off-nadir hyperspectral field data: Strengths and limitations in estimating grassland biophysical characteristics. *International Journal of Remote Sensing*, 28(7), 1547-1560.
- Gianelle, D., & Guastella, F. (2007). Nadir and off - nadir hyperspectral field data: Strengths and limitations in estimating grassland biophysical characteristics. *International Journal of Remote Sensing*, 28(7), 1547-1560.
- Gianelle, D., Vescovo, L., Marcolla, B., Manca, G., & Cescatti, A. (2009). Ecosystem carbon fluxes and canopy spectral reflectance of a mountain meadow. *International Journal of Remote Sensing*, 30(2), 435-449.
- Gibon, A. (2005). Managing grassland for production, the environment and the landscape. challenges at the farm and the landscape level. *Livestock Production Science*, 96(1), 11-31.
- Green, A. A., Berman, M., Switzer, P., & Craig, M. D. (1988). A transformation for ordering multispectral data in terms of imagequality with implications for noise removal. *IEEE Transactions on Geoscience and Remote Sensing*, 26(1), 65-74.
- Guo, X., Price, K. P., & Stiles, J. (2003). Grasslands discriminant analysis using landsat TM single and multitemporal data. *Photogrammetric Engineering and Remote Sensing*, 69(11), 1255-1262.
- Guo, X., Wilmshurst, J., McCanny, S., Fargey, P., & Richard, P. (2004). Measuring spatial and vertical heterogeneity of grasslands using remote sensing techniques. *Journal of Environmental Informatics*, 3(1), 24-32.

- Hamada, Y., Stow, D. A., Coulter, L. L., Jafolla, J. C., & Hendricks, L. W. (2007). Detecting tamarisk species (*tamarix* spp.) in riparian habitats of southern california using high spatial resolution hyperspectral imagery. *Remote Sensing of Environment*, 109(2), 237-248.
- Haralick, R. M., Shanmugam, K., & Dinstein, I. (1973). Textural features for image classification. *Systems, Man and Cybernetics, IEEE Transactions on*, 3(6), 610-621.
- Harsanyi, J. C., & Chang, C. I. (1994). Hyperspectral image classification and dimensionality reduction: An orthogonal subspace projection approach. *Geoscience and Remote Sensing, IEEE Transactions on*, 32(4), 779-785.
- He, K. S., Rocchini, D., Neteler, M., & Nagendra, H. (2011). Benefits of hyperspectral remote sensing for tracking plant invasions. *Diversity and Distributions*, 17(3), 381-392.
- Hestir, E. L., Khanna, S., Andrew, M. E., Santos, M. J., Viers, J. H., Greenberg, J. A., Rajapakse, S. S., & Ustin, S. L. (2008). Identification of invasive vegetation using hyperspectral remote sensing in the california delta ecosystem. *Remote Sensing of Environment*, 112(11), 4034-4047.
- Hill, M. J., FitzSimons, J., & Pearson, C. J. (2009). Creating land use scenarios for city greenbelts using a spatial multi-criteria analysis shell: Two case studies. *Physical Geography*, 30(4), 353-382.
- Hill, M. J., Lesslie, R., Barry, A., & Barry, S. (2005). A simple, portable, spatial multi-criteria analysis shell—MCAS-S. Paper presented at the *MODSIM 2005 International Congress on Modelling and Simulation. Modelling and Simulation Society of Australia and New Zealand*, 12-15.
- Hodkinson, D. J., & Thompson, K. (1997). Plant dispersal: The role of man. *Journal of Applied Ecology*, 34(6), 1484-1496.
- Homayouni, S., & Roux, M. (2004). Hyperspectral image analysis for material mapping using spectral matching. Paper presented at the *ISPRS Congress Proceedings, 20*
- Homer, C., Dewitz, J., Fry, J., Coan, M., Hossain, N., Larson, C., Herold, N., McKerrow, A., VanDriel, J. N., & Wickham, J. (2007). Completion of the 2001 national land cover database for the conterminous united states. *Photogrammetric Engineering and Remote Sensing*, 73(4), 337.
- Hooper, D. U., & Vitousek, P. M. (1997). The effects of plant composition and diversity on ecosystem processes. *Science*, 277(5330), 1302.
- Hurst, R. J. (2006). use of satellite imagery to measure cover of prairie vegetation for the detection of change. *Montana State University*, , 1-65.

- Isaacs, R., Tuell, J., Fiedler, A., Gardiner, M., & Landis, D. (2008). Maximizing arthropod-mediated ecosystem services in agricultural landscapes: The role of native plants. *Frontiers in Ecology and the Environment*, 7(4), 196-203.
- Jiménez-Muñoz, J. C., Sobrino, J. A., Plaza, A., Guanter, L., Moreno, J., & Martínez, P. (2009). Comparison between fractional vegetation cover retrievals from vegetation indices and spectral mixture analysis: Case study of PROBA/CHRIS data over an agricultural area. *Sensors*, 9(2), 768.
- Price, K. P., Guo, X. L., Stiles, J.M. (2002). Comparison of Landsat TM and ERS-2 SAR data for discriminating among grassland types and treatments in eastern Kansas. *Computers and Electronics in Agriculture*, 37, 157-171
- Johnson, S. (2007). Comments on “Orthogonal subspace projection (OSP) revisited: A comprehensive study and analysis”. *Geoscience and Remote Sensing, IEEE Transactions on*, 45(2), 532-533.
- Jordan, N. R., Larson, D. L., & Huerd, S. C. (2008). Soil modification by invasive plants: Effects on native and invasive species of mixed-grass prairies. *Biological Invasions*, 10(2), 177-190.
- Jupp, D., Datt, B., Lovell, J., Campbell, S., & King, E. (2002). Discussions around hyperion data: Background notes for the hyperion data users workshop. pp46.
- Kannowski, P. B. (1988). Oakville prairie. *ND Outdoors*,
- Kowarik, I. (2003). Human agency in biological invasions: Secondary releases foster naturalisation and population expansion of alien plant species. *Biological Invasions*, 5(4), 293-312.
- Küchler, A. (1964). Manual to accompany the map potential natural vegetation of the conterminous united states (with separate map at scale 1: 3,168,000), spec. *New York, American Geographical Society*, 39, pp116
- Lass, L. W., Prather, T. S., Glenn, N. F., Weber, K. T., Mundt, J. T., & Pettingill, J. (2005). A review of remote sensing of invasive weeds and example of the early detection of spotted knapweed (*centaurea maculosa*) and babysbreath (*gypsophila paniculata*) with a hyperspectral sensor. *Weed Science*, 53(2), 242-251.
- Lawrence, R. L., Wood, S. D., & Sheley, R. L. (2006). Mapping invasive plants using hyperspectral imagery and breiman cutler classifications (RandomForest). *Remote Sensing of Environment*, 100(3), 356-362.

- Lencioni, D. E., Digenis, C. J., Bicknell, W. E., Hearn, D. R., & Mendenhall, J. A. (1999). Design and performance of the EO-1 advanced land imager. Paper presented at the *SPIE Conference on Sensors, Systems, and Next Generation Satellites III*,
- Lesslie, R. G., Hill, M. J., Hill, P., Cresswell, H. P., & Dawson, S. (2008). The application of a simple spatial multi-criteria analysis shell to natural resource management decision making. *Landscape Analysis and Visualisation*, , 73-95.
- Mack, R. N., Simberloff, D., Mark Lonsdale, W., Evans, H., Clout, M., & Bazzaz, F. A. (2000). Biotic invasions: Causes, epidemiology, global consequences, and control. *Ecological Applications*, 10(3), 689-710.
- Malmstrom, C. M., McCullough, A. J., Johnson, H. A., Newton, L. A., & Borer, E. T. (2005). Invasive annual grasses indirectly increase virus incidence in california native perennial bunchgrasses. *Oecologia*, 145(1), 153-164.
- Manolakis, D., & Shaw, G. (2002). Detection algorithms for hyperspectral imaging applications. *Signal Processing Magazine, IEEE*, 19(1), 29-43.
- Miao, X., Gong, P., Swope, S., Pu, R., Carruthers, R., Anderson, G. L., Heaton, J. S., & Tracy, C. R. (2006). Estimation of yellow starthistle abundance through CASI-2 hyperspectral imagery using linear spectral mixture models. *Remote Sensing of Environment*, 101(3), 329-341.
- Miao, X., Gong, P., Swope, S., Pu, R., Carruthers, R., Anderson, G. L., Heaton, J. S., & Tracy, C. (2006). Estimation of yellow starthistle abundance through CASI-2 hyperspectral imagery using linear spectral mixture models. *Remote Sensing of Environment*, 101(3), 329-341.
- Miao, X., Patil, R., Heaton, J. S., & Tracy, R. C. (2011). Detection and classification of invasive saltcedar through high spatial resolution airborne hyperspectral imagery. *International Journal of Remote Sensing*, 32(8), 2131-2150.
- Miller, G. T. (1992). Living in the environment: An introduction to environmental science. *Wadsworth Publishing Company*. pp706
- Mooney, H. A., & Drake, J. A. (1986). Ecology of biological invasions of north america and hawaii.
- Moore, B. J., Hardisty, P. E., & Headley, J. V. (1997). Hydrocarbon attenuation in natural wetlands. Paper presented at the *Proceedings of Petroleum Hydrocarbons and Organic Chemicals in Ground Water: Prevention, Detection, and Remediation Conference*, 12-14.

- Mundt, J. T., Glenn, N. F., Weber, K. T., Prather, T. S., Lass, L. W., & Pettingill, J. (2005). Discrimination of hoary cress and determination of its detection limits via hyperspectral image processing and accuracy assessment techniques. *Remote Sensing of Environment*, 96(3-4), 509-517.
- Mushet, D. M., Euliss, N. H., Lane, S. P., & Goldade, C. M. (2004). The flora of the cottonwood lake study area, stutsman county, north dakota. *Prairie Naturalist*, 36(1), 43-62.
- Mutanga, O., & Skidmore, A. K. (2004). Narrow band vegetation indices solve the saturation problem in biomass estimation. *International Journal of Remote Sensing*, 25, 1-16.
- Mutanga, O., & Skidmore, A. (2004). Integrating imaging spectroscopy and neural networks to map grass quality in the kruger national park, south africa. *Remote Sensing of Environment*, 90(1), 104-115.
- Mutanga, O., van Aardt, J., & Kumar, L. (2009). Imaging spectroscopy (hyperspectral remote sensing) in southern africa: An overview. *South African Journal of Science*, 105(5-6), 193-198.
- Nagler, P. L., Inoue, Y., Glenn, E. P., Russ, A. L., & Daughtry, C. S. T. (2003). Cellulose absorption index (CAI) to quantify mixed soil-plant litter scenes. *Remote Sensing of Environment*, 87(2-3), 310-325.
- Noujdina, N. V., & Ustin, S. L. (2008). Mapping downy brome (*bromus tectorum*) using multivariate AVIRIS data. *Weed Science*, 56(1), 173-179.
- Parker Williams, A., Hunt Jr, E. R., & USDA, A. R. S. (2002). Estimation of leafy spurge cover from hyperspectral imagery using mixture tuned matched filtering. *Remote Sensing of Environment*, 82(2-3), 446-456.
- Pengra, B. W., Johnston, C. A., & Loveland, T. R. (2007). Mapping an invasive plant, phragmites australis, in coastal wetlands using the EO-1 hyperion hyperspectral sensor. *Remote Sensing of Environment*, 108(1), 74-81.
- Perbandt, D., Fricke, T., & Wachendorf, M. (2010). Effects of changing simulated sky cover on hyperspectral reflectance measurements for dry matter yield and forage quality prediction. *Computers and Electronics in Agriculture*, 73(2), 230-239.
- Peterson, D. L., Price, K. P., & Martinko, E. A. (2002). Discriminating between cool season and warm season grassland cover types in northeastern kansas. *International Journal of Remote Sensing*, 23(23), 5015-5030.

- Petropoulos, G. P., Arvanitis, K., & Sigrimis, N. (2012). Hyperion hyperspectral imagery analysis combined with machine learning classifiers for land Use/Cover mapping. *Expert Systems with Applications*, 39(3), 3800-3809
- Pfiftner, K., Bollhofer, A., & Carr, G. (2006). A standard design for collecting vegetation reference spectra: Implementation and implications for data sharing. *Journal of Spatial Science*, 51(2), 79-92.
- Price, K. P., Guo, X., & Stiles, J. M. (2002). Optimal landsat TM band combinations and vegetation indices for discrimination of six grassland types in eastern kansas. *International Journal of Remote Sensing*, 23(23), 5031-5042.
- Questad, E. J., Foster, B. L., Jog, S., Kindscher, K., & Loring, H. (2011). Evaluating patterns of biodiversity in managed grasslands using spatial turnover metrics. *Biological Conservation*, 144(3), 1050-1058
- Raddi, S., Cortes, S., Pippi, I., & Magnani, F. (2005). Estimation of vegetation photochemical processes: An application of the photochemical reflectance index at the san rosso test site, 3rd CHRIS. Paper presented at the *PROBA Workshop, ESRIN, Frascati*, 21-23.
- Ramsey, E., Rangoonwala, A., Nelson, G., & Ehrlich, R. (2005). Mapping the invasive species, chinese tallow, with EO1 satellite hyperion hyperspectral image data and relating tallow occurrences to a classified landsat thematic mapper land cover map. *International Journal of Remote Sensing*, 26(8), 1637-1657.
- Ramsey, R. D., Wright, D. L., & McGinty, C. (2004). Evaluating the use of landsat 30m enhanced thematic mapper to monitor vegetation cover in shrub-steppe environments. *Geocarto International*, 19(2), 39-47.
- Redmann, R. E. (1972). Plant communities and soils of an eastern north dakota prairie. *Bulletin of the Torrey Botanical Club*, 99(2), 65-76.
- Reduction, D. (1994). Hyperspectral image classification and dimensionality reduction: An orthogonal subspace projection approach. *IEEE Transactions on Geoscience and Remote Sensing*, 32(4), 179.
- Ricketts, T. H., Dinerstein, E., & Olson, D. M. (1999). Terrestrial ecoregions of north america: A conservation assessment. *Island Pr.* pp508.
- Samson, F., & Knopf, F. (1994). Prairie conservation in north america. *Bioscience*, 44(6), 418-421.

- Sawyer, H., Lindzey, F., McWhirter, D., & Andrews, K. (2002). Potential effects of oil and gas development on mule deer and pronghorn populations in western wyoming. Paper presented at the *Transactions of the North American Wildlife and Natural Resources Conference*, 67, 350-365.
- Schaepman, M. E., Ustin, S. L., Plaza, A. J., Painter, T. H., Verrelst, J., & Liang, S. (2009). Earth system science related imaging spectroscopy--an assessment. *Remote Sensing of Environment*, 113, S123-S137.
- Schut, A. G. T., & Ketelaars, J. (2003). Monitoring grass swards using imaging spectroscopy. *Grass and Forage Science*, 58(3), 276-286.
- Schwab, A., Dubois, D., Fried, P. M., & Edwards, P. J. (2002). Estimating the biodiversity of hay meadows in north-eastern switzerland on the basis of vegetation structure. *Agriculture, Ecosystems & Environment*, 93(1-3), 197-209.
- Sedivec, K., Tober, D., & Berdahl, J. (2009). Grass varieties for north dakota.
- Spitz, H., Lovins, K., & Becker, C. (1997). Evaluation of residual soil contamination from commercial oil well drilling activities and its impact on the naturally occurring background radiation environment. *Soil and Sediment Contamination: An International Journal*, 6(1), 37-59.
- Stuffer, T., Kaufmann, C., Hofer, S., Forster, K. P., Schreier, G., Mueller, A., Eckardt, A., Bach, H., Penne, B., & Benz, U. (2007). The EnMAP hyperspectral imager--an advanced optical payload for future applications in earth observation programmes. *Acta Astronautica*, 61(1-6), 115-120.
- Thenkabail, P. S., Enclona, E. A., Ashton, M. S., Legg, C., & De Dieu, M. J. (2004). Hyperion, IKONOS, ALI, and ETM sensors in the study of african rainforests. *Remote Sensing of Environment*, 90(1), 23-43.
- Thulin, S. M. (2009). Hyperspectral remote sensing of temperate pasture quality.
- Thulin, S., Hill, M., & Held, A. (2004). Spectral sensitivity to carbon and nitrogen content in diverse temperate pastures of australia. Paper presented at the *2004 IEEE International Geoscience and Remote Sensing Symposium, 2004. IGARSS'04. Proceedings*, 2
- Underwood, E., Ustin, S., & DiPietro, D. (2003). Mapping nonnative plants using hyperspectral imagery. *Remote Sensing of Environment*, 86(2), 150-161.
- Underwood, E. C., Mulitsch, M. J., Greenberg, J. A., Whiting, M. L., Ustin, S. L., & Kefauver, S. C. (2006). Mapping invasive aquatic vegetation in the sacramento-san joaquin delta using hyperspectral imagery. *Environmental Monitoring and Assessment*, 121(1), 47-64.

- Underwood, E. C., Ustin, S. L., & Ramirez, C. M. (2007). A comparison of spatial and spectral image resolution for mapping invasive plants in coastal California. *Environmental Management*, 39(1), 63-83.
- Ustin, S. L., DiPietro, D., Olmstead, K., Underwood, E., & Scheer, G. J. (2001). Hyperspectral remote sensing for invasive species detection and mapping. *Papers of the American Chemical Society*, 221
- Vitousek, P. M., Mooney, H. A., Lubchenco, J., & Melillo, J. M. Human domination of Earth's ecosystems. *Urban Ecology*, 3-13.
- Whitman, W. C., & Barker, W. T. (1994). Wheatgrass-bluestem-needlegrass SRM 606. *Rangeland cover types of the United States* (pp. 75-75)
- Yang, C., Everitt, J. H., & Johnson, H. B. (2009). Applying image transformation and classification techniques to airborne hyperspectral imagery for mapping aspen-juniper infestations. *International Journal of Remote Sensing*, 30(11), 2741-2758.
- Yang, C., Everitt, J., & Johnson, H. (2009). Applying image transformation and classification techniques to airborne hyperspectral imagery for mapping aspen-juniper infestations. *International Journal of Remote Sensing*, 30(11), 2741-2758.
- Yuan, R. H., Goetz, A. F. H., & Boardman, J. W. (1992). Discrimination among semi-arid landscape endmembers using the spectral angle mapper (SAM) algorithm. Paper presented at the *Summaries of the Third Annual JPL Airborne Geoscience Workshop*, 1, 147-149.
- Zhang, C. (2006). Monitoring biological heterogeneity in a northern mixed prairie using hierarchical remote sensing methods. pp.146.
- Zhang, C., & Guo, X. (2007). Measuring biological heterogeneity in the northern mixed prairie: A remote sensing approach. *Canadian Geographer/Le Géographe Canadien*, 51(4), 462-474.
- Zhang, Q., Middleton, E. M., Gao, B. C., & Cheng, Y. B. Using EO-1 Hyperion to simulate HypIRI products for a coniferous forest: The fraction of PAR absorbed by chlorophyll and leaf water content (LWC). *Geoscience and Remote Sensing, IEEE Transactions* (99), 1-10.